12-9-2006

Diagonal And Horizontal Stiffeners For Shear Transfer In Rigid Frame Square Knees

William Franklin Heard

DIAGONAL AND HORIZONTAL STIFFENERS FOR SHEAR TRANSFER IN RIGID FRAME SQUARE KNEES

By

William Franklin Heard

A Thesis
Submitted to the Faculty of
Mississippi State University
in Partial Fulfillment of the Requirements
for the degree of Master of Science
in Civil Engineering
in the Department of Civil Engineering

Mississippi State University

December 2006

DIAGONAL AND HORIZONTAL STIFFENERS FOR SHEAR TRANSFER IN RIGID FRAME SQUARE KNEES

By

William Franklin Heard

Approved:

R. Ralph Sinno Professor of Civil Engineering Committee Chairman	William H. McAnally Graduate Coordinator Associate Professor of Civil Engineering
Stan C. Woodson Adjunct Professor of Civil Engineering Committee Member	Thomas Slawson Adjunct Professor of Civil Engineering Committee Member

Kirk Schulz
Dean of the College of Engineering

Name: William Franklin Heard

Date of Degree: December 8, 2006

Institution: Mississippi State University

Major Field: Civil Engineering

Major Professor: Dr. Ralph Sinno

Title of Study: DIAGONAL AND HORIZONTAL STIFFENERS FOR SHEAR TRANSFER IN RIGID FRAME SQUARE KNEES

Pages in Study: 130

Candidate for Degree of Master of Science

The research addresses the effect of diagonal and horizontal stiffeners on shear transfer in rigid frame square knees. Rigid frame square knees are an integral component of pre-manufactured metal building systems. This paper examined a more efficient design of the rigid frame square knee.

Five full-scale laboratory tests on square knee joints were performed to verify the effects of a diagonal stiffener on shear transfer. Two frames were fabricated without diagonal stiffeners, and three frames were fabricated with 1/8- inch- thick diagonal stiffeners, not extending the full diagonal length of the knee web. Experimental results, coupled with a finite element analysis, are compared to AISC provisions in Section F4: shear yielding and shear buckling, and in Section G3: tension field action. This research shows that if diagonal stiffeners are needed, then thin, shortened diagonal stiffeners are sufficient to restrain shear buckling of the knee web until shear yielding occurs.

TABLE OF CONTENTS

APPENDIX Page

LIST OF TABLES

LIST OF FIGURES

FIGURE Page

CHAPTER I

INTRODUCTION

1.1 General

Grossing sales of over $2.5 billion a year and shipping over 2.8 billion pounds of steel last year alone [1], the pre-manufactured and pre-engineered metal building industry has become a popular alternative to conventional steel construction. These metal building systems are used in a wide variety of applications, such as complex production facilities, retail stores, shopping centers, warehouses and distribution centers, motels, automobile dealerships, office complexes, schools, and churches. By using highly efficient designs and requiring minimal skilled labor to erect and install, the metal building industry has become a highly competitive market.

In order to stay competitive in this changing market, a pre-manufactured and pre-engineered metal building company must continually seek a more innovative and efficient design that provides structural safety and economy. This research addresses an area of design that is unique to the metal building rigid frame, commonly called the square knee joint. Square knee joints are used exclusively by the metal building industry to frame rafters to columns. Typical square knee joints are constructed in the shop with or without a diagonal stiffener as an integral component of the column section. The rafters are then field connected to the columns by end plates that serve as a bolted

moment resistant transfer connection. This general connection concept has proven to be safe and cost-effective because it allows for quick and easy installation in the field.

Present design practice requires the knee joint to be conservatively rigid. Special efforts are commonly made to fabricate a tight fit diagonal member within the square knee joint. When needed, the tight fit diagonal stiffener serves as a lateral restraint to the web as well as a compression strut to strengthen the knee joint.[2] As an alternative to the use of a diagonal stiffener, the web of the square knee may be designed and fabricated with a minimum required web thickness that is often thicker than the required web thickness of the column and rafter. Both of these common practices either result in special fabrication techniques or additional material requirements; therefore, both are either difficult to fabricate or proven to be more expensive. Figure 1.1 shows a typical metal building frame, while Figure 1.2 is a close up view of the knee joint used in the frame shown in Figure 1.1.

Figure 1.1 A typical frame showing a commonly used square knee joint design

Figure 1.2 A commonly used design for a square knee joint (from figure 1.1)

The shear transfer between the rafter and the column is the main concern in the design of a square knee, as it often results in shear buckling of the web plate.[3] Figure 1.3 shows the load transfer and the resulting tendency for web deformation due to shear. This research addresses a more efficient design of the square knee joint by employing a shortened diagonal stiffener, if used, to serve as a means of lateral constraint. In addition to a shortened diagonal stiffener, this research will also address the effects of detaching the horizontal stiffener to the outside column flange. Figure 1.4 shows the design that will be discussed and investigated throughout this paper.

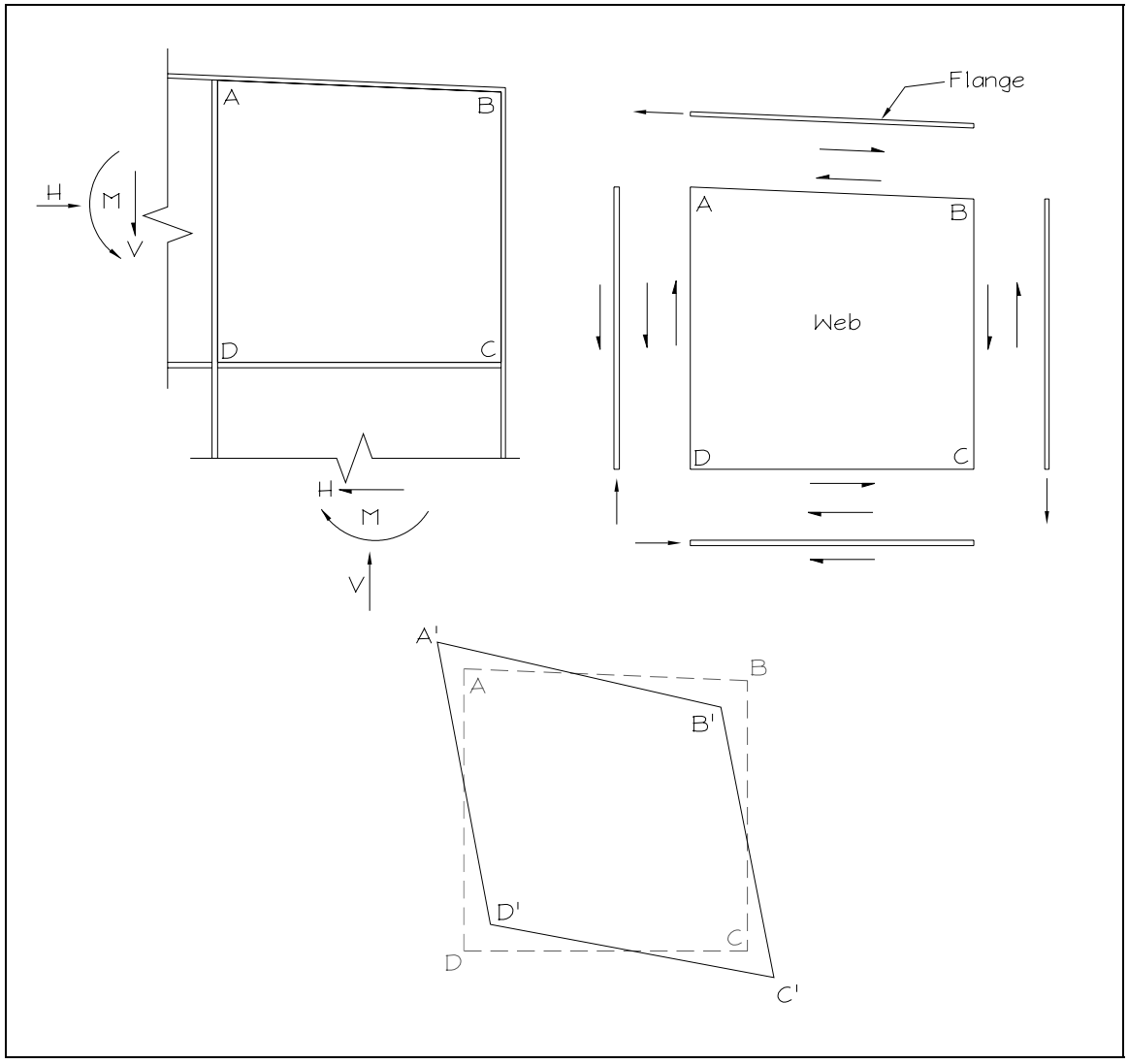

Figure 1.3 Shear transfer and web deformation in the knee panel

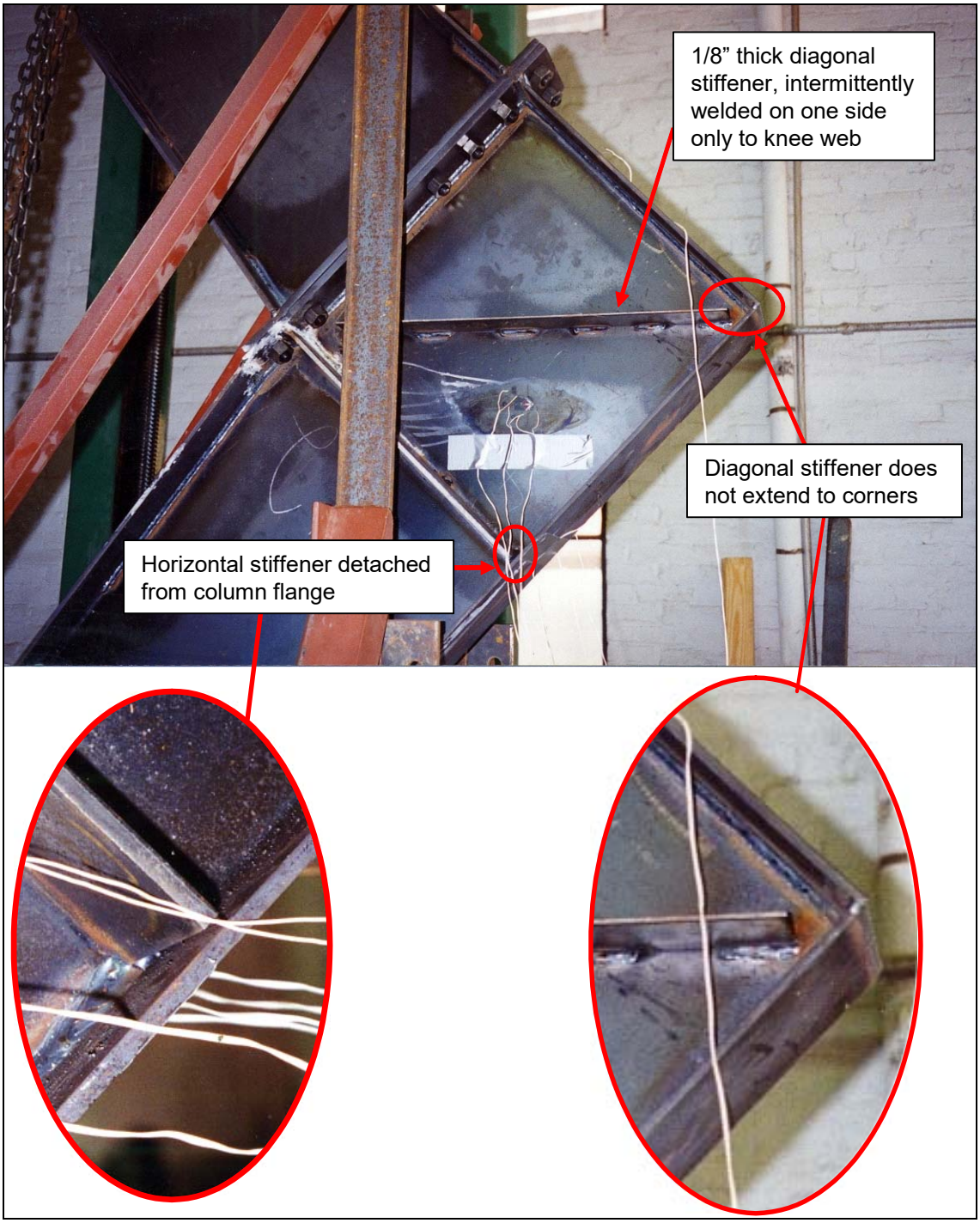

Figure 1.4 A proposed more efficient design of the square knee joint

1.2 Scope

Through a process of finite element analysis and consulting with a metal building manufacturer, five rigid metal frames were constructed and tested in the laboratory for investigating the following:

1. The need and performance of a shortened diagonal stiffener
2. The effects of detaching the horizontal column stiffener
3. The effects of tension field action
4. The failure mode of each rigid frame
5. A comparison of the actual laboratory results and the finite element analysis predicted values

1.3 Objectives

The research addressed in this paper intended to accomplish the following objectives:

1. Determine if a shortened diagonal stiffener will adequately arrest shear buckling of the web in the square knee.
2. Determine if a detached horizontal column stiffener will affect the structural strength of the rigid frame.
3. Verify the findings from a finite element analysis with those from the actual laboratory tests.

CHAPTER II

EXPERIMENTAL APPROACH

2.1 General

Five full-scale prototype rigid frames were fabricated and donated by Ceco Metal Building Systems of Columbus, Mississippi. Each frame was composed of a tapered column and a tapered rafter connected together by a square knee joint. Two main variables were addressed:

1. Contribution of the diagonal stiffener, when used, to the failure mode
2. Effectiveness of welding the lower horizontal stiffener in the square knee to the outside flange of the column

These two variables were considered as the major items that make the fabrication of the square knee connection convenient, fast, and less labor intensive. In addition, the need for a diagonal stiffener serving as a compression strut was investigated. A theoretical engineering investigation on the need of a diagonal stiffener is presented in Appendix A. The mathematical calculations indicated that bracing the web plate of the knee against shear buckling is the major concern to the structural integrity of the square knee. This was accomplished by using a single thin diagonal stiffener placed on one side only, and welded intermittently on one side along its length to the web plate.

2.2 Testing Program

Table 2.1 gives a description of the five frames used in the laboratory testing program. All frames were fabricated from the same structural steel, ASTM A572 with A325 bolts, with properties and dimensions shown in Table 2.2 and shown in Figures 2.1 through 2.5.

Table 2.1 Description of frames used in the laboratory tests

Test # / Frame #	Description
Test 1 / Frame 1	Knee without diagonal stiffener, the horizontal stiffener of the lower side of the square knee welded to the outside flange of the column. See Figure 2.2
Test 2 / Frame 2	Same as Test 1 / Frame 1, except a single diagonal stiffener is added; b_{st} = 2-3/4", t_{st} = 0.138", and length = 22-1/2". The diagonal stiffener was welded intermittently on one side using 3/16" fillet welds, 2" long at 4" centers. The diagonal stiffener is recessed 2-1/2" from both corners of the square knee. See Figure 2.3
Test 3 / Frame 3	Same as Test 1 / Frame 1, except the stiffener of the lower side of the square knee was not welded to the outside flange of the column. A gap of 1/8" was left intentionally. See Figure 2.4
Test 4 / Frame 4	Same as Test 2 / Frame 2, except the stiffener of the lower side of the square knee was not welded to the outside flange of the column. A gap of 1/8" was left intentionally. See Figure 2.5
Test 5 / Frame 5	Same as Test 4 / Frame 4, this test was used to confirm the results of Test 4.

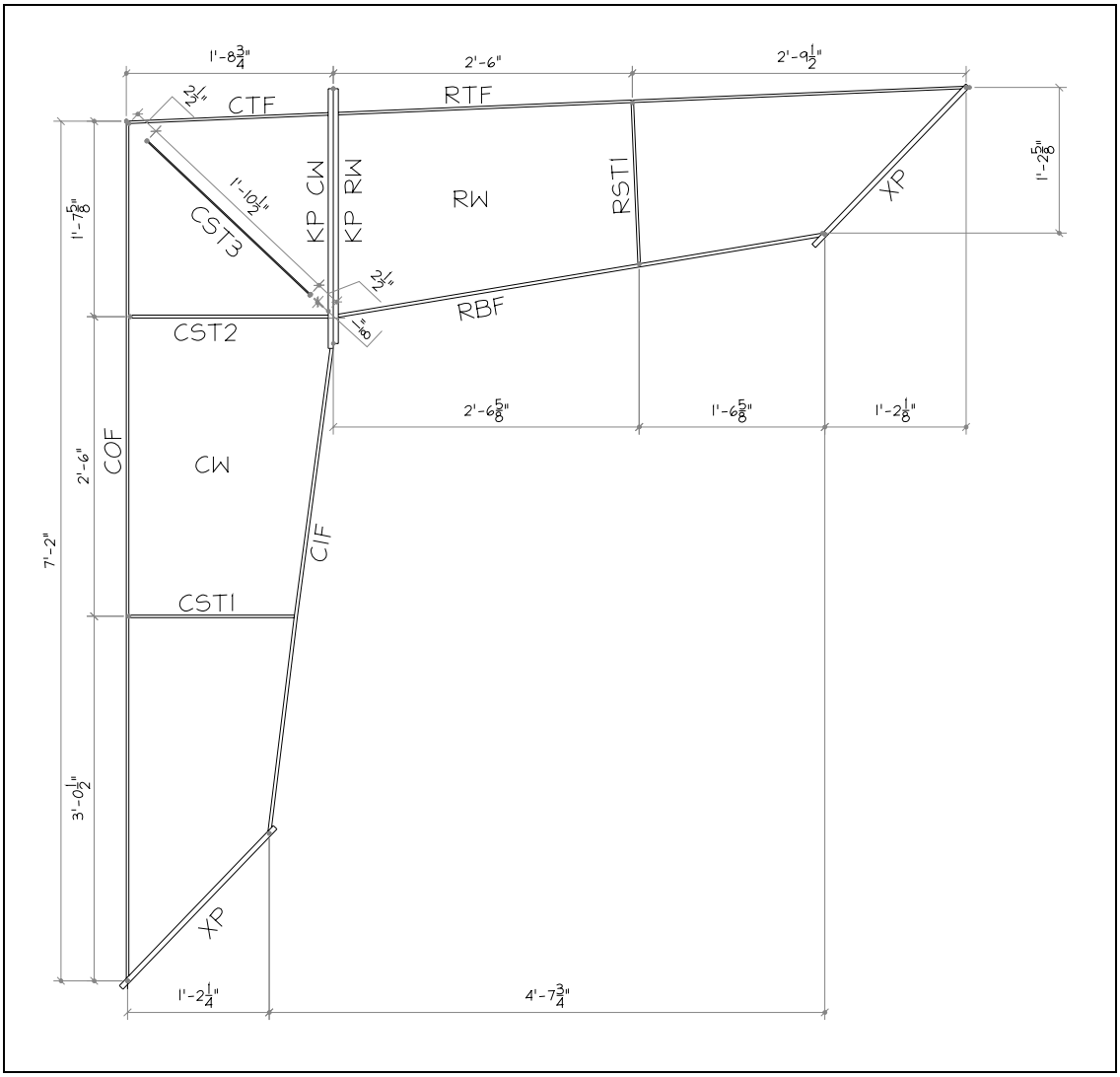

Figure 2.1 Frame showing plate fabrication nomenclature and overall dimensions

Table 2.2 Size of frame plates and components

Name	**Description**	Size
RTF	Rafter top flange	$PL\frac{1}{4}$" x 6" x 5'-2$\frac{9}{16}$"
RBF	Rafter bottom flange	$PL\frac{5}{16}$" x 6" x 4'-1"
COF	Column outer flange	$PL\frac{1}{4}$" x 6" x 6'-11$\frac{1}{2}$"
CIF	Column inner flange	$PL\frac{5}{16}$" x 6" x 3'-10$\frac{7}{16}$"
CTF	Column top flange	$PL\frac{1}{4}$" x 6" x 1'-8$\frac{1}{16}$"
CST1	Lower column web stiffener	$PL\frac{1}{4}$" x 2$\frac{3}{4}$" x 6'-11$\frac{1}{2}$"
CST2	Upper column web stiffener	$PL\frac{1}{4}$" x 6" x 6'-11$\frac{1}{2}$"
CST3	Knee web stiffener	$PL\frac{1}{8}$" x 2$\frac{3}{4}$" x 1'-10$\frac{1}{2}$"
RST	Rafter web stiffener	$PL\frac{1}{4}$" x 2$\frac{3}{4}$" x 1'-4"
RW	Rafter web	$PL\frac{1}{8}$" x varies
CW	Column web	$PL\frac{1}{8}$" x varies
KP CW	Column end plate	$PL\frac{1}{2}$" x 6" x 2 - 2"
KP RW	Rafter end plate	$PL\frac{1}{2}$" x 6" x 2 - 1$\frac{1}{2}$"
XP	End loading plate	$PL\frac{1}{2}$" x 6" x 1 - 10$\frac{1}{4}$"
Bolt	Bolt for end plates	$\phi = \frac{3}{4}$"

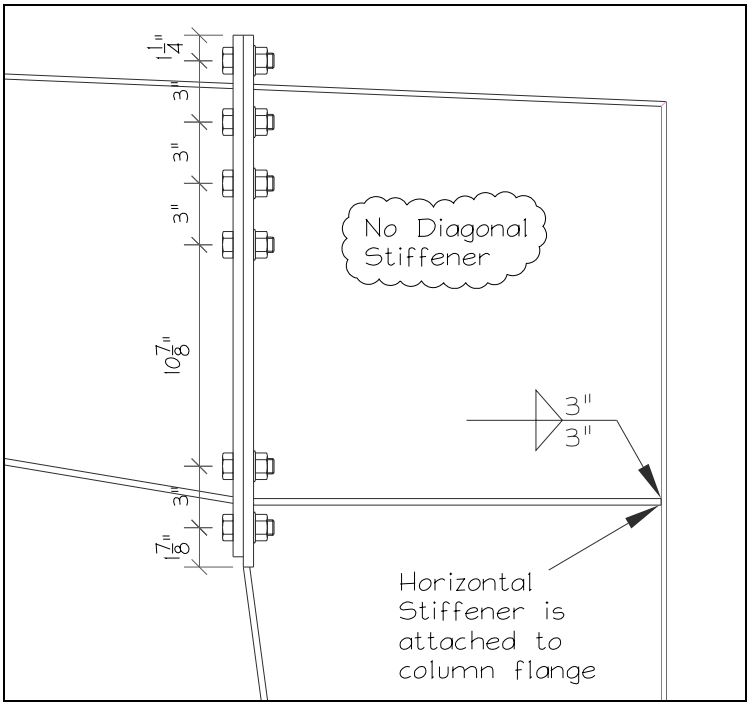

Figure 2.2 Frame 1, no diagonal stiffener and the horizontal stiffener is attached

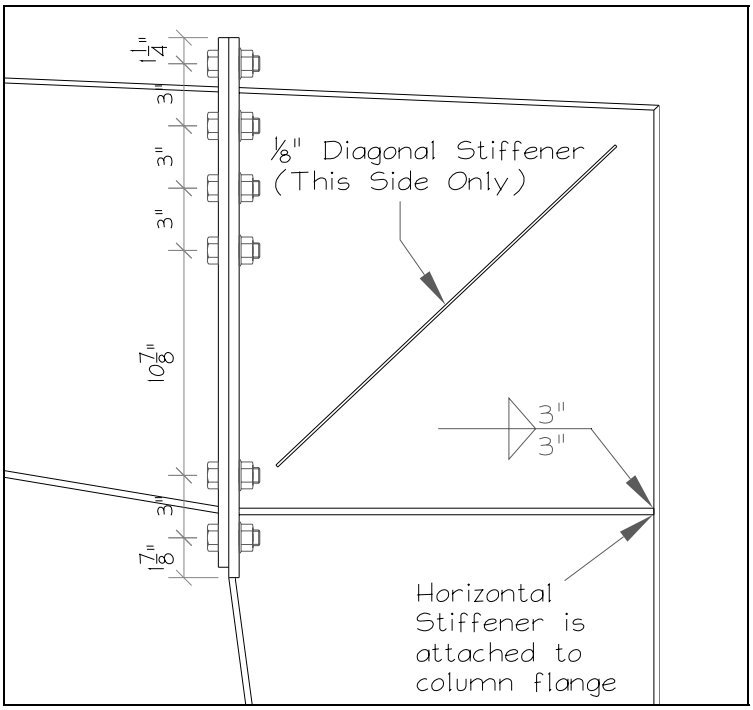

Figure 2.3 Frame 2, diagonal stiffener and the horizontal stiffener is attached

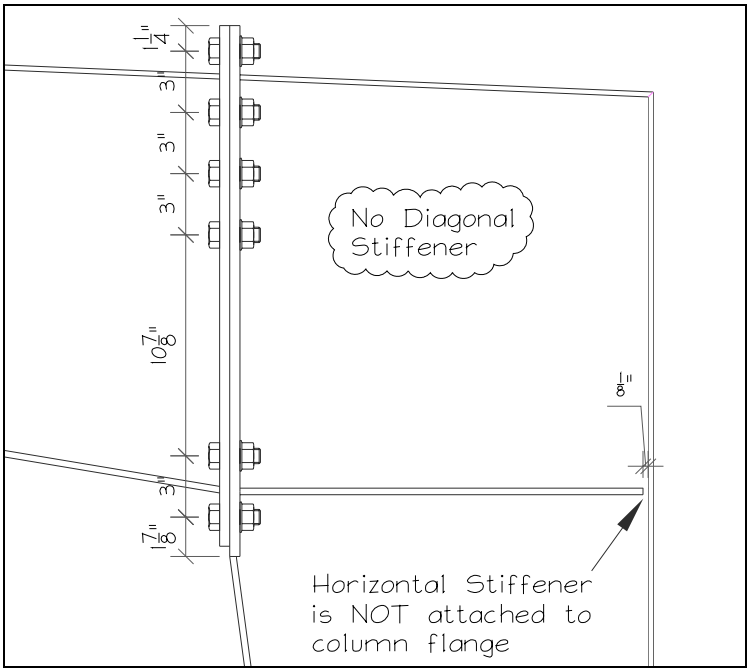

Figure 2.4 Frame 3, no diagonal stiffener and the horizontal stiffener is detached

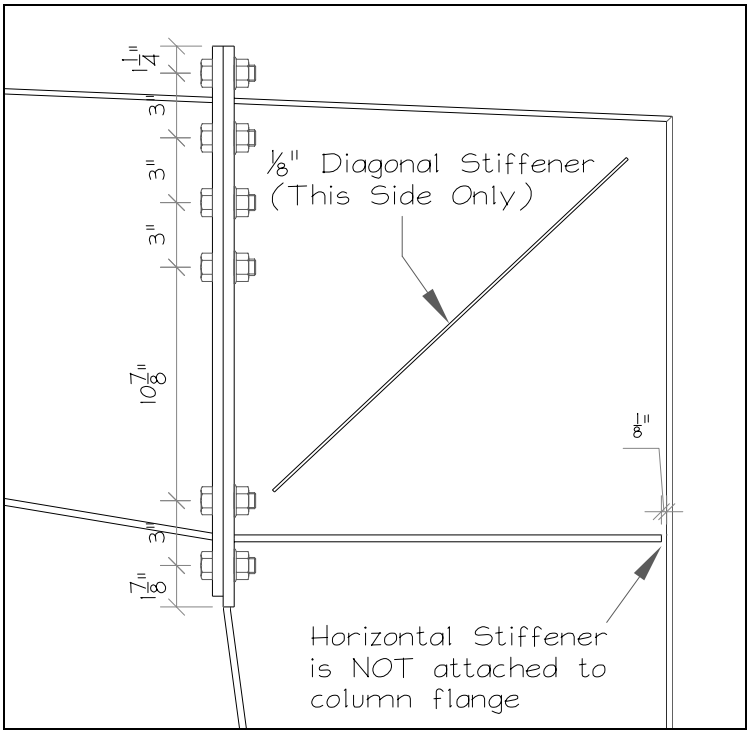

Figure 2.5 Frame 4, diagonal stiffener and the horizontal stiffener is detached

The frames were tested in the structures laboratory at Mississippi State University. Figures 2.6 and 2.7 show test specimens under load in the testing machine. The test setup was designed to physically apply a unidirectional concentrated load to the full-scale rigid frame section as shown. By adding the independent guide angles, as shown in Figure 2.8, the frame was constrained on both sides to prevent lateral translation. The entire test setup of the rigid frame, including the square knee junction, was free to glide vertically between the two guide angles. The test setup proved to be highly reliable and free from any indirect secondary loading, it also provided very clear and direct observation of the failure mode as it developed.

Figures 2.6, 2.7 and 2.8 Test setup for all five frames with lateral guide angles

2.3 Data Collection

The five frames were set in the testing machine using identical set-ups and loading procedures. Loading was monitored throughout the incremental loading. The load was applied continuously by positive vertical displacement between the head and the table of the testing machine. Strain measurements were collected using electrical strain gages and visual inspection. The strain gages were positioned to monitor critical points of interest. Figures 2.9 to 2.12 show the locations of the strain gages for each test.

Direct tension test coupons were taken from the web steel of each test frame to establish the basic mechanical properties. The coupon test results are presented in Appendix B. A typical stress-strain curve was produced from this data and is also shown in Appendix B.

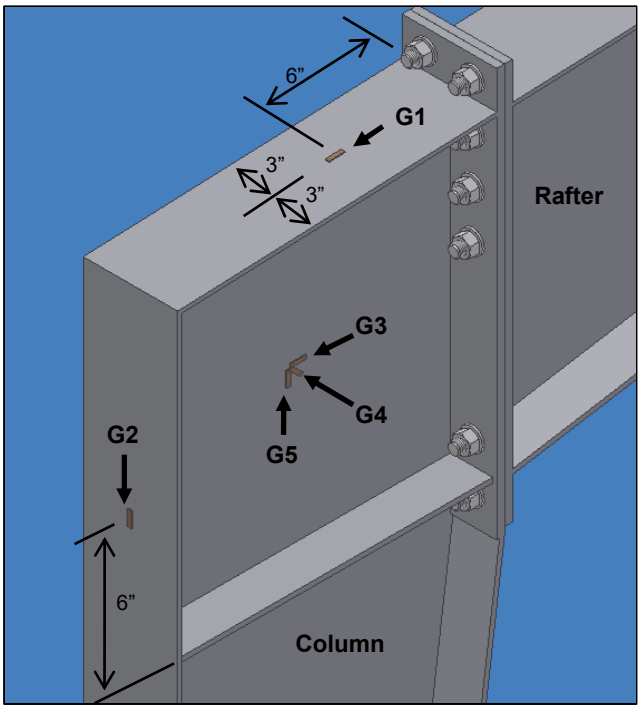

Figure 2.9 Frame 1 showing locations of strain gages (G1-G5)

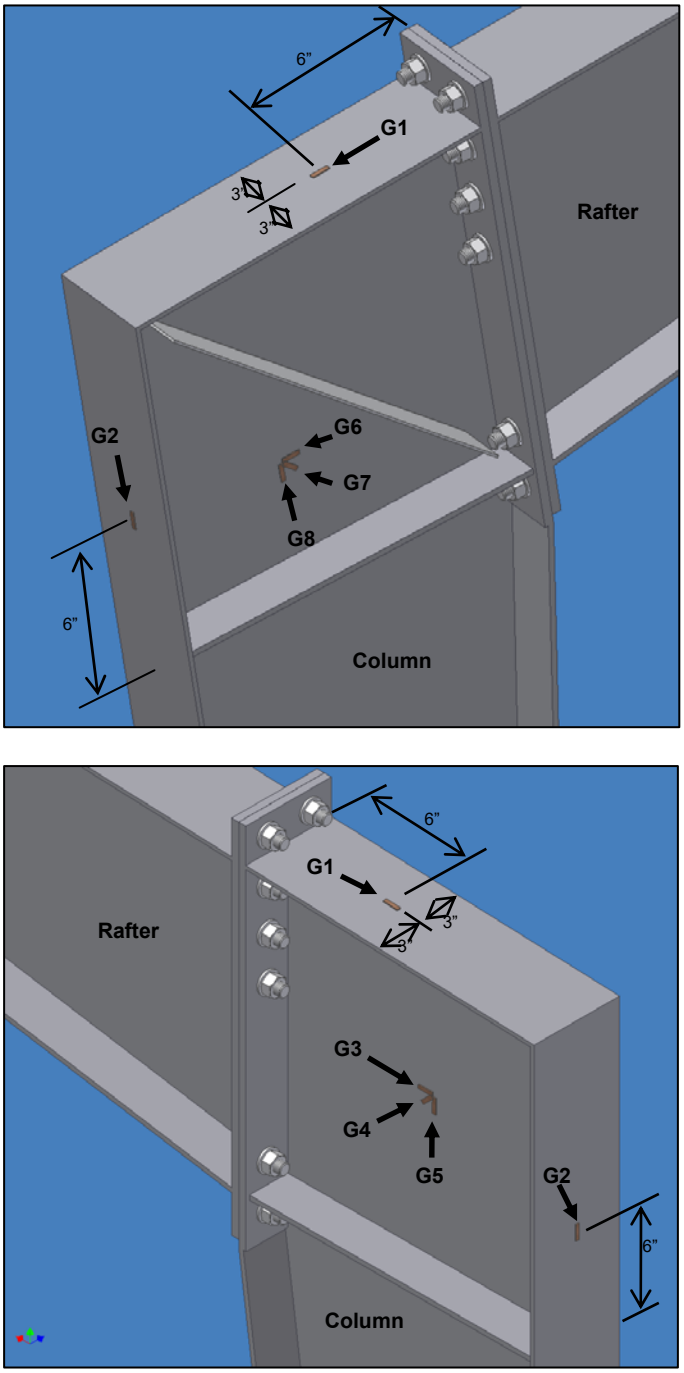

Figure 2.10 Frame 2 showing locations of strain gages (G1-G8)

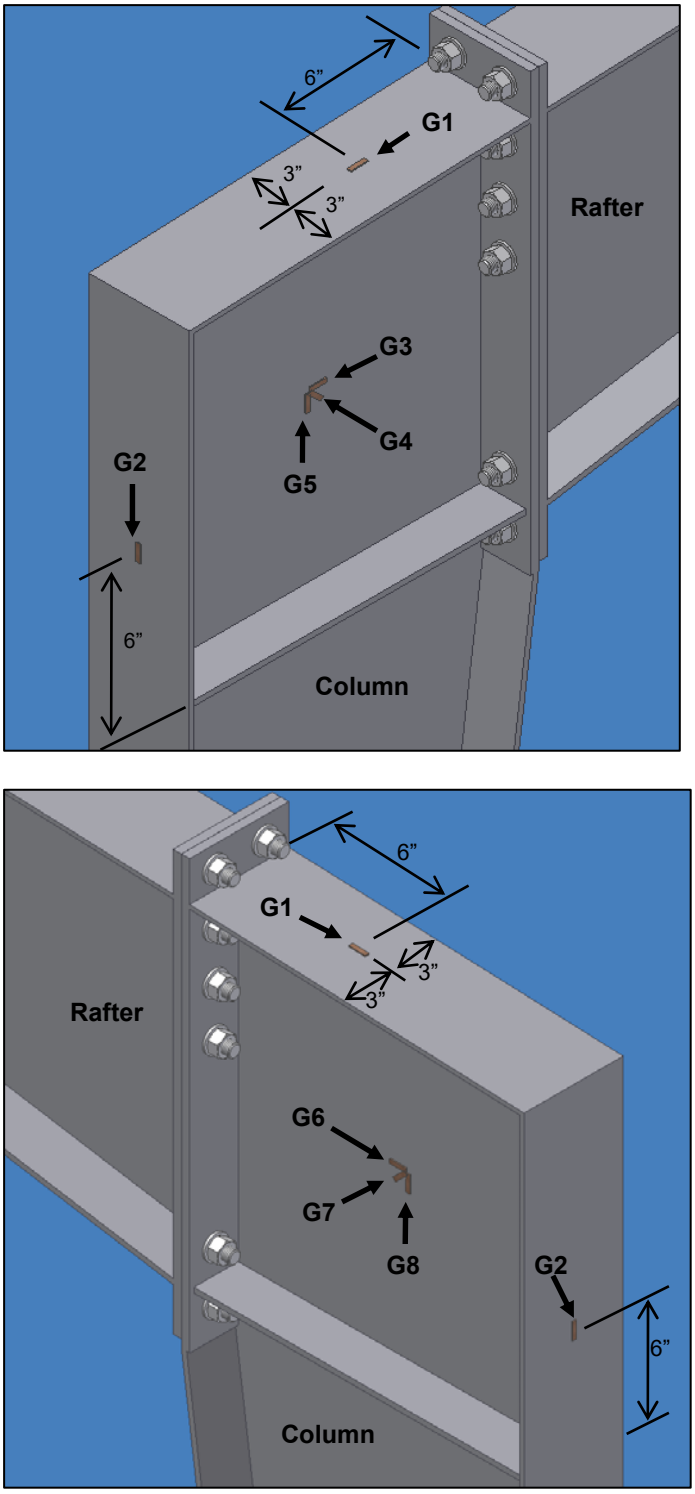

Figure 2.11 Frame 3 showing locations of strain gages (G1-G8)

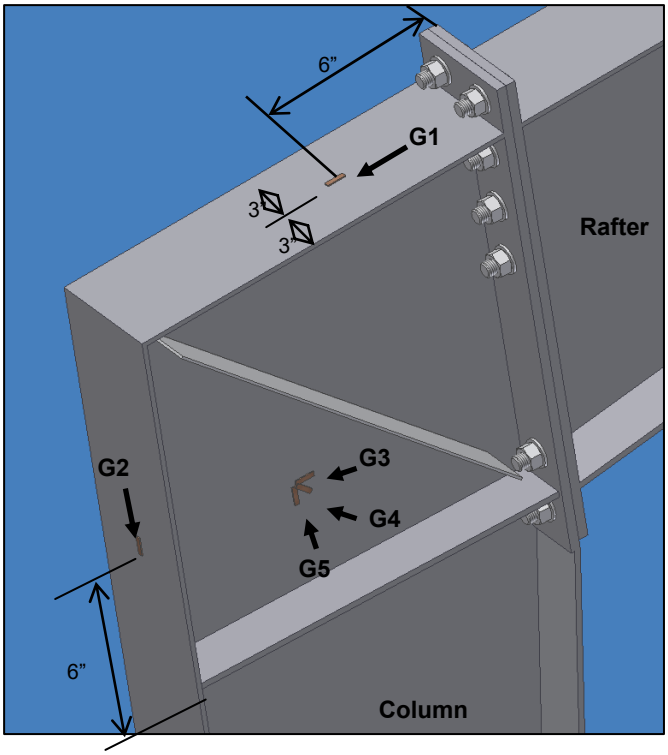

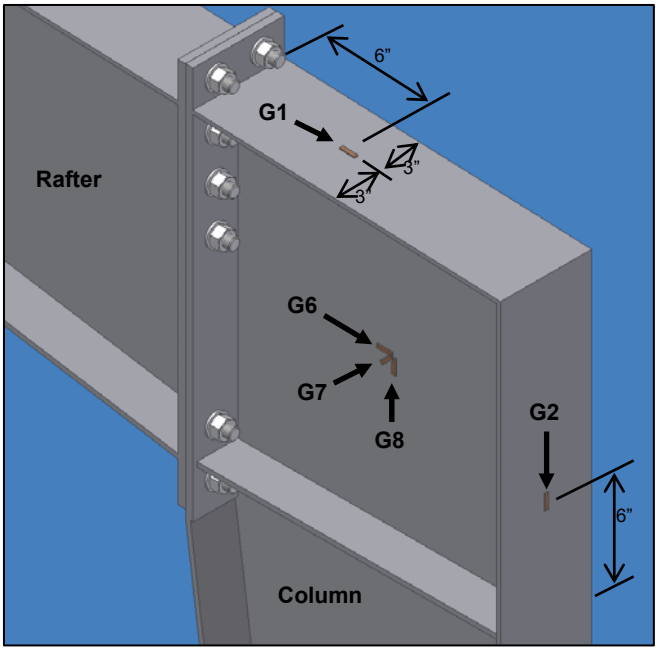

Figure 2.12 Frames 4 and 5 showing locations of strain gages (G1-G8)

CHAPTER III

FINITE ELEMENT ANALYSIS

3.1 General

The frames were modeled with ALGOR™ v19.2, a finite element analysis (FEA) program.[4] ALGOR™ FEA is a code primarily developed to run on a personal computer and is mainly used in industry for simulating mechanical events, computational fluid dynamics, and linear / nonlinear static stress analyse. Although some of the preliminary models were conducted as a nonlinear static stress analysis, computer processing capacity and lack of frame symmetry, ultimately limited the study to the ALGOR™ static stress linear material model core package. Furthermore, as shown in the engineering □athematical calculations presented in Appendix A and stated as a primary objective of this study, premature buckling of the knee web is expected to occur in the linear elastic region. Given this, the FEA approach was a linear static stress elastic analysis, coupled with an investigation of the critical buckling load due to geometric instability of the knee web.

3.2 Developing the FEA Mesh

The frames were modeled with the corresponding variables shown in Table 2.1. Initially, the modeling process began with an attempt to use solid or brick elements, but the resulting model was much too computationally intensive for a personal computer.

Therefore, the final model was a combination of plate elements, beam elements, and gap elements. Plate elements represented most of the web, flange, and stiffener components. Of the plate elements, a vast majority were four-node quadrilaterals. Due to the taper of the column and rafter, three-node triangular plate elements were also used to transition the mesh geometry while maintaining reasonable aspect ratios for the individual elements. ALGOR™ offers four options for plate element formulation; the models developed for this linear static stress analysis used the default setting, Veubeke. The Veubeke option is based on the theory by B. Fraeijs de Veubeke for plate formulation for displaced and equilibrium models [5]. Figures 3.1 and 3.2 show the overall model mesh, and additional views of the knee joint mesh for frames 1, 2, and 5 are shown in Figures 3.3 and 3.5. Figures 3.4 and 3.6 show the knee joint mesh geometry for frames 1 and 3.

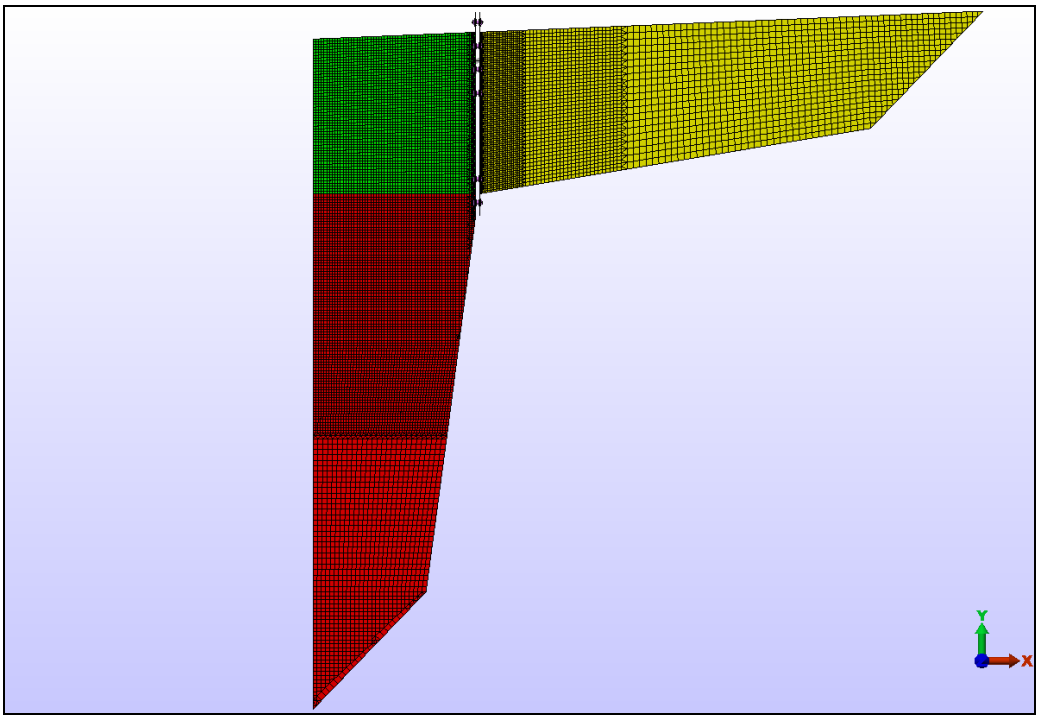

Figure 3.1 Overall view of model mesh for frame 1 and frame 3

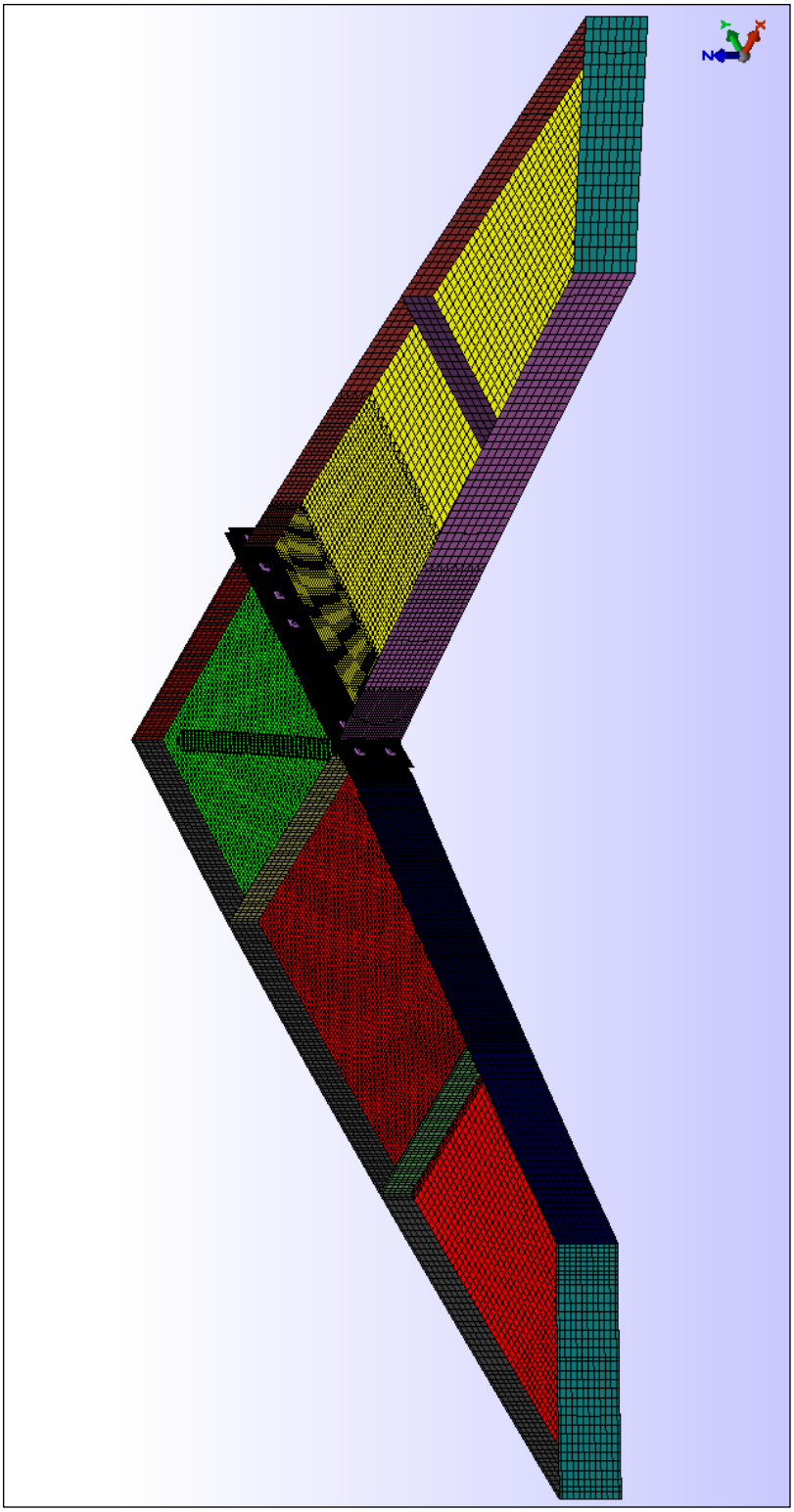

Figure 3.2 Isometric view of model mesh for frames 2, 4, and 5

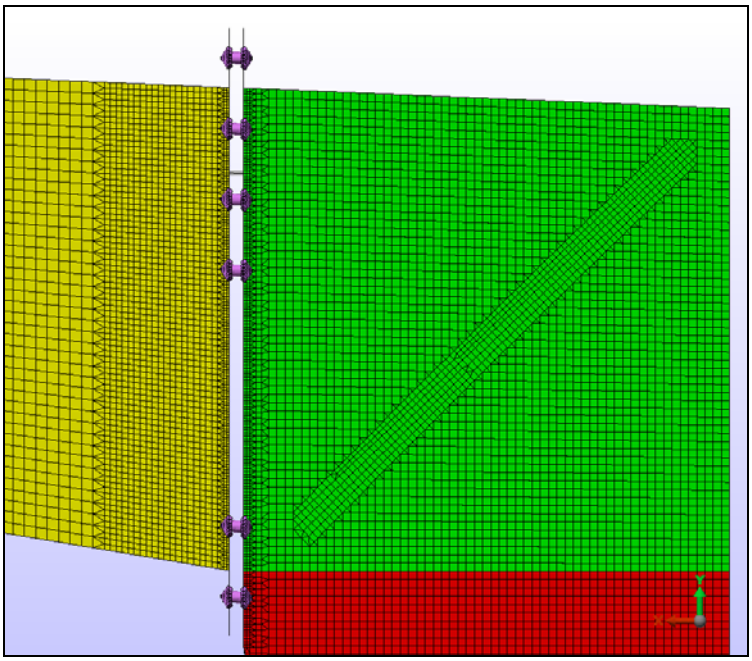

Figure 3.3 Mesh for the knee web for frames 2, 4, and 5

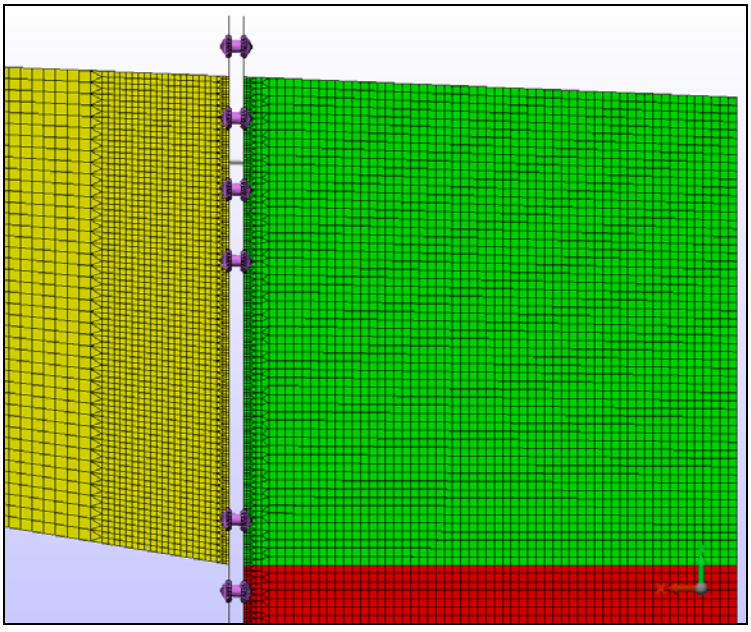

Figure 3.4 Mesh for the knee web for frames 1 and 3

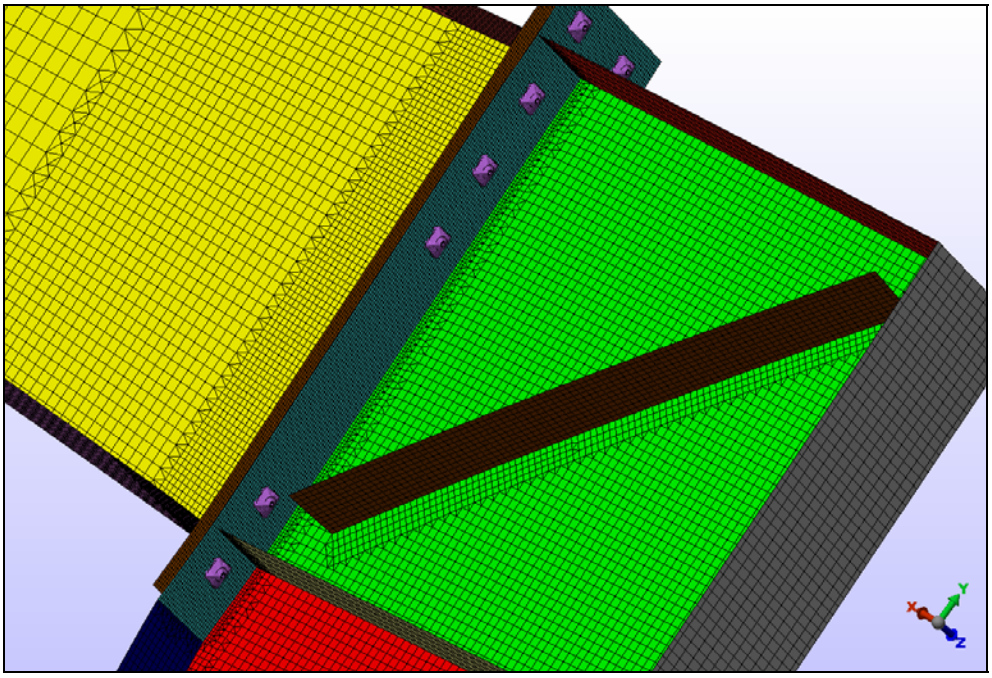

Figure 3.5 Mesh for the knee joint flanges, stiffener, and end plate of frames 2, 4, and 5

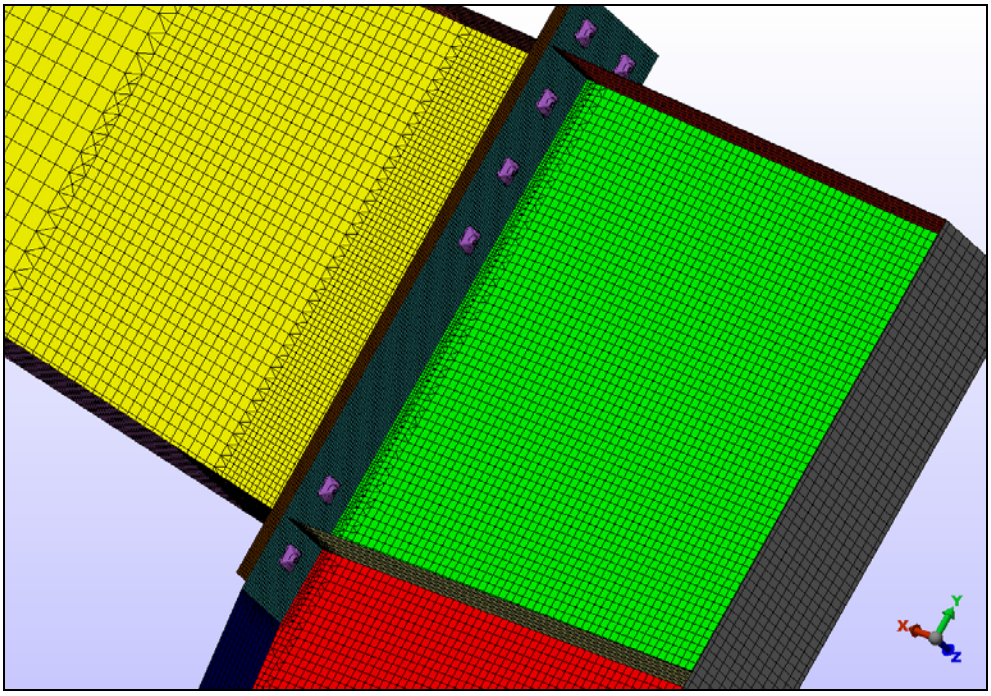

Figure 3.6 Mesh for the knee joint flanges, stiffener, and end plate for frames 1 and 3

Shop fabrication welds between the web, flanges, and stiffeners within the knee joint of the frames were replicated in the model with coexisting or coincidental nodes between adjoining plate elements. Element nodes located in gaps between shop welds of adjoining plates were simply offset a distance of 0.01 inch. This technique allowed ALGOR™ to correctly represent welded and non-welded areas when formulating the stiffness matrix. Welding details of the knee joint are shown in Figure 3.7.

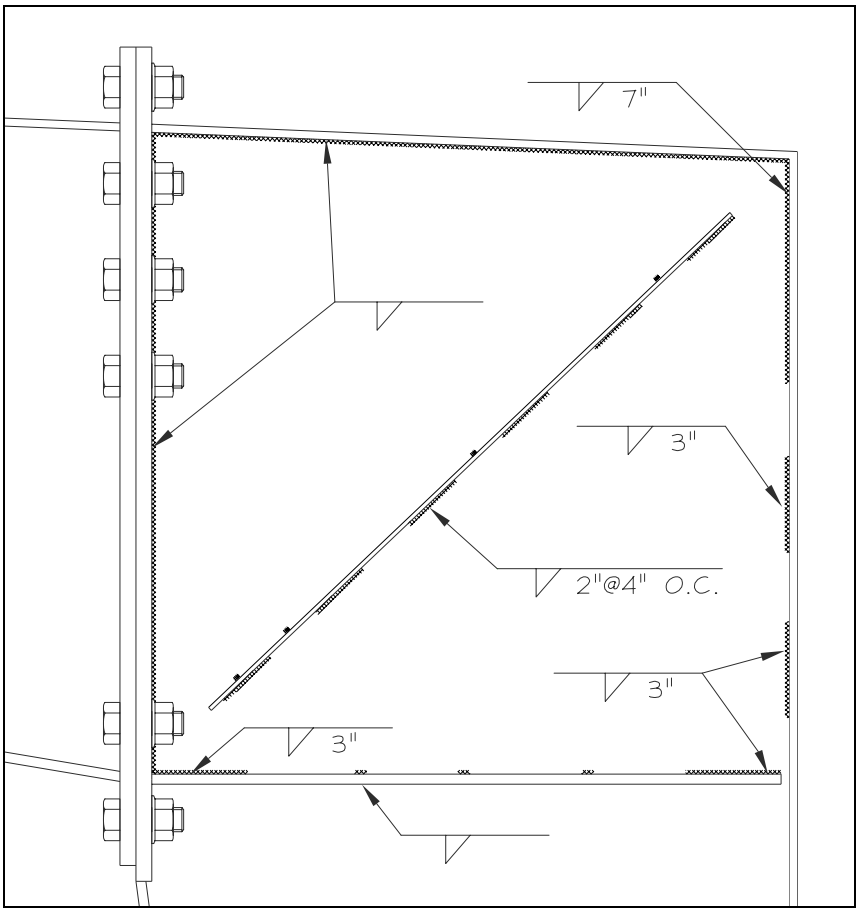

Figure 3.7 Welding details for the knee

Beam elements were used to model the bolts, bolt heads, and nuts. A single beam element, representing the shaft of the bolt, was located at the center of each bolt hole in the end plate (KP RW or KP CW). Since this investigation did not include a study of precise stresses in the bolt, using a single beam element for the bolt shaft reduced the number of elements but still provided a useful check of axial load in the bolt. Bolt stress could be estimated with the axial load and area of the bolt shaft. The bolt shaft was held in position with 24 additional beam elements, each individually extending radially from the end of the bolt shaft to a node of an adjacent plate element of the rafter or column end plate. Bolt heads and nuts were both modeled with this technique and are depicted in Figure 3.8. This technique is one of several recommended approaches found in the ALGOR online tutorials for modeling connections. [6]

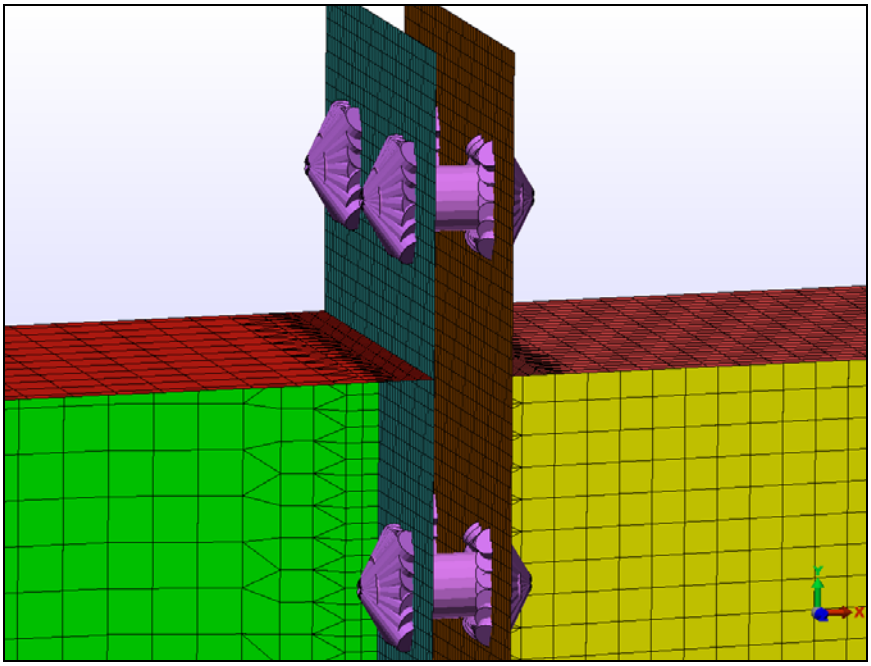

Figure 3.8 Beam elements used to represent bolt, bolt heads, and nuts

Gap elements are a useful modeling tool that ALGOR provides for elements making contact with each other during a linear static stress analysis. Gap elements can be used to model the effects of a spring (compression only) or cable (tension only) where the assigned stiffness is not always present and is a function of the magnitude and direction of the load. These two node elements do not transfer any load until displacement of their nodes are initiated from an adjacent plate or solid element. They force the solution to become an iterative process. Until deflections are calculated, it is not known which gap elements are in contact. However, deflections are influenced by the quantity and locations of those gap elements in contact. Therefore, ALGOR's iterative process is the following: [5]

1) Determine which gap elements are in contact on the first iteration

2) Calculate deflections

3) Determine which gap elements would have been in contact

4) Add these additional gap elements to the solution

5) Repeat the process until all gap element status is constant

Clearly this process can be taxing on processing time. As a result, gap elements were strategically placed to ensure proper interaction between the two members. Placement of the gap elements was determined with a level of assurance that the column and rafter plate elements were transferring compressive forces while limiting individual, non-composite movement of a single plate element between contacting members. Specifically, 1,974 nodes of the total 9,907 nodes were connected to gap elements. Although connecting all 9,907 nodes would have been an accurate representation, the

iterative solving process would have been grossly inefficient. Therefore, gap elements were strategically placed and located more densely in regions prone to compression. This approach of using plate, beam, and gap elements to model the bolted moment connection adequately represented the structural response and significantly reduced computation time over the more conventional method of using brick or solid elements. Figure 3.9 shows gap elements connecting the column and rafter end plates.

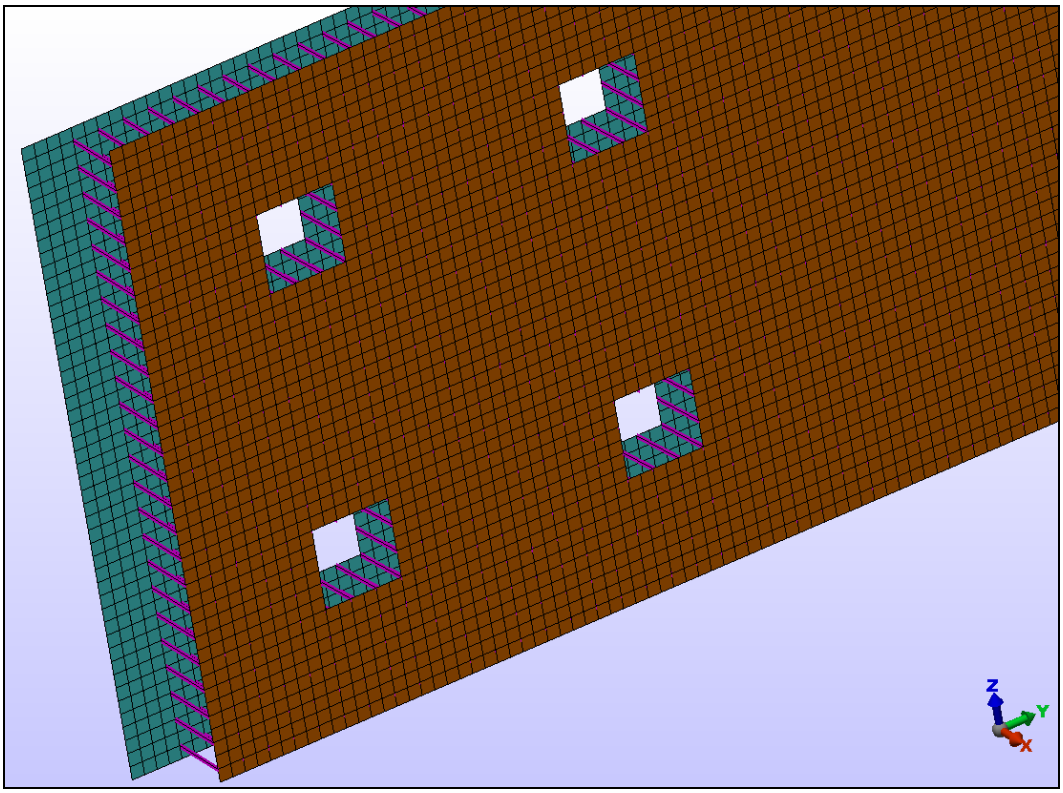

Figure 3.9 Gap elements connecting the column and rafter end plates

During the modeling process, several iterations were conducted to determine the optimum mesh refinement. The final mesh is a result of this process. Upon completing the final mesh, FEMPRO (ALGOR's graphical preprocessor), checks model geometry

and provides several element geometric properties. This function is a useful tool to identify any final adjustments or problem zones with the mesh. The final mesh aspect ratios are shown in Figure 3.10 and Figure 3.11. Figure 3.12 and Figure 3.13 show maximum and minimum node angles for the model. Table 3.1 is a summary of model components, element types, and final element totals for each component.

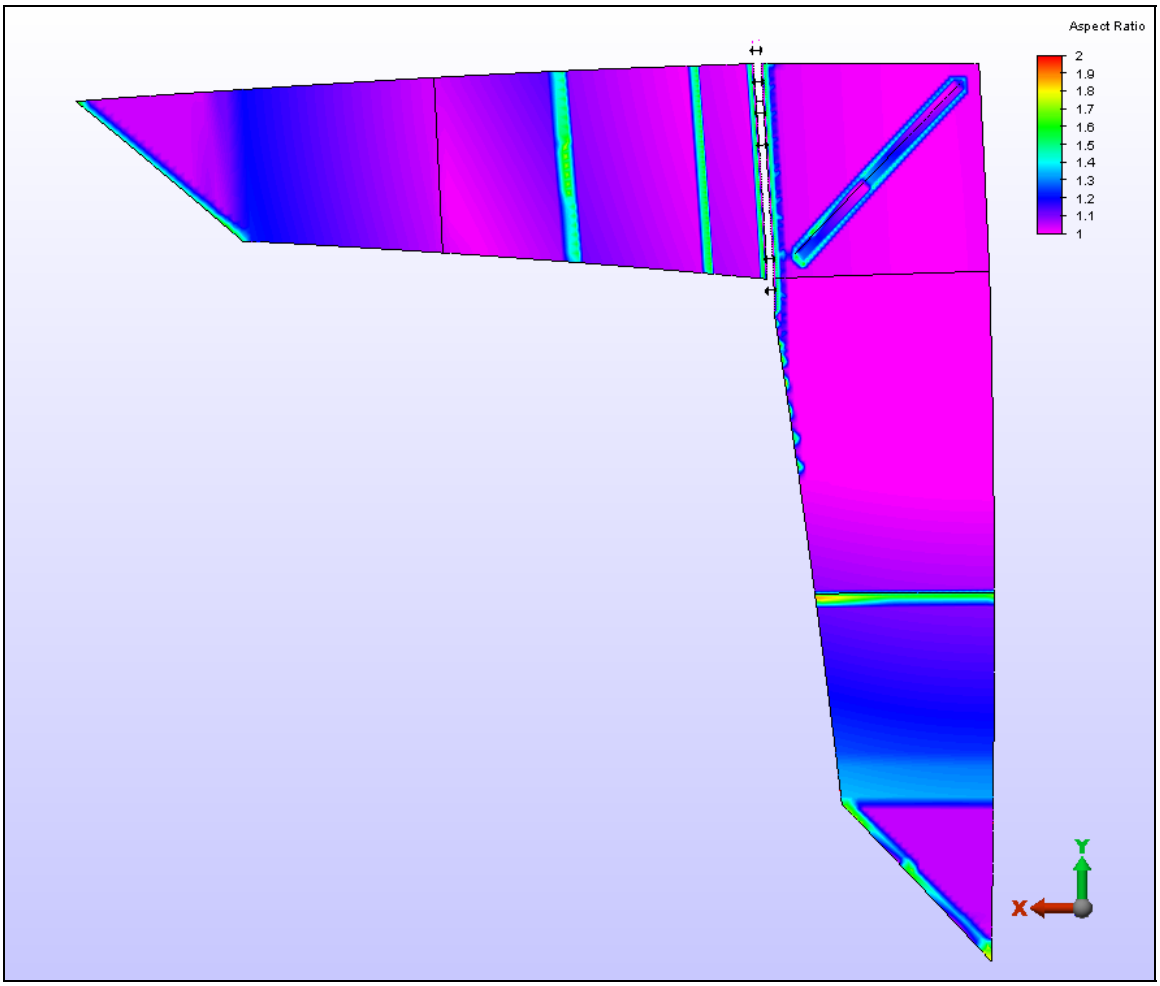

Figure 3.10 Aspect ratios of the web, values range from 1.0 to 2.0

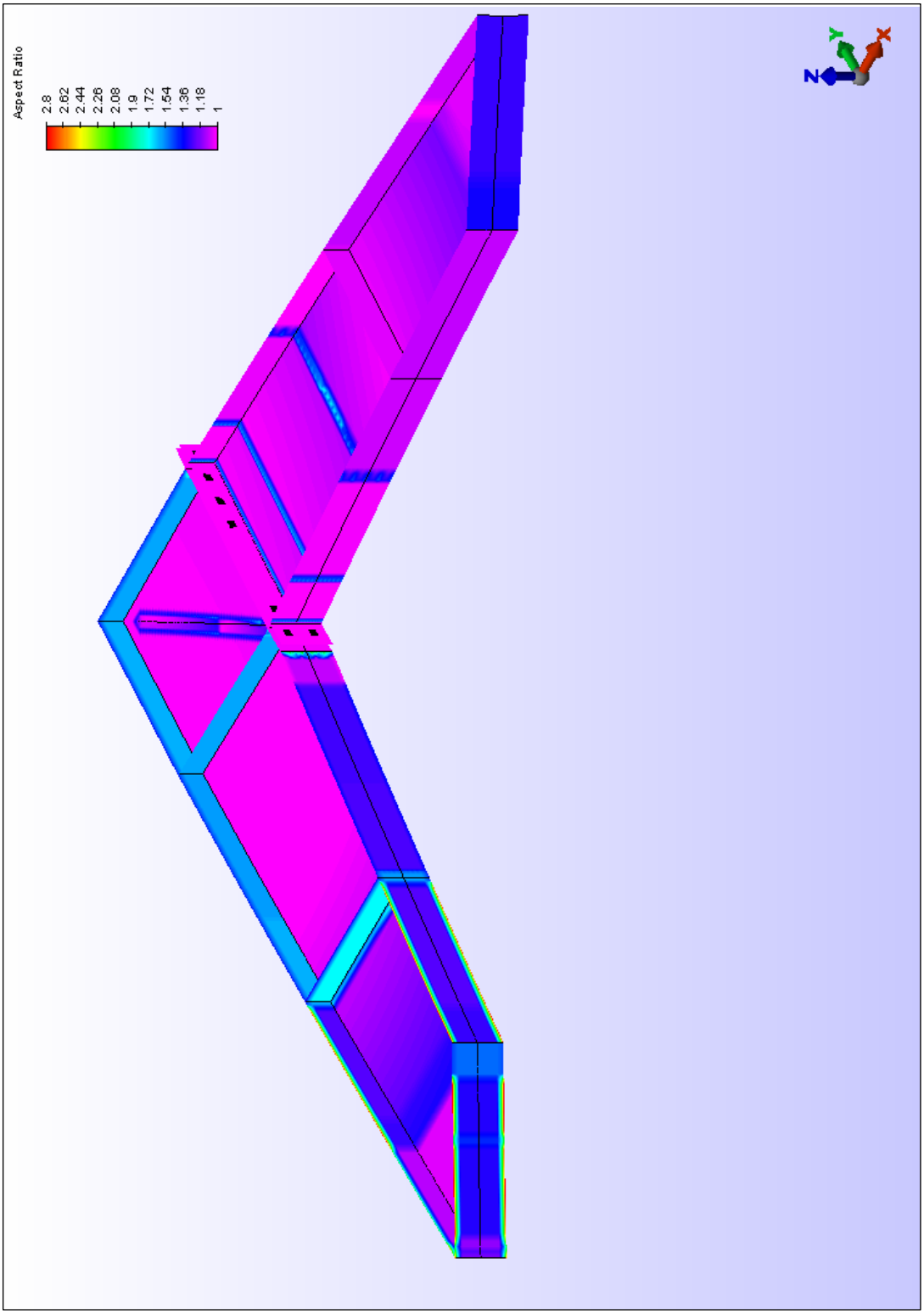

Figure 3.11 Aspect ratios of flanges and stiffeners, values ranging from 1.0 to 2.8

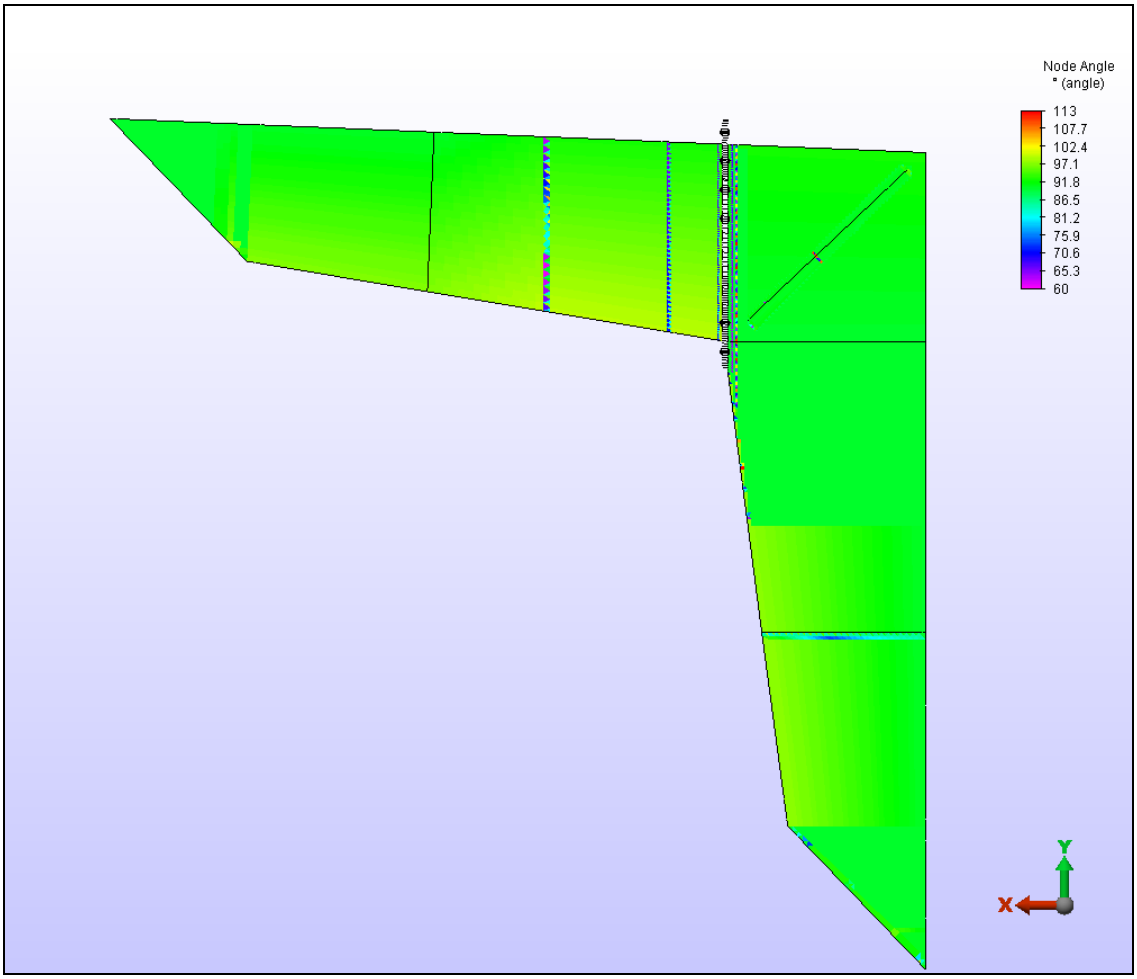

Figure 3.12 FEMPRO node angle results

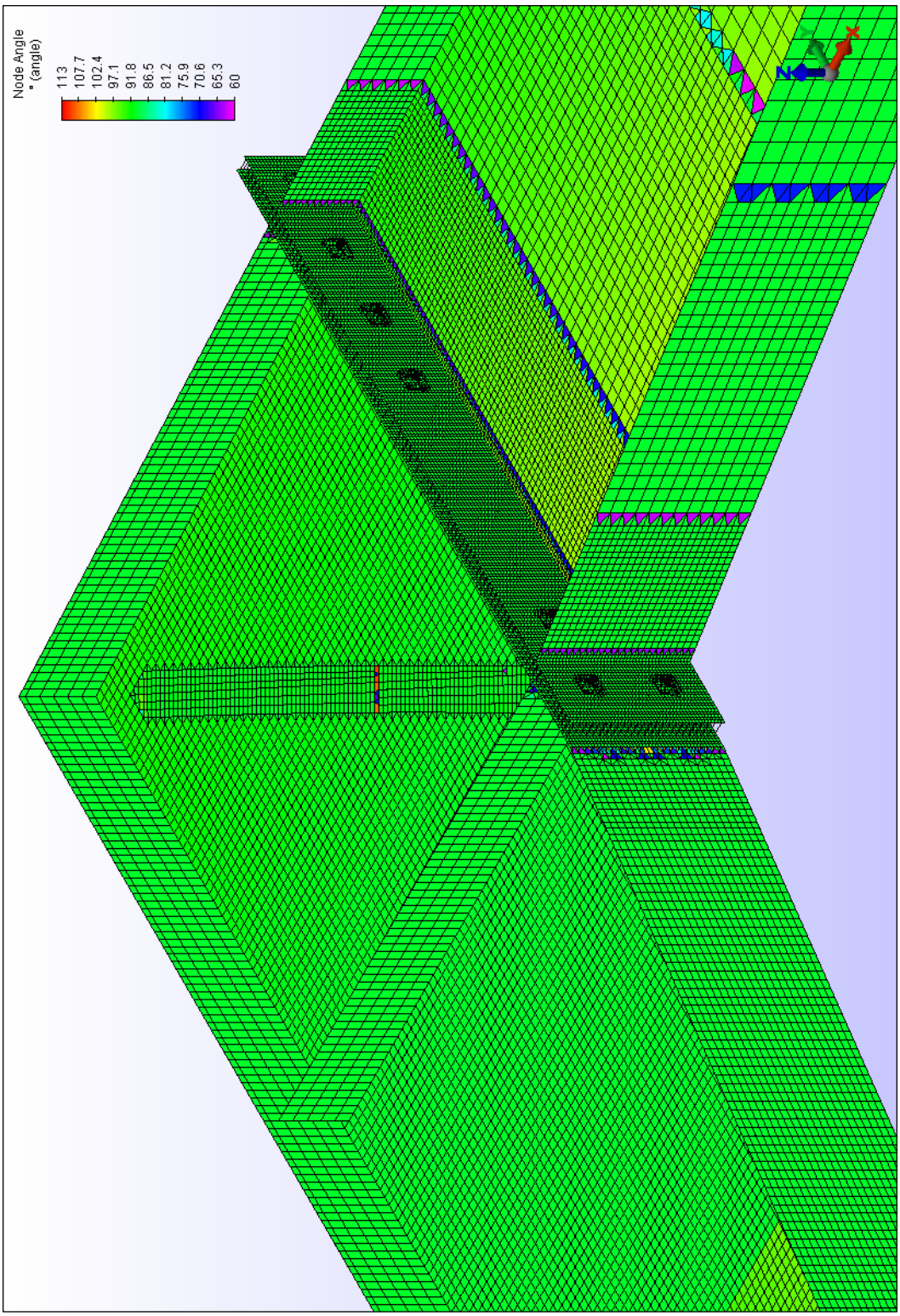

Figure 3.13 FEMPRO node angle results for flanges, stiffeners, and end plates

Table 3.1 Summary of FEA model components

Component Name	Description	Element Type	# of Elements
CW knee web	Col. knee web	Plate	4387
CW col.	Col. web	Plate	6257
RW	Rafter web	Plate	4383
KP CW	Col End Plate	Plate	9728
KP RW	Rafter End Plate	Plate	9536
CTF	Col. top flange	Plate	882
COF	Col. outer flange	Plate	2436
Gap Elements	Compression elements	Gap	630
Primary Gap Elements	Compression elements	Gap	1344
CIF	Col. inner flange	Plate	2254
XP	Loading plate	Plate	576
CST1	Col stiffener #1	Plate	636
CST2	Col. stiffener #2	Plate	802
CST3	Diagonal stiffener	Plate	1023
RTF	Rafter top flange	Plate	1452
RBF	Rafter bottom flange	Plate	1284
RST1	Rafter stiffener	Plate	168
Bolts	Bolts	Beam	12
RW Spokes	Bolt head	Beam	288
CW Spokes	Nut for bolt	Beam	290
		Total =	48,368

3.3 Material Properties, Boundary Conditions, and Loads

Consistent with the material used to fabricate the frames, all plate elements were assigned ASTM A572 material properties. Young's Modulus, yield stress, and ultimate tensile stress were adjusted to match actual values determined from coupon tension tests. Coupon test data is presented in Appendix B. Bolts used for all frames were ASTM A325; however, the ALGOR™ material models have a limited selection of available similar material. Again, since bolts were not an intended topic of study for this experiment, ASTM A514 was selected for all bolts, bolt heads, and nuts. ASTM A514 was selected for its higher yield stress, and somewhat similar properties, among other available material in ALGOR™. After each analysis, the stress in bolts was checked to ensure values were well below the yielding limit. Each of the 24 beam elements that comprised a single bolt head or nut was given an arbitrary diameter of 0.5". Obviously, the intention was to have the bolt, bolt head, and nut significantly capable of transferring load to the plate elements, the intended subject of investigation. As previously discussed, loads were transferred between the column and rafter end plates with gap elements. ALGOR™ provides four options for gap elements: [5]

1) Compression only with a gap
2) Compression only without a gap
3) Tension only with a gap
4) Tension only without a gap

Since the column and rafter end plates were initially in contact and load transfer would occur immediately, compression only without a gap was selected. During development

of the model mesh, a 0.1 inch gap was intentionally left between the two end plates. Therefore, gap elements were set precisely as 0.1 inch long with an arbitrary stiffness of 1,000,000 lbs/in, guaranteeing immediate transfer of compressive loads while disregarding any tensile loads transferred exclusively by the beam elements representing the bolts.[1]

Boundary conditions were selected and applied to replicate experimental conditions. As seen in Figure 3.14 and Figure 3.15, the intersection of the column outer flange and the adjacent support plate (XP) was fixed in all six degrees of freedom, global X, Y, and Z translation and X, Y, and Z rotation. Although the frames were not entirely restrained in all six degrees of freedom, this boundary condition was required to stabilize the model to successfully run the analysis. The intersection of the rafter top flange and adjacent loading plate (also noted as XP) was restrained only against translation in global Z direction. As presented in the preceding chapter, the frames were restrained from lateral translation by independent guide angles (see Figure 2.8). This condition was duplicated in the model with a boundary restraint in the global Z direction and was applied to only five nodes on each side along the outer edge of the flange. Boundary conditions can be seen in Figures 3.14 and 3.15, where FEMPRO uses a triangle to represent restraint for all six degrees of freedom and a circle to represent restraint in the Z direction.

Loading of the model was simply a concentrated nodal load applied to the intersection of the rafter web, rafter top flange, and loading plate, XP. The load was applied parallel to both the loading and support plates denoted as XP. ALGOR™ offers

an option for multiple load cases in a single analysis; however, the iterative processes required for gap elements conflict with this option. Therefore, upon completing a successful model run, the results were saved, and the magnitude of the concentrated load was increased for the next analysis.

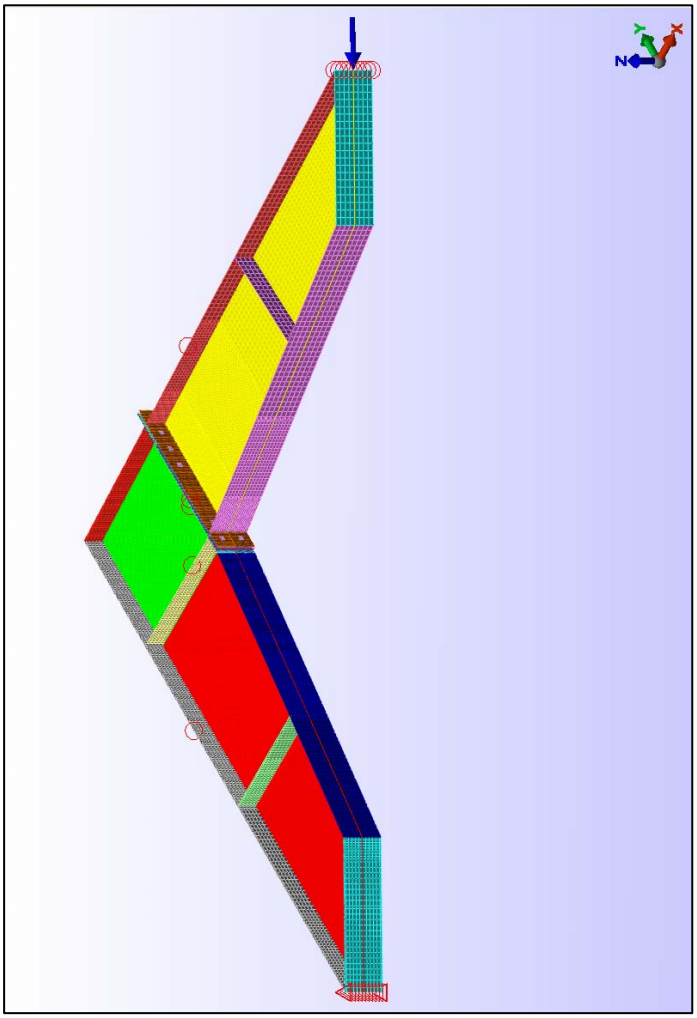

Figure 3.14 Boundary conditions and concentrated nodal load

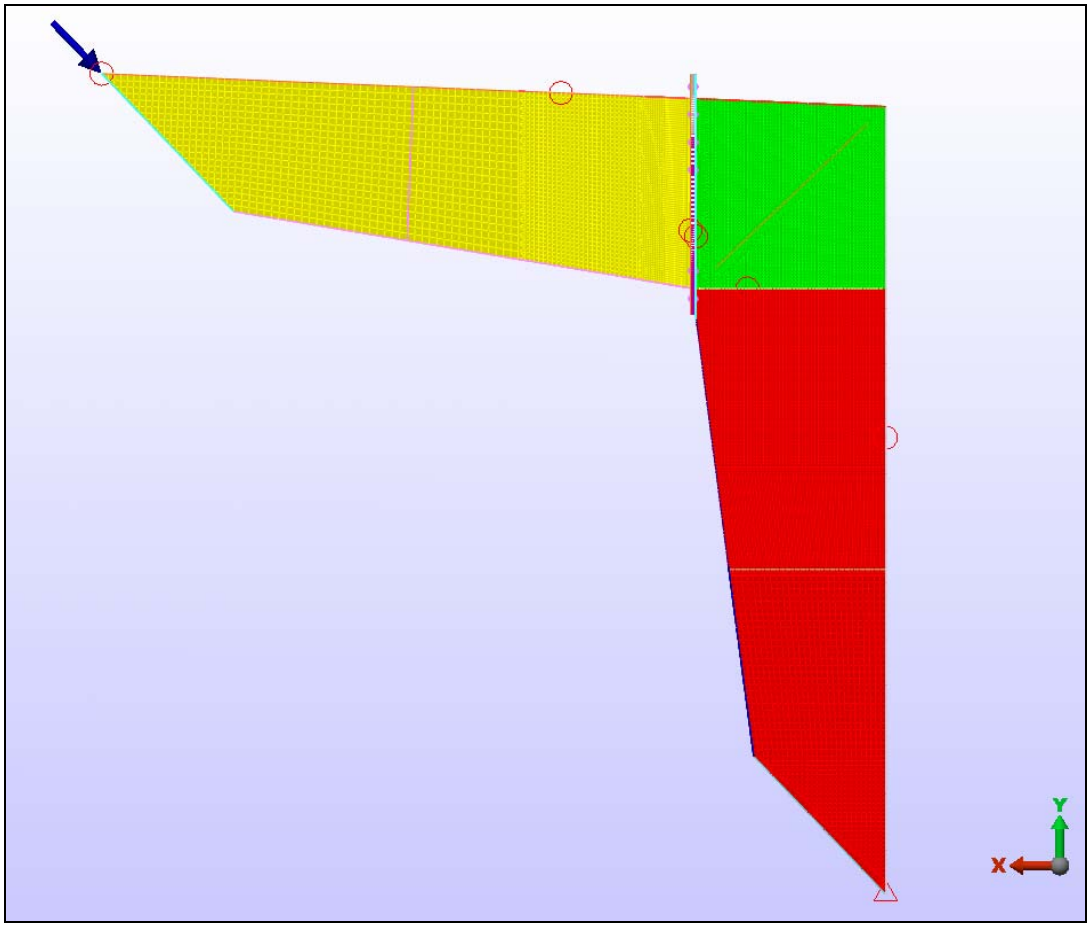

Figure 3.15 The model is ready for analysis

CHAPTER IV

RESULTS

4.1 Experimental Results

Data collected during the laboratory experiment are presented in Appendix C. Sample calculations and all calculated values are tabulated in Appendix C as well. This chapter will present further analysis of this data and discuss results of each test frame, resulting failure modes, and observed influence of the test variables between different test frames.

All five frames were carefully monitored throughout application of the load, and were loaded to a point of obvious failure. Figures 4.1 through 4.5 show graphical plots of collected strain data versus associated load. To help demonstrate the relative performance between frames, all five graphs maintain the same scale and range of values for both vertical and horizontal axes. To simplify the graphs, absolute values were used for compressive strain and are noted on graphs where applicable. Furthermore, strain is always noted as "1E-6 in. / in." and load is shown as "pounds." Strain gage locations are shown in Figure 2.9 through Figure 2.12. However, "G1" is always located at the centerline of the rafter flange, 6 inches inside the knee; and "G2" is always located at the centerline of the column flange, 6 inches above the horizontal stiffener of the knee. "G3"

through “G7” are rectangular rosettes at the center of the web, or the centroid of the lower triangle formed by the diagonal stiffener.

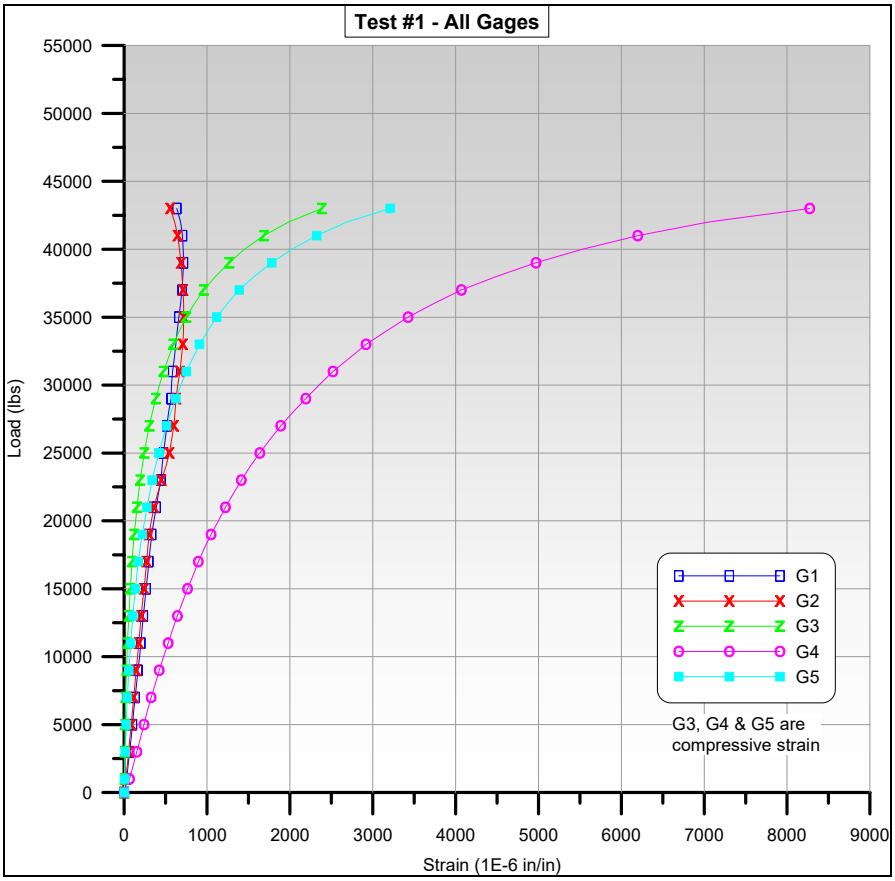

Figure 4.1 Measured strain data versus load for frame 1

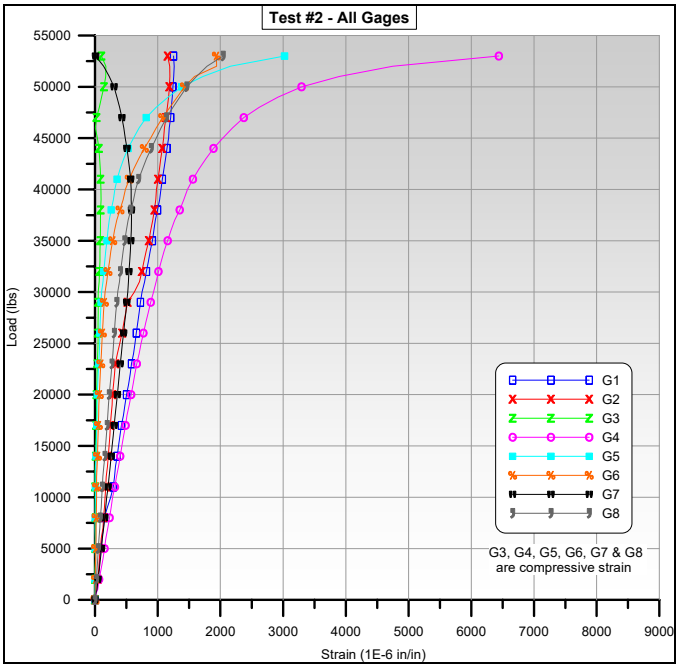

Figure 4.2 Measured strain data versus load for frame 2

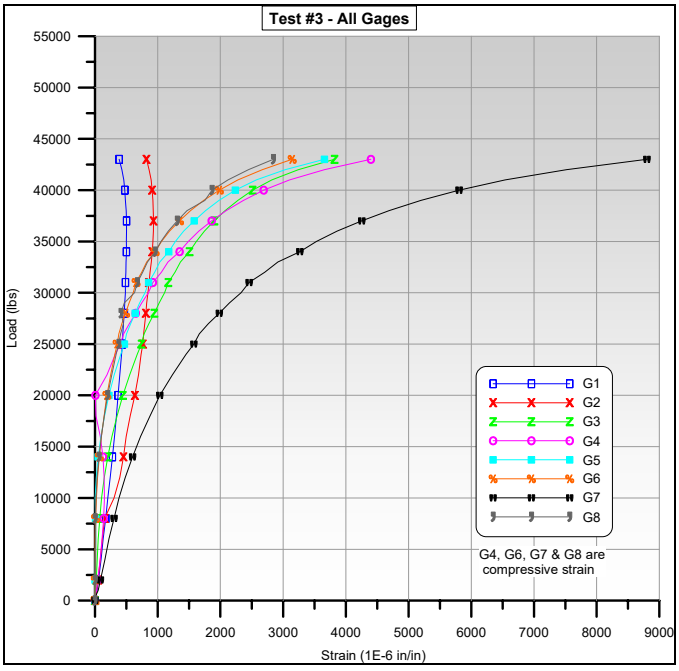

Figure 4.3 Measured strain data versus load for frame 3

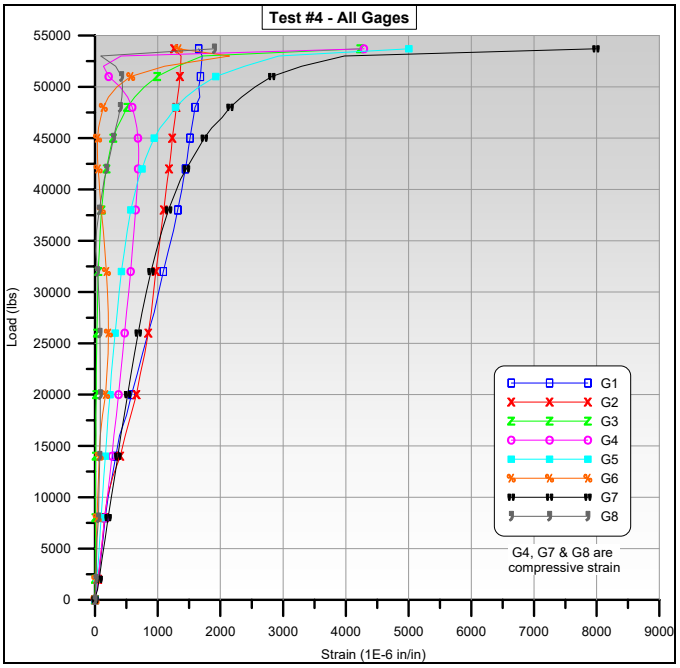

Figure 4.4 Measured strain data versus load for frame 4

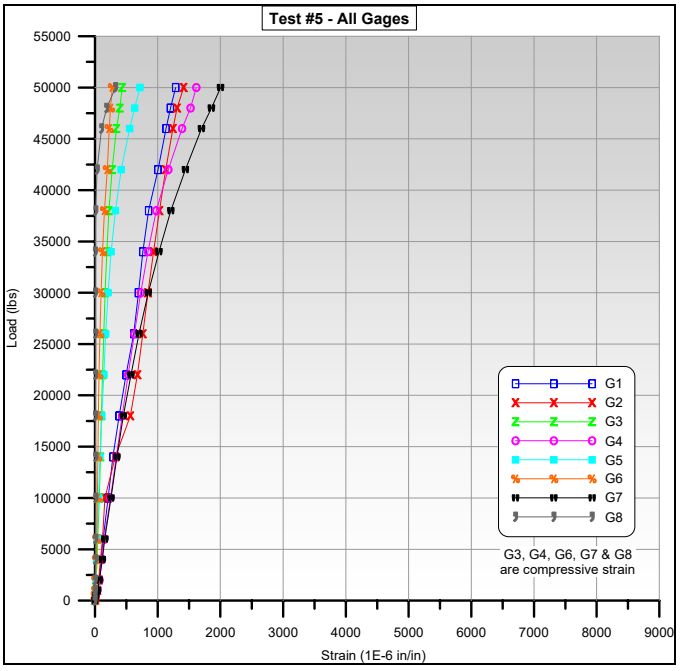

Figure 4.5 Measured strain data versus load for frame 5

The knee web of frames 1 and 3 began to show signs of buckling under a load of approximately 36 kips. Frame 1 had clearly buckled at 43 kips and beyond that, could not adequately support additional load. Similarly, frame 3 experienced buckling in the knee web under a 45 kip load and could not support additional load beyond 45.9 kips. Figures 4.1 and 4.3 support this as gage 3, 4 and 5 (the 0, 45, and 90 degree components of the three element rectangular strain gage rosette at the center of the knee web for frame 1) and gage 6, 7 and 8 (the 0, 45, and 90 degree components of the strain gage rosette at the center of the knee web for frame 3), clearly began to undergo much more significant strain under increasing load while gages 1 and 2 (rafter flange and column flange for frames 1 and 3) continue to maintain a constant linear increase in strain before the knee web buckled. Figures 4.6 and 4.7 are photos that show buckling of the knee web of frames 1 and 3, respectively. The theoretical investigation of the knee web, as presented in Appendix A, predicted shear web buckling to occur under a 15.3 kip load. As stated in Appendix A, this buckling load will occur if lateral restraint of the knee web is not provided. Clearly, frames 1 and 3 do not have any lateral restraint for the knee web. However, AISC also allows for an exception to exceed this shear web buckling limit, provided criteria are met for tension field action. As shown in Appendix A, tension field action will increase the limitation of a shear web buckling load to 35.9 kips. This provision of tension field action clearly agrees much better with the experimental results and observed buckling in the knee web.

In contrast, frames 2, 4, and 5 performed significantly different. The diagonal stiffener provided the required minimal restraint to prevent lateral translation of the knee

web. This is observed in Figures 4.2, 4.4, and 4.5. Strain gages oriented at a forty five degree angle and located in the middle of the knee web (G4 for frames 1 and 2, and G7 for frames 3, 4 and 5) show a reduction in strain, compared to frames 1 and 3, in the region prone to buckling. This is more easily seen in Figure 4.8, which compares this individual gage for all five tests.

Figure 4.6 Buckling in knee web of frame 1 (frame 3 was identical)

Figure 4.7 Buckling in knee web of frame 3

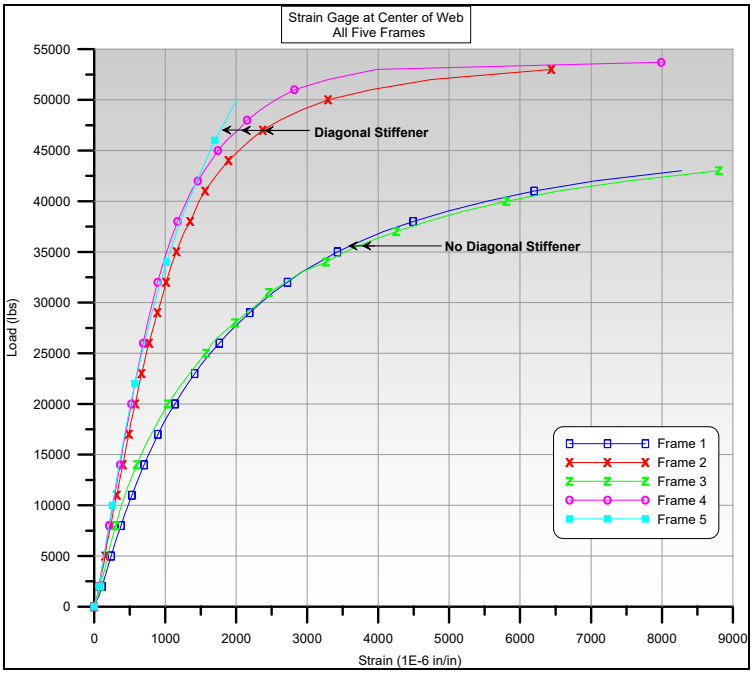

Figure 4.8 Comparison of individual strain gage at the center of web and oriented parallel to the direction of the diagonal stiffener (when present) for all five frames

Using data provided by the three components of the strain gage rosette located at the center of the web, shear strain can be calculated (see Appendix C). Further influence from the diagonal stiffener is seen in Figure 4.9, which shows this same trend, but in terms of measured shear strain versus load for each test. Assuming a state of plane stress and given the focus of pre-mature buckling of the knee web while still in the linear elastic region, Hooke's law for a linear homogeneous, isotropic material is used to solve for stresses (also see Appendix C). Figure 4.10 shows a calculated maximum shear stress at the location of the strain gage rosette in the center of the knee web for each frame.

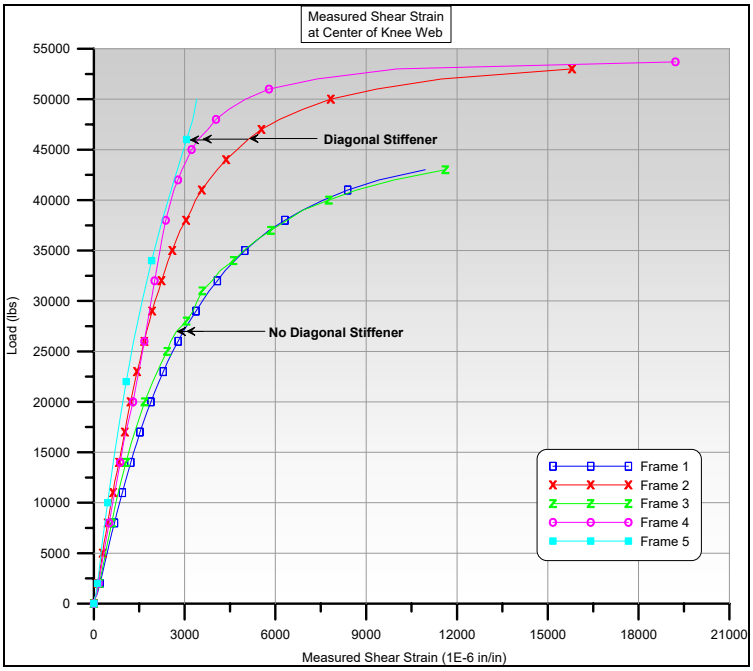

Figure 4.9 Measured shear strain at center of knee web for all five frames

As shown in these graphs, the knee web of frames 2, 4, and 5 were adequately restrained from buckling. Furthermore, Appendix A suggests that if the knee web is sufficiently restrained from buckling, it would reach a point of shear yielding prior to

experiencing buckling issues in the knee web. This was observed in the laboratory. Both frames 2 and 4 began experiencing shear yielding in the web. However, both frames ultimately failed due to buckling of the column web and flange, below the knee joint. Frame 5, which was identical to frame 4, did not experience shear yielding in the knee web. However, the mode and location of buckling for frame 5 was identical to frames 2 and 4. Buckling occurred before the onset of shear yielding and at a loading that was 2.7 kips less than the buckling load of frames 2 and 4. This can be seen in Figures 4.8, 4.9 and 4.10 when comparing curves for frames two and four to the curve for frame 5. Ultimately, the shortened diagonal stiffener sufficiently restrained the knee web from buckling in frames 2, 4 and 5 and all failed by buckling in the column below the knee joint. Frames 2 and 4 both reached an ultimate load of 53.7 kips before this failure occurred. Frame 5 buckled at 51 kips. Figure 4.11 and Figure 4.12 show pictures the buckling failure of the column web and flange below the knee joint.

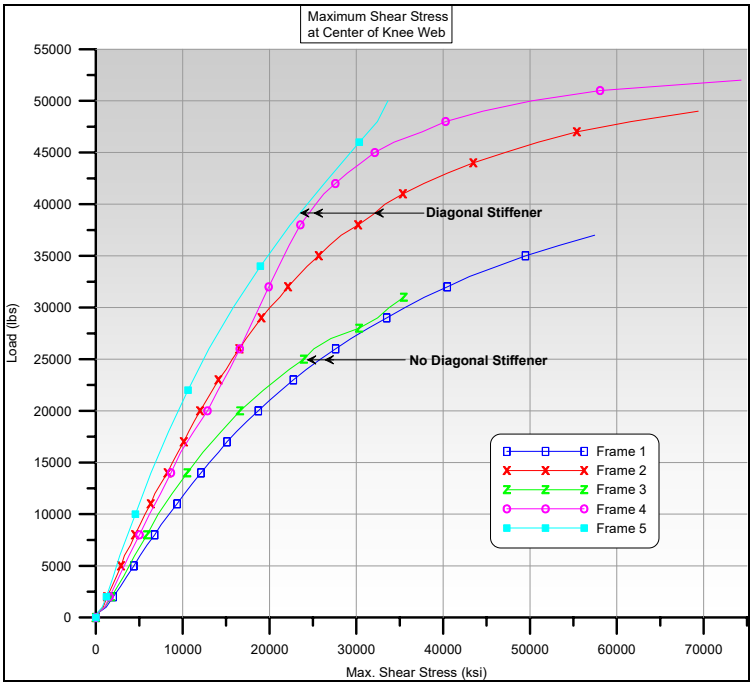

Figure 4.10 Calculated maximum shear stress at center of knee web for all five frames

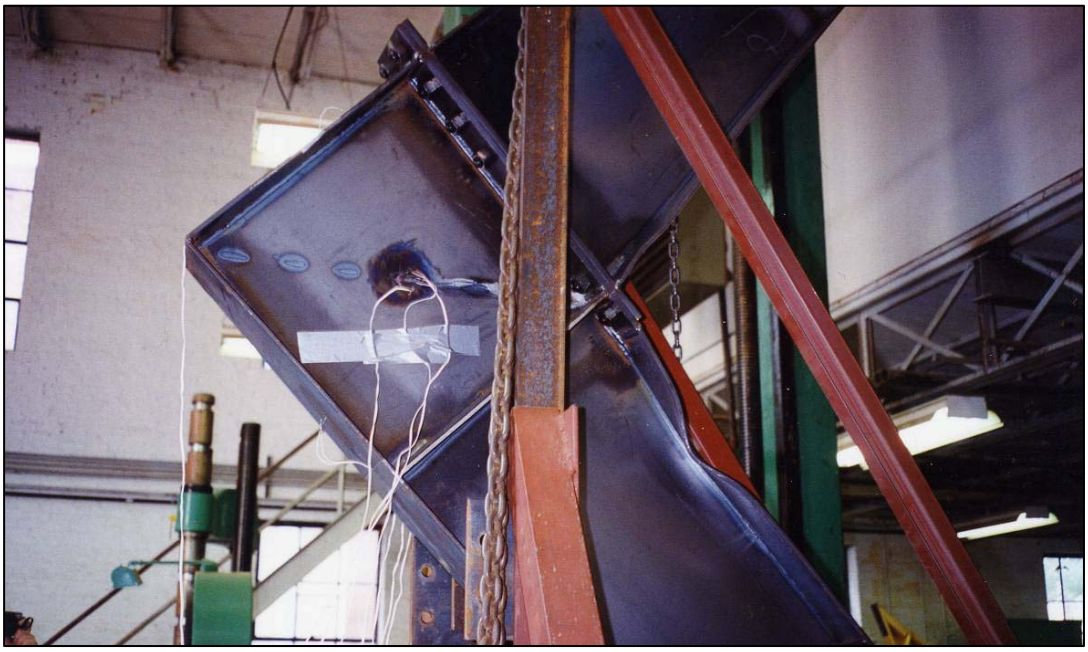

Figure 4.11 Buckling in the column web and flange for frames 2, 4, and 5

Figure 4.12 Close-up view of web and flange buckling for frames 2, 4, and 5

Detaching the horizontal stiffener in the column from the flange appeared to have no or minimal effect on the overall performance of all five frames. Strain data from "G2" on the flange of the column was converted to normal stress using the equation generated from the stress strain curve of the coupon test presented in Appendix B. Figure 4.13 is a comparison of normal stress in the column flange of frames 1 and 3, where the horizontal stiffener is attached to the column flange for frame 1, and it is detached from the column flange for frame 3. Both frames failed by buckling of the knee web and reached approximately the same ultimate load. For the curve representing frame 3, there is a minor shift to higher strains (this occurred under a load of approximately 8 to 10 kips).

This same shift is seen in Figure 4.14, which is the same graph as Figure 4.13, but represents frames 2, 4 and 5. Again, the only difference between frames 2, 4 and 5, is the detached horizontal stiffener from the column flange of frames 4 and 5. Failure mode of these three frames was the same, as was the ultimate load at failure.

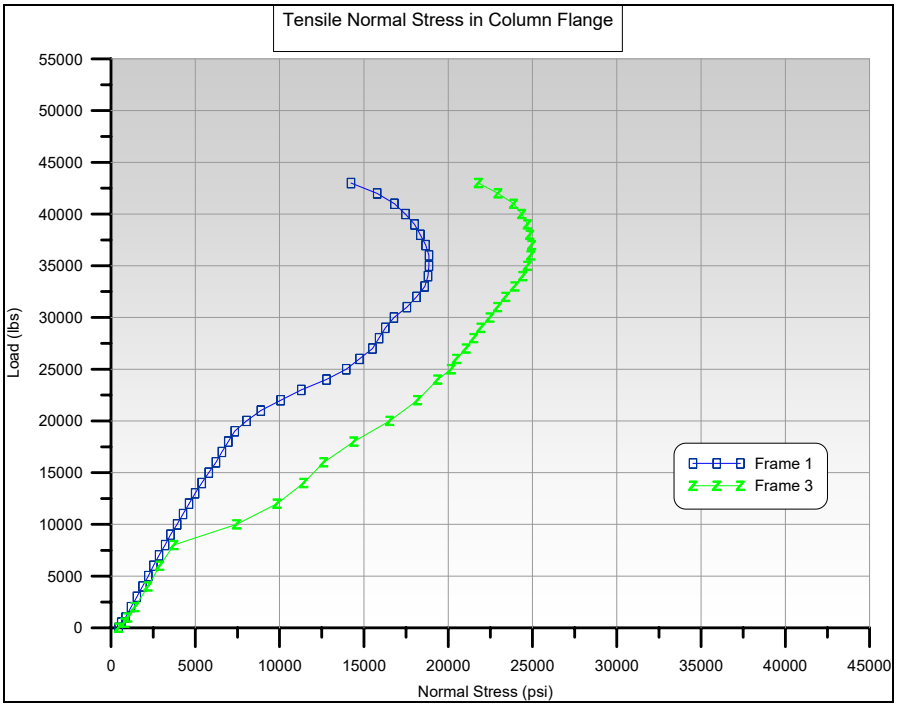

Figure 4.13 Measured normal stresses in column flange, showing effects of a detached horizontal stiffener for frames 1 and 3

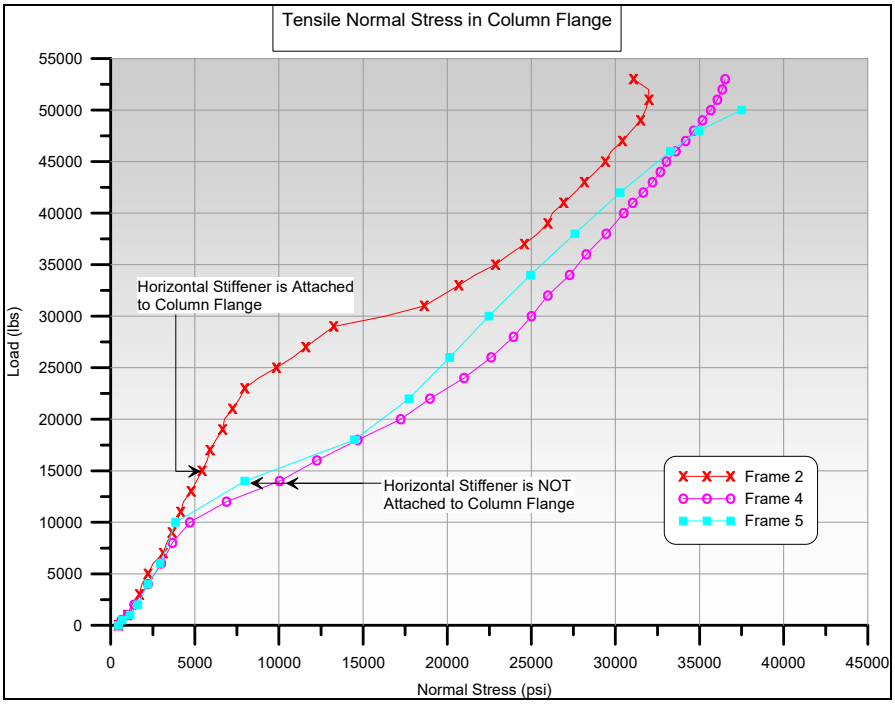

Figure 4.14 Measured normal stresses in column flange, showing effects of detached horizontal stiffener for frames 2, 4, and 5

4.2 Finite Element Analysis Results

To check the overall general validity of the model results, and the general approach to efficiently model the bolted moment connection, Figure 4.15 shows the axial loads for gap elements in frame 4. As depicted in this graphic, the gap elements performed the intended function - to only transfer compressive loads between the rafter end plate (KP RW) and column end plate (KP CW). The compressive loads ranged from 0 to 1000 pounds in compression for an applied load of 40,000 pounds to frame 4. Under this same applied load, frames 1, 2 and 3 performed very similarly. Additionally, bolt axial loads are shown in Figure 4.16, while the associated von Mises stresses for the column end plate are seen in Figure 4.17. Further, Figure 4.18 shows all element node

rotations in the column end plate. As anticipated, larger rotations, higher von Mises stresses and axial loads occur in areas prone to tension and at the interface of the column or rafter flanges and end plates. As a final check for reasonable model results, Figure 4.19 shows the deflected shape of frame 4 at the 40 kip applied load. All of these values appear to be within reasonable limits of expected values.

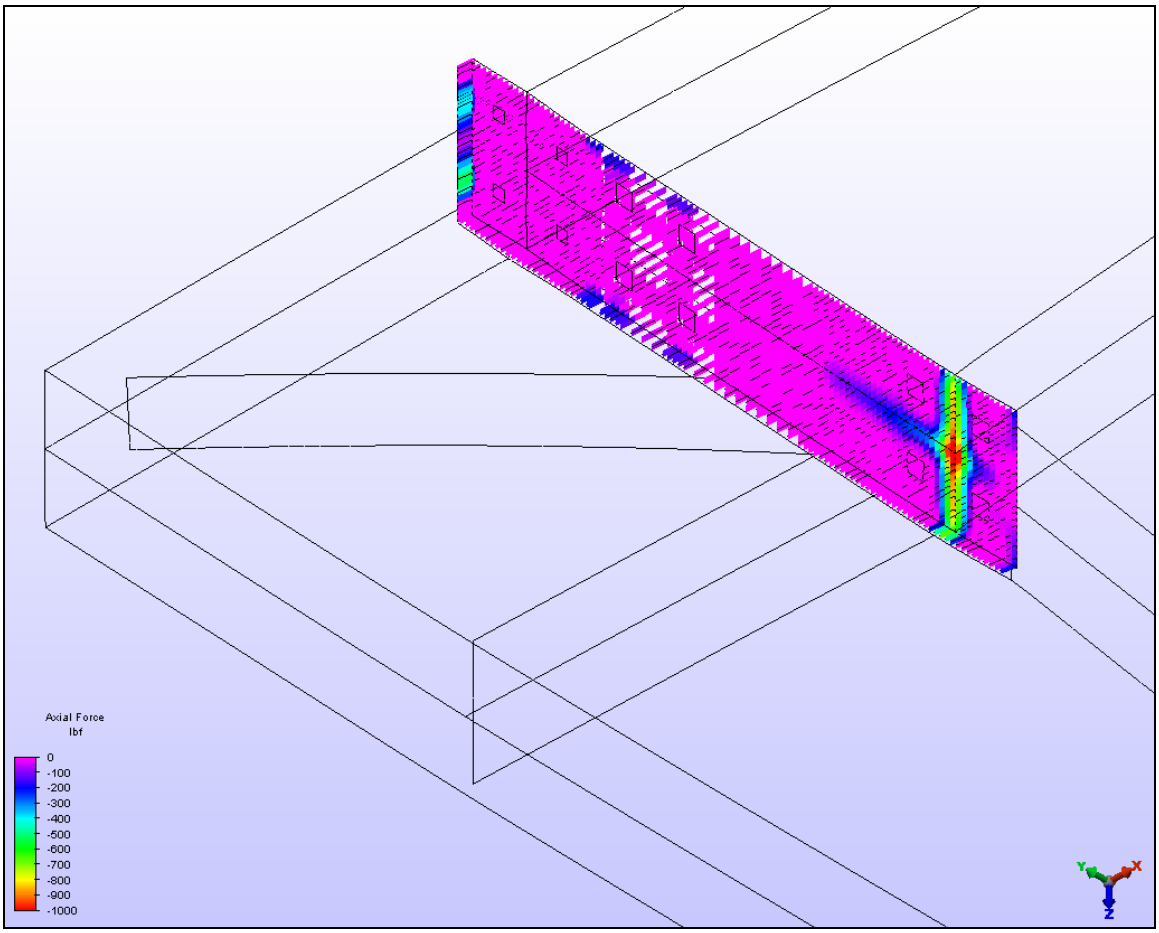

Figure 4.15 Axial loads for the compression only gap elements in frame 4 at a load equal to 40 kips

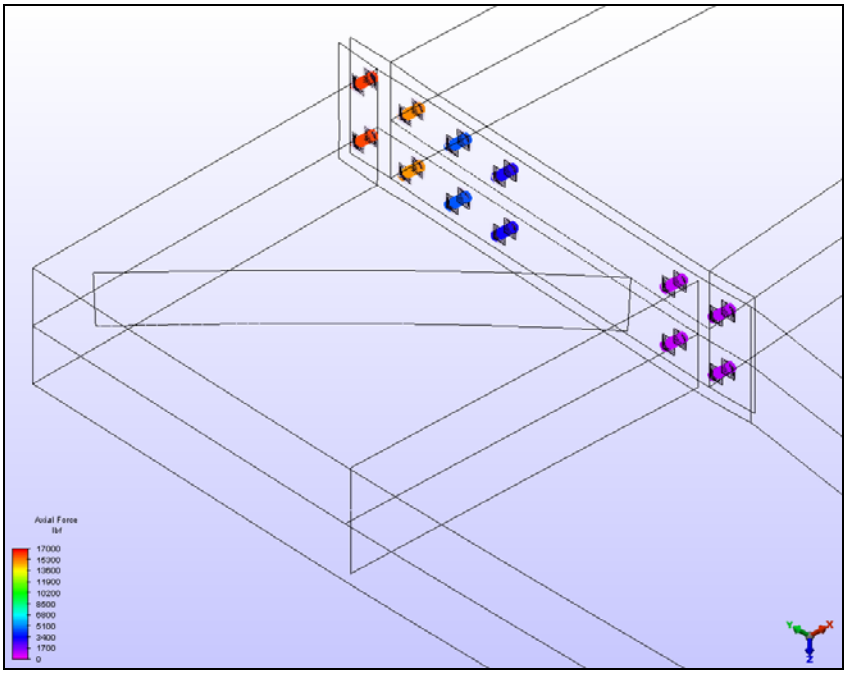

Figure 4.16 Bolt axial loads in the knee joint moment connection for frame 4 at a load equal to 40 kips

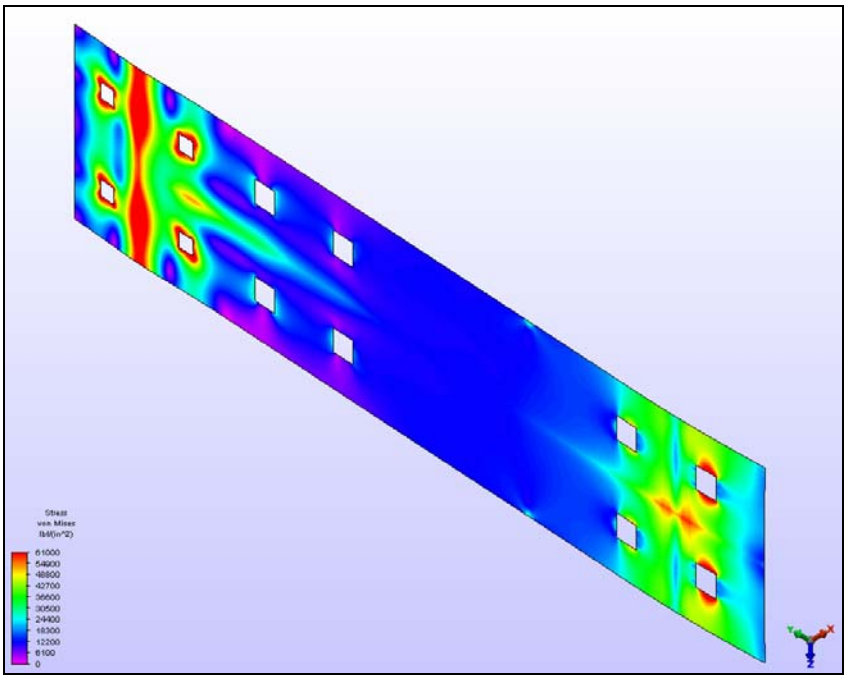

Figure 4.17 von Mises stresses in the column end plate of frame 4 at a load equal to 40 kips

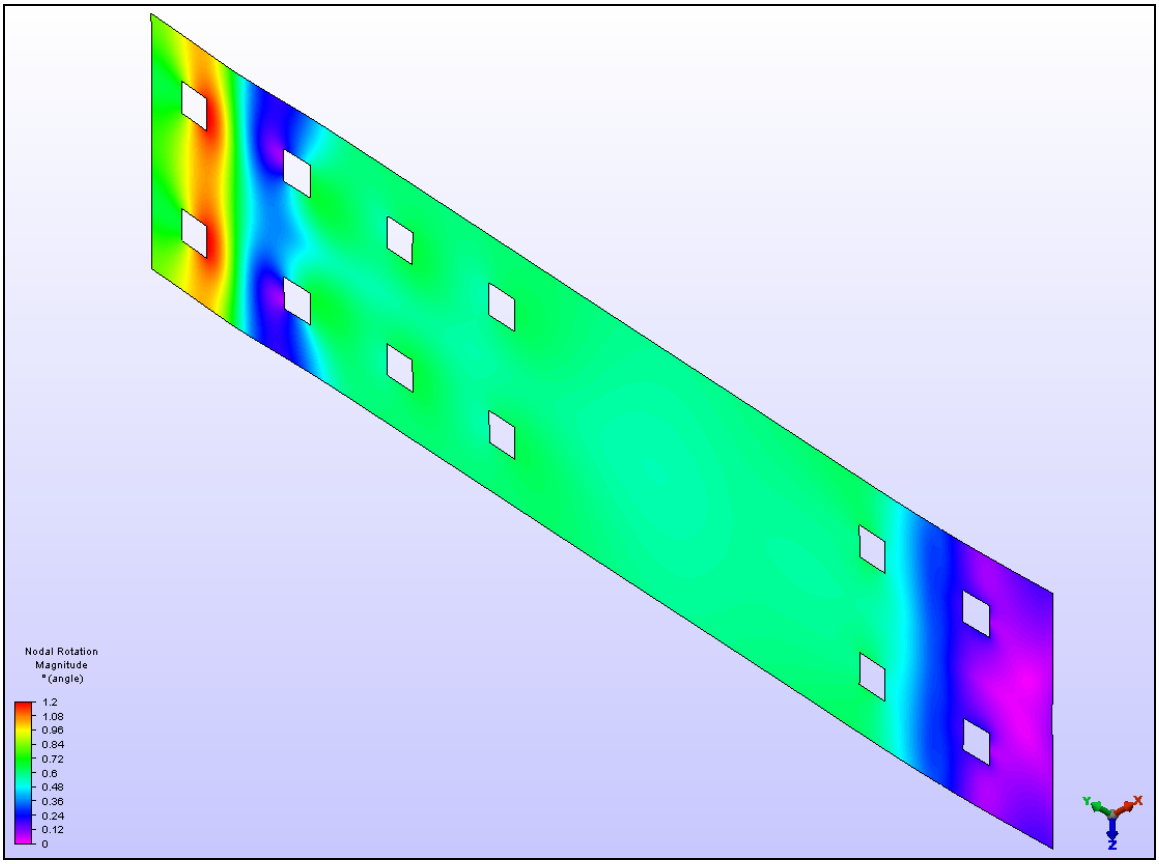

Figure 4.18 Rotation of element nodes in the column end plate (KP CW), frame 4 at a load equal to 40 kips

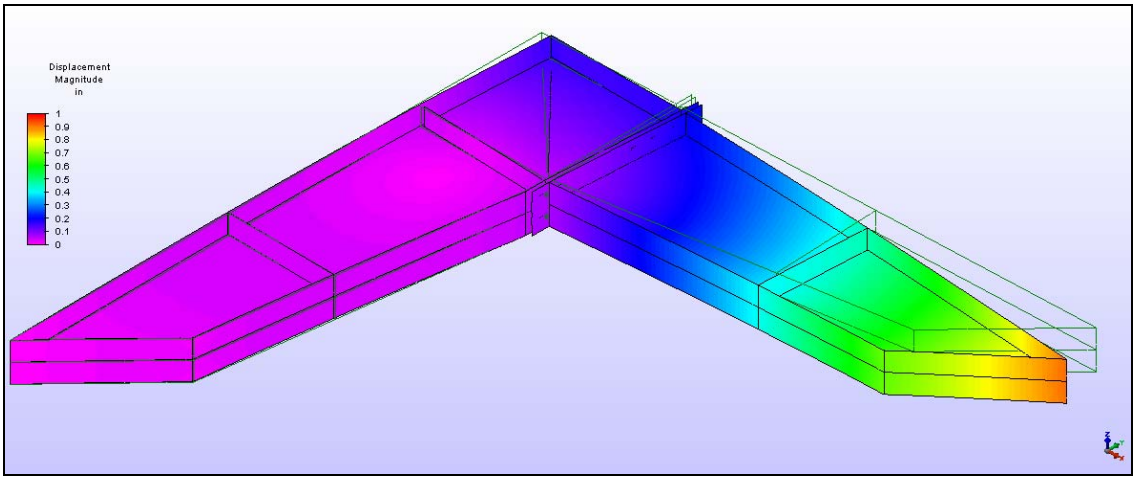

Figure 4.19 Displacement of frame 4 at a load equal to 40 kips (scale factor of 5.0 applied for viewing purposes)

All frames were analyzed with the ALGOR critical buckling load program. During program execution, ALGOR incrementally increases the load until the model becomes geometrically unstable. To prevent enormous processing times, ALGOR does not provide detailed output of stresses during the critical buckling load execution; rather, it provides graphical output of the buckling mode and associated load at an occurrence of buckling. Detailed stresses at the buckling load are then determined from a separate static stress analysis.

Frames 1 and 3 performed identically during the critical load buckling analysis. Figure 4.20 shows the ALGOR predicted buckling mode for frames 1 and 3. As expected, buckling occurred in the knee web. Figure 4.21 shows a close-up view of the buckling shape in the knee web. Buckling occurred under a 29.6 kip load. Figures 4.22 and 4.23 show the associated stresses at this point of instability for frame 1. Figures 4.24 and 4.25 show stresses for frame 3. The analysis reinforces the assumption of premature buckling in the linear elastic region. As seen, stresses are still relatively low at the occurrence of buckling for both frames with a laterally unrestrained knee web.

With a laterally restrained knee web, frames 2 and 4 performed much differently than frames 1 and 3 in the buckling analysis. Most importantly, as seen in Figure 4.26, the shortened diagonal stiffener adequately suppressed buckling in the knee web. Under a 35.7 kip load, the column web (below the horizontal stiffener of the knee joint) buckled, as well as the column inner flange. Figures 4.27 and 4.28 show the stresses at the point of buckling in frame 2, while Figures 4.29 and 4.30 show the associated stresses in frame 4 and 5.

An additional FEA buckling analysis was conducted on frames 2 and 4. The length of the diagonal stiffener was varied from 22.5 inches long to 7 inches long. The purpose of this analysis was to determine the minimal length of diagonal stiffener that would still adequately prevent buckling of the knee web. The results are presented in Appendix E.

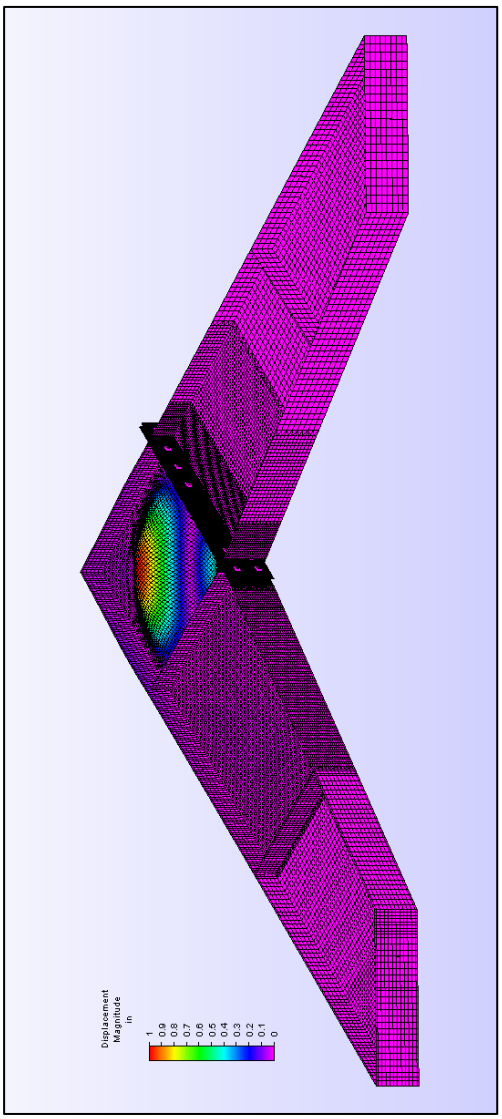

Figure 4.20 FEA buckling in knee web of frames 1 and 3 at a load equal to 29.6 kips

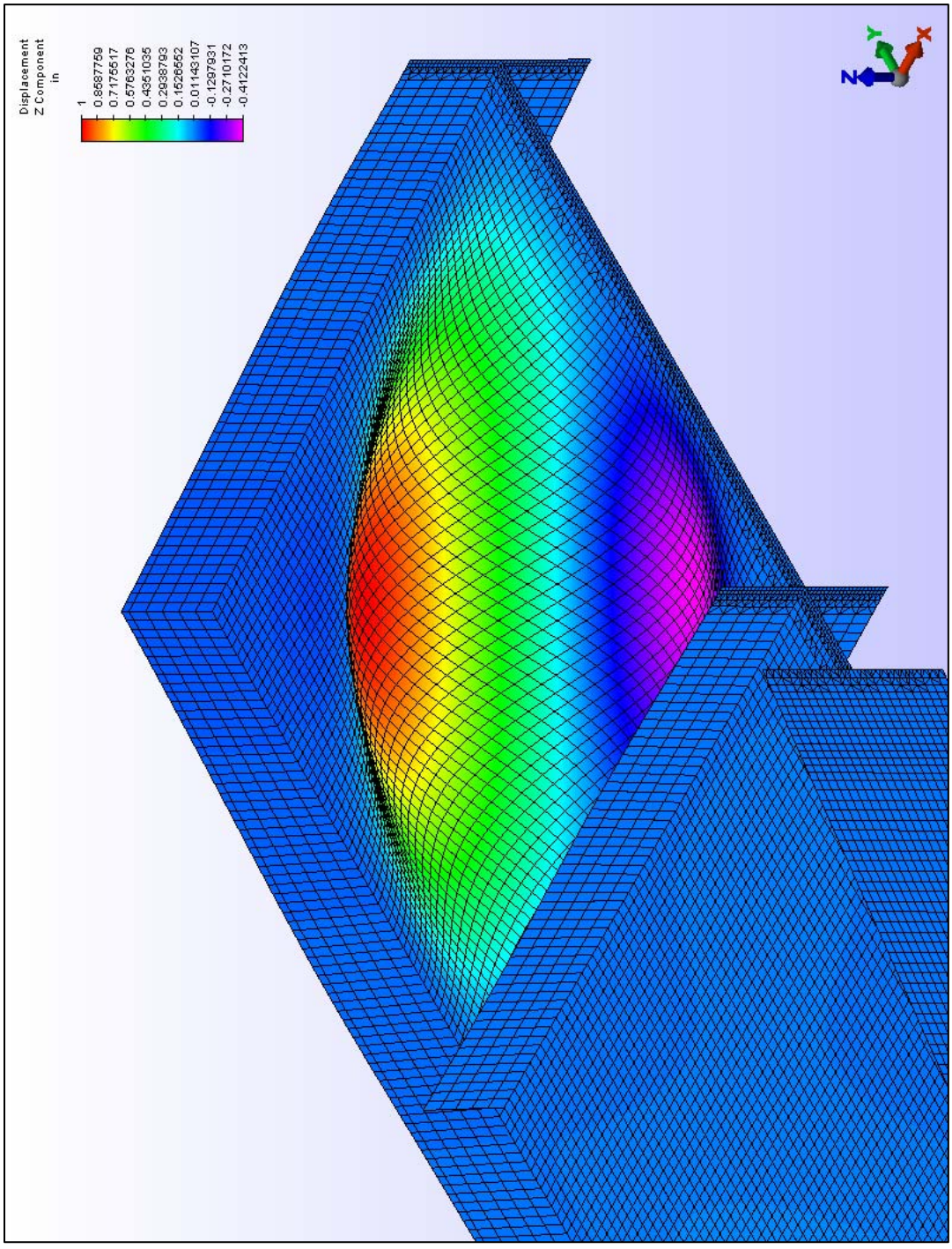

Figure 4.21 Close-up view of the buckled knee web of frames 1 and 3, occurring under a a load equal to 29.6 kip (rafter and end plates were removed for viewing purpose)

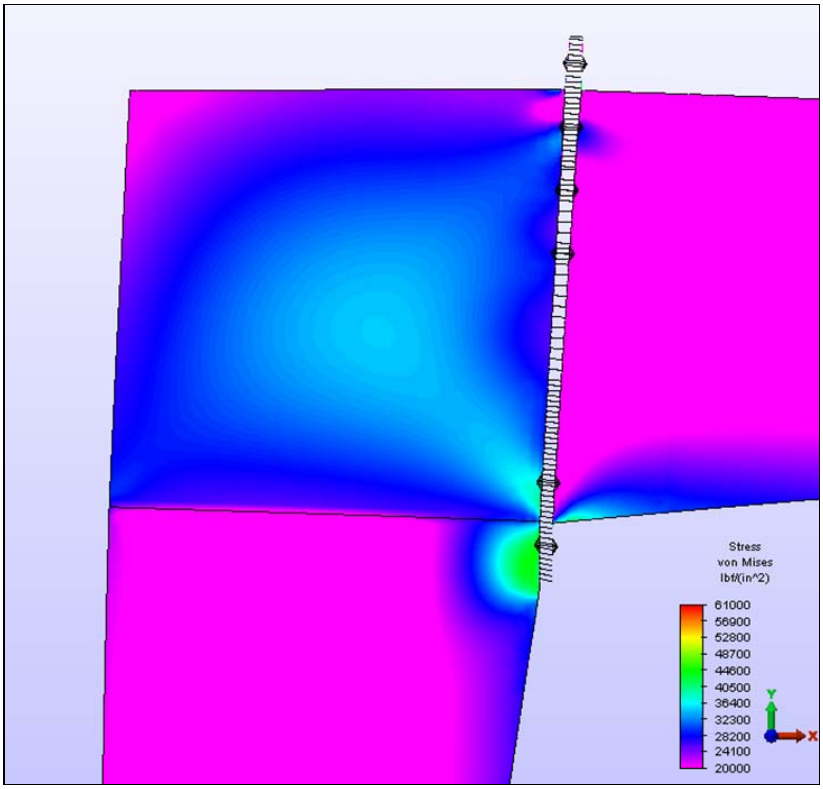

Figure 4.22 Frame 1 von Mises Stress in knee web at the buckling load of 29.6 kips

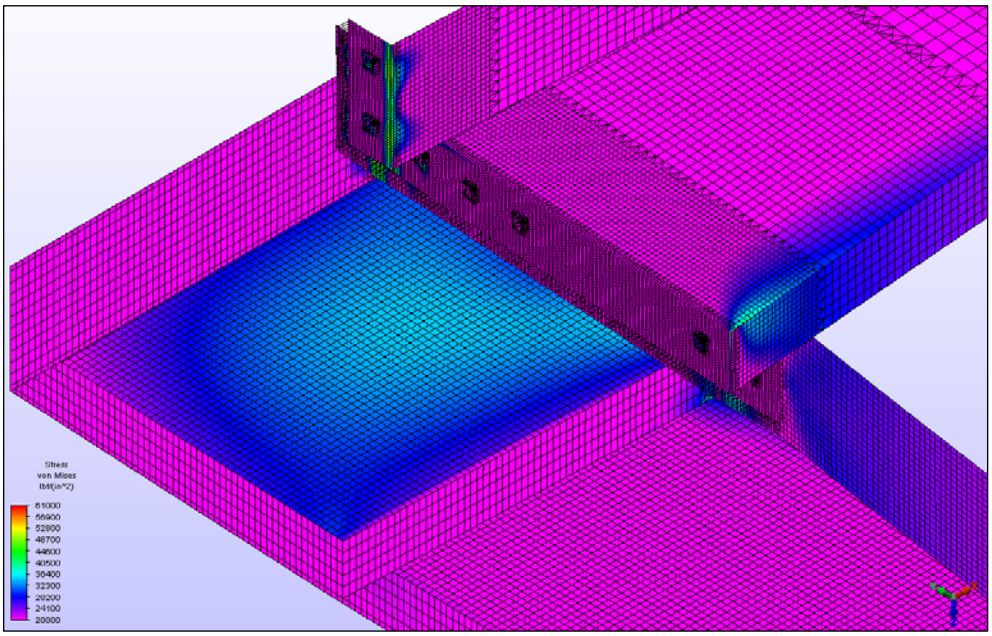

Figure 4.23 Frame 1 von Mises Stress in the knee at the buckling load of 29.6 kips

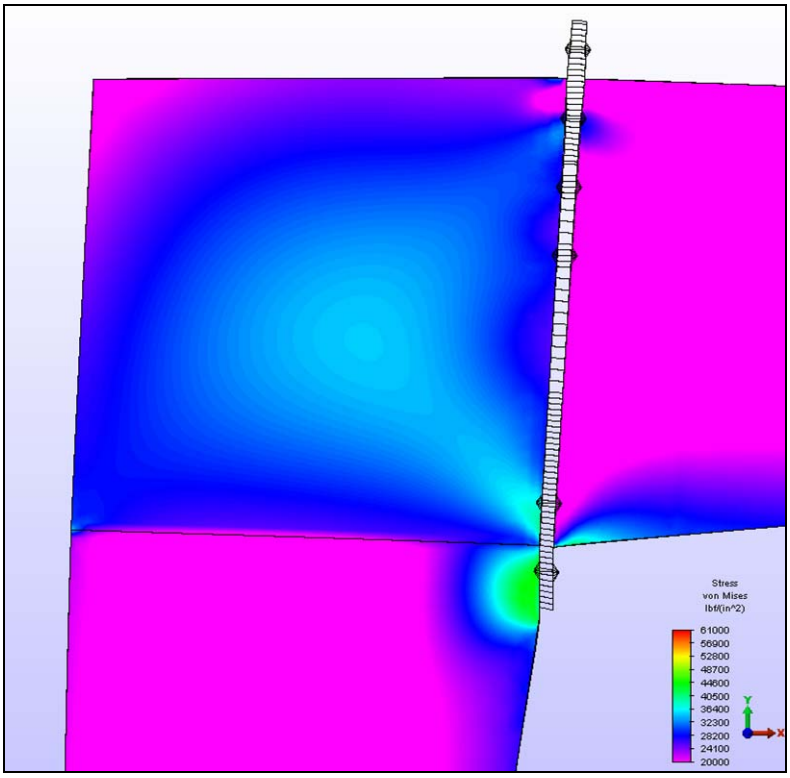

Figure 4.24 Frame 3 von Mises Stress in knee web at the buckling load of 29.6 kips

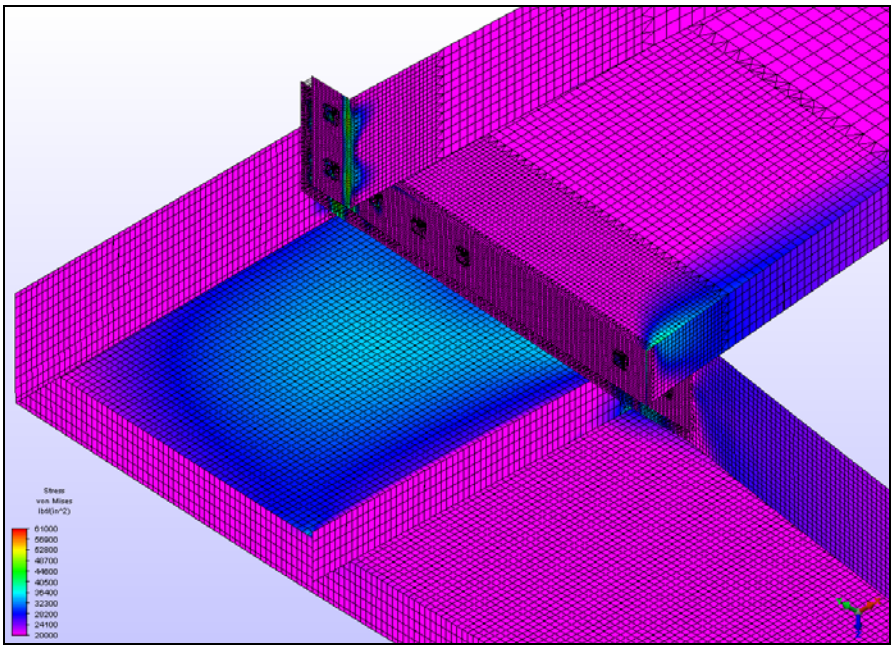

Figure 4.25 Frame 3 von Mises Stress in the knee at the buckling load of 29.6 kips

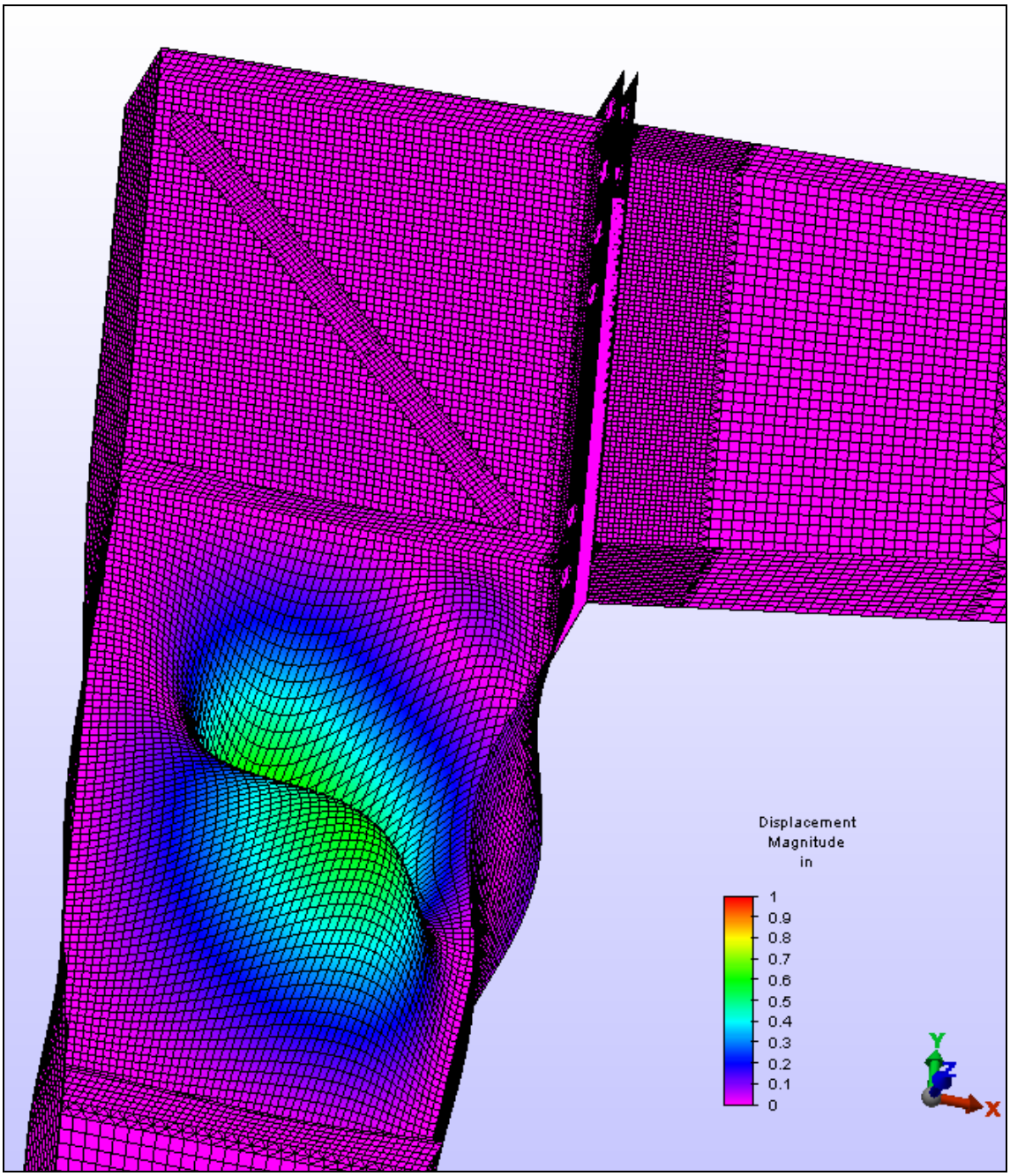

Figure 4.26 FEA failure mode for frames 2, 4 and 5 under a 35.7 kip load (the diagonal stiffener adequately suppressed buckling of the knee web)

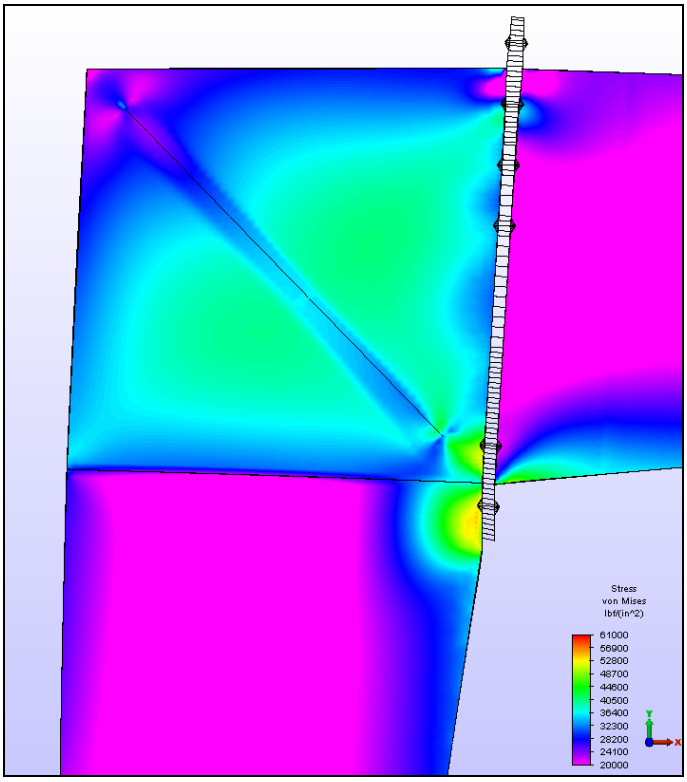

Figure 4.27 Frame 2 von Mises Stress in knee web at the buckling load of 35.7 kips

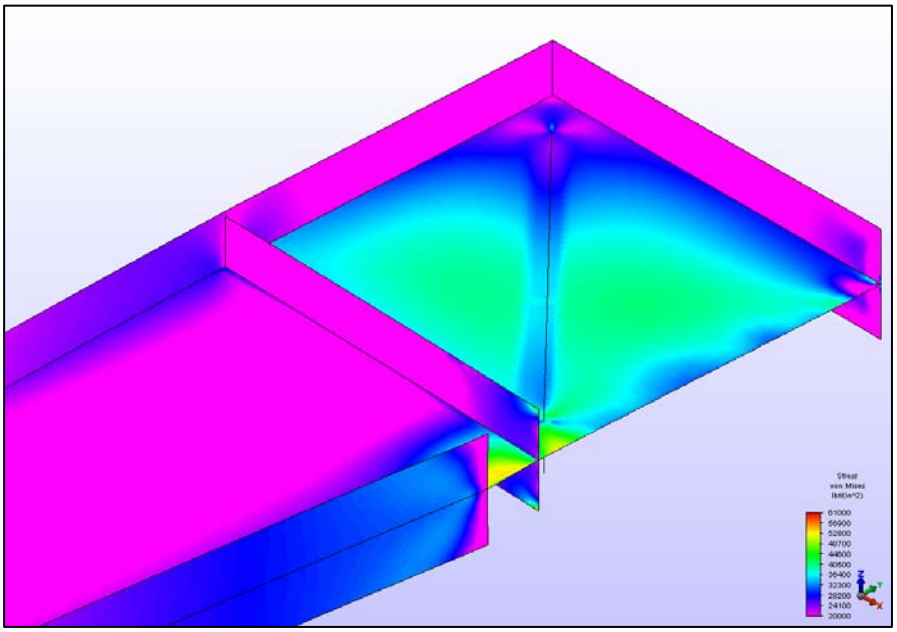

Figure 4.28 Frame 2 von Mises Stress at 35.7 kips (rafter is removed from this view)

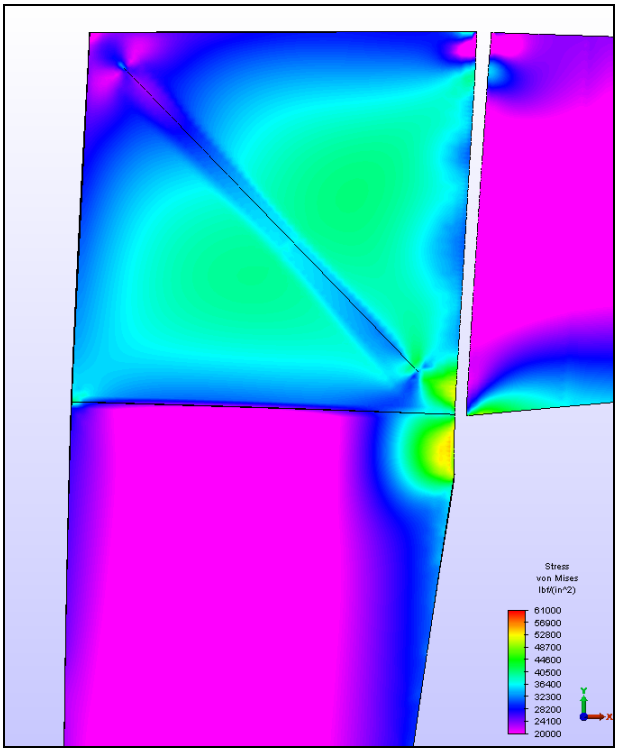

Figure 4.29 Frame 4 von Mises Stress in knee web at the buckling load of 35.7 kips

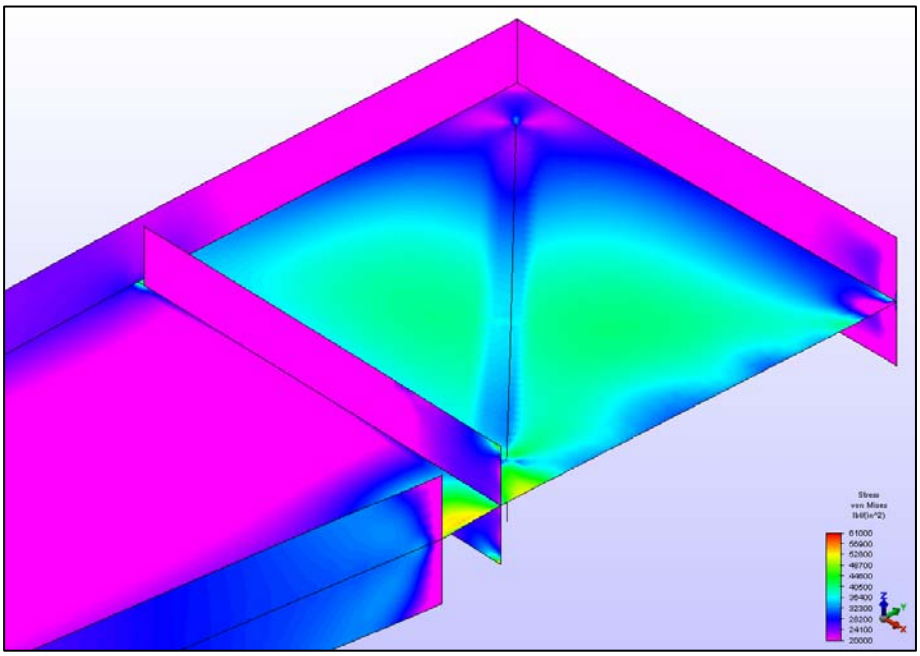

Figure 4.30 Frame 4 von Mises Stress at 35.7 kips (rafter is removed from this view)

As found in the laboratory data and presented in the preceding section, detaching the horizontal stiffener from the column outer flange has very little impact on the overall performance of each modeled frame. Small increases of approximately 6 ksi were found in the column web. This increase in the local stresses was located directly in the gap where the horizontal stiffener is detached. This is seen when comparing Figure 2.28 to Figure 2.30. Upon further investigation of the column outer flange, there is minimal difference in frame 2 (attached horizontal stiffener) and frame 4 (detached horizontal stiffener). Figure 2.31 shows a minor difference in the distribution of stress from the horizontal stiffener to the column outer flange. There appears to be almost no effect to the stresses or strain in the knee web if the horizontal stiffener is detached.

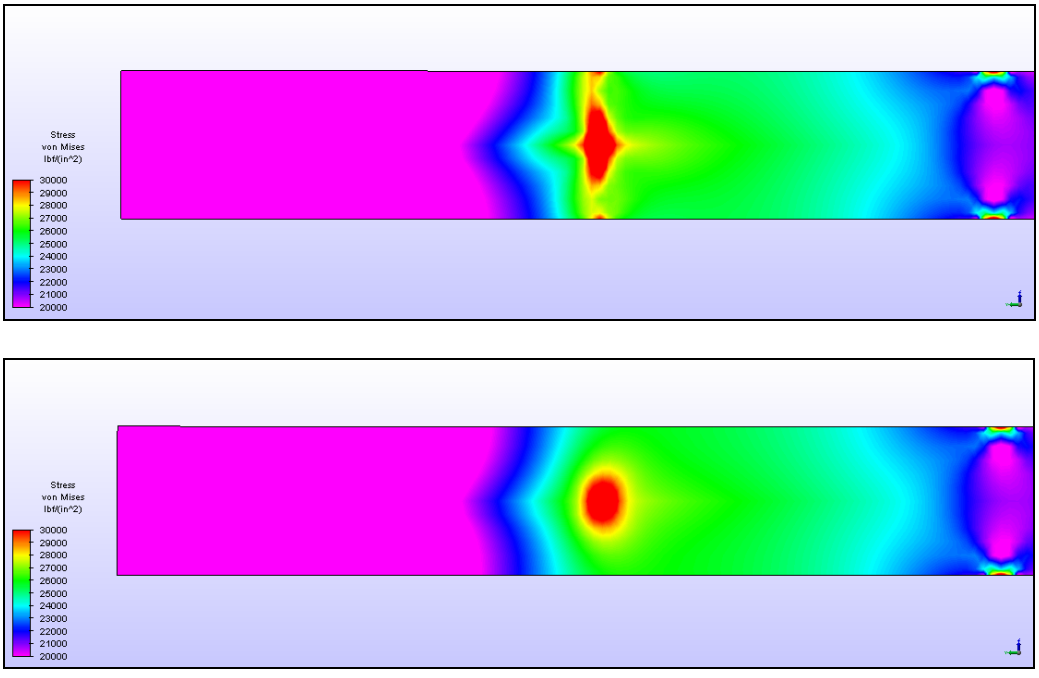

Figure 4.31 Both contour plots are from the column outer flange at a 35.7 kip load. The top is from frame 2 (horizontal stiffener is attached), while the bottom is from frame 4 (horizontal stiffener is detached)

4.3 Comparison of Experimental Test and FEA Results

Assuming a state of plane stress in the linear elastic region, the rosette strain gage provides the necessary information to calculate the principal stresses. Therefore, principal stresses can be determined at the center of the knee web throughout the incremental loading. In addition to the equations from Hooke's Law for determining the principal stresses, Appendix C presents the equation for von Mises stress as a function of the principal stresses. Once the von Mises stresses are calculated, the laboratory data can be compared to the finite element data at the center of the knee web. This comparison is made in Figure 4.32. It is evident that there were insignificant differences in the finite element von Mises stress and measured test results for frames 2, 4 and 5. This is shown in Figure 4.32. Likewise, measured laboratory test results and theoretically calculated von Mises stress for frames 2 (Lab), 4 (Lab), and 5 (Lab) all follow similar trends, showing minimal influence from the attached or detached horizontal stiffener. However, the most important observation from Figure 4.32 is the similar values all along the loading sequence between finite element stress and laboratory stress for each of the three frames. The slope of the lines of measured data and finite element analysis is the same for all practical purposes. In fact, frame 4 (FEA) falls almost directly between the curves for frame 4 (Lab), and frame 5 (Lab), where frame 5 was fabricated identically to frame 4 to confirm test results in the laboratory. Frame 2 (FEA) also compares well to frame 2 (Lab); however, as the load increases, the laboratory data diverges from the linear finite element data. This is certainly to be expected and an accepted limitation of the linear finite element static stress and buckling analysis. To employ a nonlinear finite element

analysis would require substantially more computer processing capability. Figure 4.33 is similar to Figure 4.32, but for frames 1 and 3 that do not have a diagonal stiffener in the knee web. Once again, the laboratory data begins to diverge from the linear finite element stress with increasing load.

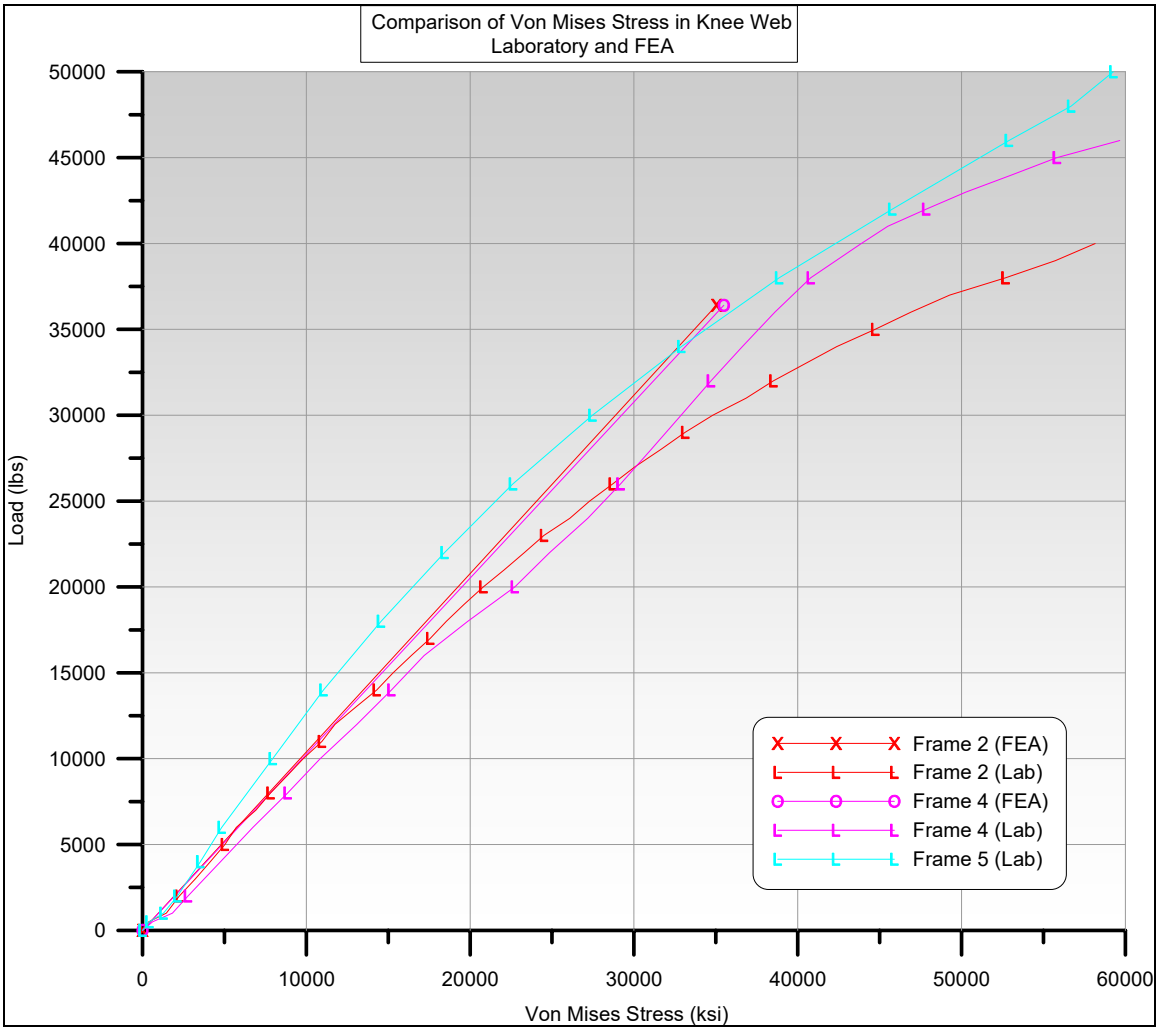

Figure 4.32 A comparison of finite element results to laboratory test results for frames 2, 4, and 5, having a diagonal stiffener in the knee web

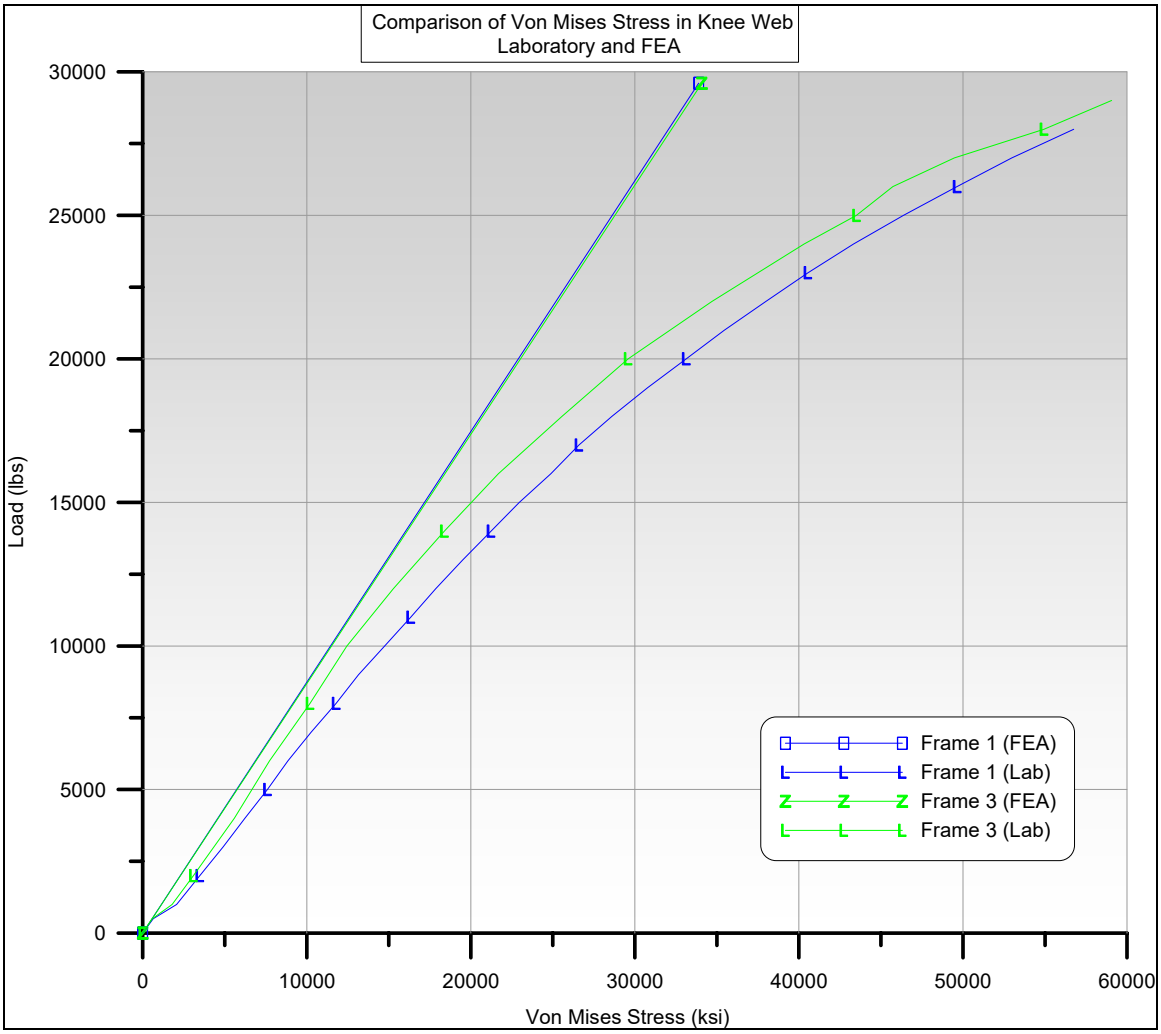

Figure 4.33 A comparison of finite element results to laboratory results for frames 1 and 3, having no diagonal stiffener in the knee web

The finite element buckling analysis predicted buckling to occur in the knee web for frames 1 and 3. Comparative views of the FEA predicted web buckling and the actual buckling observed during testing are shown in Figure 4.34. The knee web buckling was expected and the FEA buckling prediction closely resembled that from laboratory tests. Likewise, the FEA buckling analysis for frames 2, 4 and 5 clearly resemble the actual failure mode in the laboratory, see Figure 4.35.

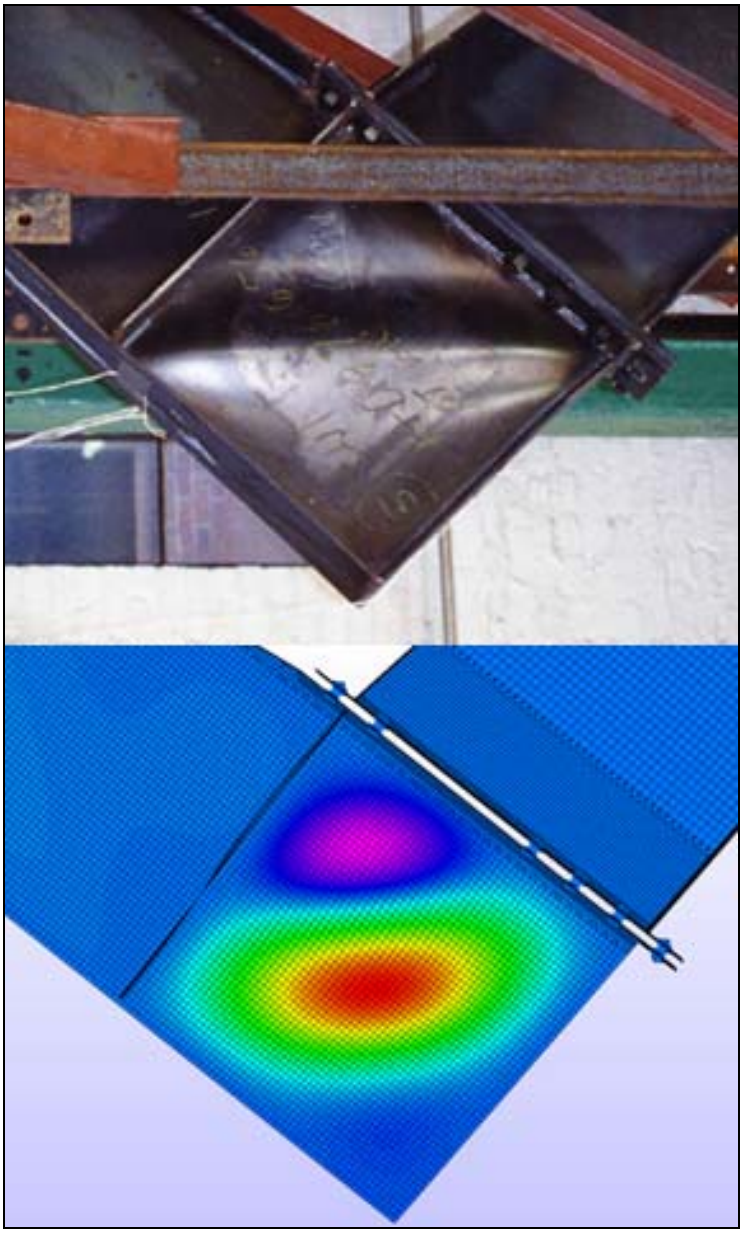

Figure 4.34 Comparative views of laboratory test results and predicted FEA buckling mode for frame 3 (frame 1 was identical)

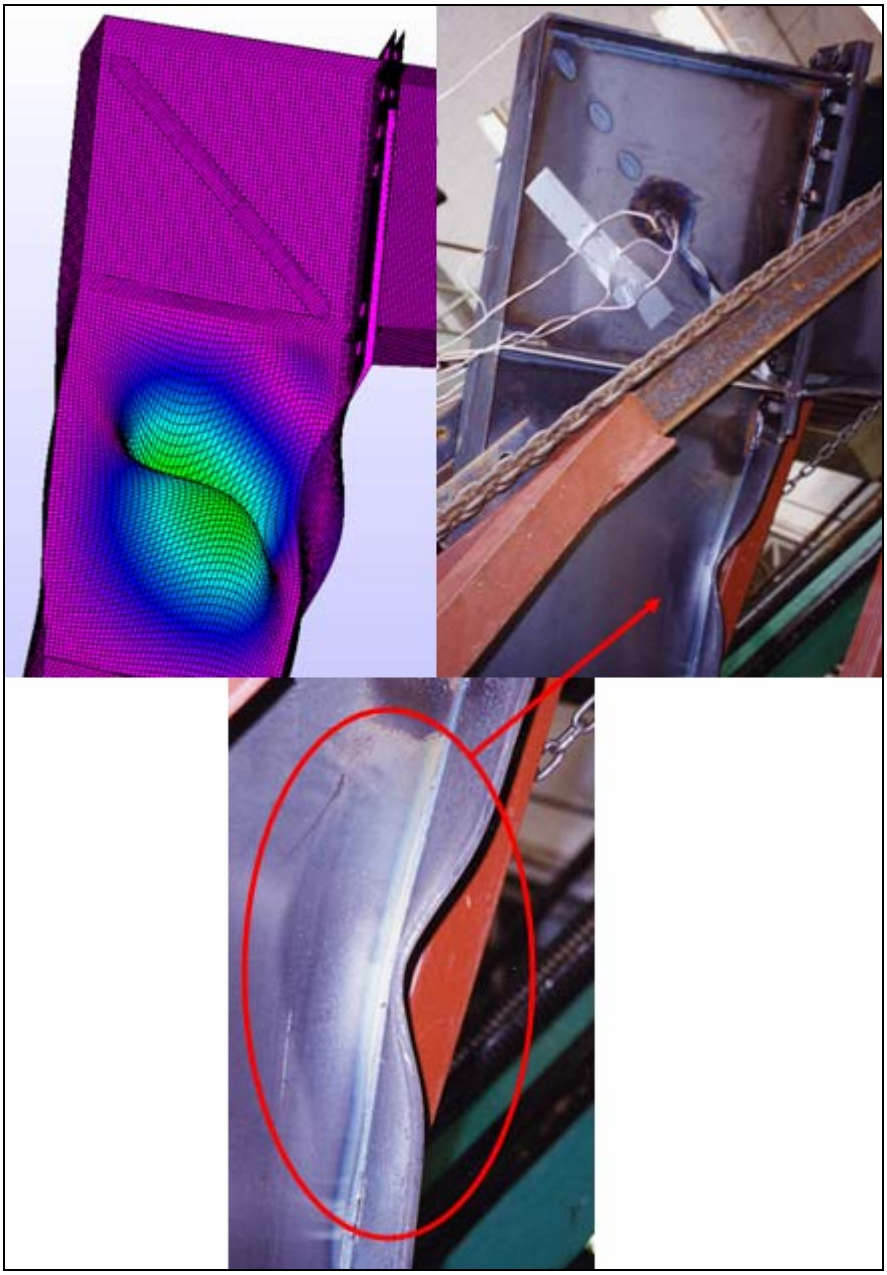

Figure 4.35 Comparative views of buckling from test results and predicted FEA for frame 4 (frame 2 was identical)

While the FEA von Mises stress and buckling modes all appeared to match well with actual laboratory values and results, the FEA buckling load value was consistently

conservative when compared to experimental results. In all cases for all frames, the FEA predicted buckling load was approximately 66% to 70% of the actual load that caused the frame to buckle in the laboratory. This could be attributed to the linear stress strain assumption and use of plate elements in the linear static stress finite element analysis. Using solid or brick elements in a nonlinear finite element buckling analysis would likely result in buckling loads that more closely matched laboratory test results. However, a nonlinear FEA with solid elements was not practical with current computer processor limitations.

Table 4.1 shows the comparative results between the experimental lab data, the finite element analysis, and the predicted values as per the AISC provisions. It is very clear that the finite element analysis accurately predicted stresses and modes of failure, but was considerably conservative with the prediction of actual load values causing the buckling to occur. Table 4.1 also illustrates that the AISC provisions are conservative. Without the use of a diagonal stiffener, shear buckling loads as predicted by the AISC provisions are extremely safe, and shear buckling with tension field action tracks more closely with actual experimental results, though still on the safe side. Table 4.2 tabulates the ratio of actual failure loads to the FEA and AISC predicted failure loads.

Table 4.1 Summary of results

	Actual	**FEA**	**AISC – ASD 9th**
Frame 1	Knee web buckled at 43 kips	Knee web buckled at 29.6 kips	16.0 kips (without TFA) 37.6 kips (with TFA)
Frame 2	Column web / flange buckled (below the knee joint) at 53.7 kips	Column web / flange buckled (outside of knee joint) at 35.7 kips	48.6 kips – limited by shear yielding
Frame 3	Knee web buckled at 45 kips	Knee web buckled at 29.6 kips	15.7 kips (without TFA) 36.8 kips (with TFA)
Frame 4	Column web / flange buckled (below the knee joint) at 53.7 kips	Column web / flange buckled (outside of knee joint) at 35.7 kips	50.2 kips – limited by shear yielding
Frame 5	Column web / flange buckled (below the knee joint) at 51 kips	Column web / flange buckled (outside of knee joint) at 35.7 kips	49.2 kips – limited by shear yielding

Table 4.2 Ratio of actual buckling load to predicted buckling load

	Ratio of Actual / FEA	**Ratio of Actual / AISC**
Frame 1	1.45	1.14 (with TFA)
Frame 2	1.5	1.10
Frame 3	1.52	1.22 (with TFA)
Frame 4	1.5	1.07
Frame 5	1.43	1.04

Table 4.3 Ratio of actual to FEA von Mises stress at center of knee web

	Ratio of Actual / FEA
Frame 1	1.42
Frame 2	1.12
Frame 3	1.33
Frame 4	1.16
Frame 5	0.92

CHAPTER V

SUMMARY AND CONCLUSIONS

Frames 1 and 3 had less load carrying structural capacity than frames 2, 4 and 5. This was confirmed by the actual test results and the finite element analysis. Frames 1 and 3 clearly failed by shear buckling of the knee web. Tension field action developed in these two tests and the load carrying capacity at failure for both frames agreed fairly well, on the conservative side, to the AISC provisions for shear buckling with tension field action.

Frames 2 and 4 had a diagonal stiffener, and failed clearly by shear yielding of the stiffened web in the knee joint, followed by buckling of the column web and flange below the knee joint. The diagonal stiffener prevented web buckling in all tests. Frame 5 exhibited the same identical performance as frames 2 and 4, but did not experience shear yielding in the knee web before buckling in the column web and flange below the knee joint. The ultimate load-carrying capacity for all three frames was practically the same.

The role of the diagonal stiffener, when used in preventing premature shear buckling of the knee web, was achieved easily. Furthermore, it is now clear that the diagonal stiffener does not need to be the primary load-carrying member, but rather a lateral restraint that prevents shear web buckling and allows the knee web panel to provide a significant contribution to the structural capacity of the knee joint. Therefore, a

thin, short diagonal stiffener, not extending to the column and rafter flanges, is adequate to resist shear buckling until shear yielding of the web plate occurs. This observation was theoretically evident before this research, but is not commonly used for the design of rigid square knee connections by the metal building industry.[5] The common practice of a tight fit diagonal stiffener serving as a lateral restraint to the web, as well as a compression strut to transfer load between flanges, is clearly not necessary.

It is also evident, on the basis of these tests, that there is no difference in the overall capacity of the square knee if the horizontal stiffener is attached or detached from the column outer flange. Both the finite element analysis and experimental tests results agreed that only very minimal influence can be noted from variation in construction technique.

On the basis of the findings of laboratory testing of five full-scale rigid square knee frames and that from a finite element analysis, the following conclusions can be made:

1) The AISC provisions for shear buckling of square knees without diagonal stiffeners render very conservative results, and should be ignored in actual design practice.
2) When tension field action is included in the design provisions, as allowed by the AISC specifications, the predicted load carrying capacity remains slightly conservative, but reasonable as it approaches the actual test results.
3) A shortened diagonal stiffener placed only on one side of the square knee and welded on one side only, will effectively retard shear web buckling until shear

yielding occurs. The diagonal stiffener does not need to be designed as an axial compression member between flanges, but rather to simply restrain the web from buckling. This can be accomplished with a relatively thin member.

4) When using a diagonal stiffener, failure loads as predicted by the AISC provision for shear yielding, are in good agreement with the actual test results. On average, the AISC predicted loads were within 7%, on the conservative side, of the actual test results.

5) A linear static stress finite element analysis coupled with a finite element critical buckling load analysis predicted stresses and buckling modes that compared very well with actual test results. Actual loads that caused buckling were significantly conservative.

6) Detaching the horizontal stiffener from the column flange has no apparent effect to overall capacity of the square knee joint.

BIBLIOGRAPHY

1. MBMA, *Industry Trends, 2005 MBMA Business Review*, www.mbma.com, 2006.

2. American Society of Civil Engineers. *Plastic Design in Steel: A Guide and Commentary,* Manuals and Reports on Engineering Practice No. 41. ASCE, 1971, pp. 167-186.

3. Salmon, Charles G., and Johnson, John E.. Steel *Structures: Design and Behavior,* Harper & Row, 1990, pp. 919-922.

4. ALGOR. *Products and Core Packages,* www.algor.com/products/default.asp, 2006.

5. ALGOR. *ALGOR Help file User's Guide V19.2*, 28 June 2006.

6. ALGOR. *Modeling Bolts and Fasteners, www.etechlearning.com,* 29 November 2005.

7. American Institute of Steel Construction, *Manual of Steel Construction, Allowable Stress Design*, 9th Edition, 1989.

8. Young, Warren C., Budynas, Richard G. *Roark's Formulas for Stress and Strain* 7th Edition. McGraw-Hill, 2002, pp. 15-32.

9. Boresi, Arthur P., and Schmidt, Richard J. *Advanced Mechanics of Materials,* Wiley & Sons, 2003.

APPENDIX A

AISC ASD PROVISIONS

The following calculations are based on guidelines from AISC, Allowable Stress Design, 9th edition.[7] Material properties and dimensions were obtained from frame 2 during the tension coupon tests and are listed below:

- h = 19.9375" clear distance between flanges of the section
- a = 19.75" clear distance between transverse stiffeners
- tw = 0.1347"
- Fy = 61.536 ksi
- Fv = allowable shear stress as calculated by ASD

1) Shear Yielding

$$Fv = 0.4 * Fy \quad \text{[AISC Equation F4-1]} \tag{A-1}$$

$$Fv = 0.4 * 61.536 = 24.6 \text{ ksi}$$

From AISC Commentary Chapter F4, removing the factor of safety from equation F4-1:

$$Fv = \frac{Fy}{\sqrt{3}} = \frac{61.536}{1.7321} = 35.5 \text{ ksi for shear yielding;} \tag{A-2}$$

Therefore, the associated moment for this stress:

$$M_{n1} = Fv * (a * H * tw) = 35.53 * (19.75 * 19.9375 * 0.1347) = 1884.6 \text{ k-in} \tag{A-3}$$

However:

$$\frac{h}{tw} = \frac{19.9375}{0.1347} = 148 \le \frac{380}{\sqrt{Fy}} \quad \text{but} \quad \frac{380}{\sqrt{61.536}} = 48.4 \tag{A-4}$$

Since 148 > 48.4, must check Shear Buckling [AISC Equation F4-2]

2) Shear Buckling

$$Fv = \frac{Fy}{2.89} * Cv \le Fv \le 0.4 * Fy; \quad \text{[AISC Equation F4-2]} \tag{A-5}$$

With $Fv \le 0.4 * Fy = 0.4 * 61.536 = 24.6$

And Cv is the buckling coefficient and is calculated as:

$$Cv = \frac{45{,}000 * kv}{Fy * \left(\frac{h}{tw}\right)^2} : \quad \text{When Cv} < 0.8 \tag{A-7}$$

or

$$Cv = \frac{190}{\left(\frac{h}{tw}\right)} * \sqrt{\frac{kv}{Fy}} : \quad \text{When Cv} > 0.8 \tag{A-8}$$

$$kv = 4.00 + \frac{5.34}{\left(\frac{a}{h}\right)^2}; \text{ when } \frac{a}{h} < 1.0 \tag{A-9}$$

or

$$kv = 5.34 + \frac{4.00}{\left(\frac{a}{h}\right)^2}; \text{ when } \frac{a}{h} > 1.0 \quad \text{since} \tag{A-10}$$

$$\text{Since } \frac{a}{h} = 0.996 < 1.0 : \quad kv = 4.00 + \frac{5.34}{\left(\frac{a}{h}\right)^2} = 4.00 + \frac{5.34}{(0.9906)^2} = 9.4418$$

Therefore,

$$Cv = \frac{45{,}000 * 9.44}{61.536 * (48.4)^2} = 0.3152 \le 0.8 \text{ ; Hence}$$

$$Fv = \frac{Fy}{2.89} * Cv = \frac{61.536}{2.89} * 0.3152 = 6.711 < 24.6 \tag{A-5}$$

Removing the factor of safety from AISC equation F4-2:

$Fv = 6.711 * 1.67 = 11.2$ ksi for shear web buckling (without tension field action)

Therefore, the associated moment for this stress:

$$M_{n2} = Fv * (a * H * tw) = 11.2 * (19.75 * 19.9375 * 0.1347) = 594 \text{ k-in} \quad \text{(A-3)}$$

3) Shear Buckling with Tension Field Action:

Alternative knee panel design with Tension Field Action (from AISC G3)

From AISC G3, we must satisfy AISC F5 and Cv > 1.0

$$\frac{a}{h} \le \left[\frac{260}{\left(\frac{a}{tw}\right)} \right]^2 \text{ and } 3.0 \quad \text{[AISC Equation F5-1]} \quad \text{(A-11)}$$

$$0.9906 \le \left[\frac{260}{(148)} \right]^2 = 3.09 \text{ and } 3.0 \quad OK$$

$$Fv = \frac{Fy}{2.89} * \left[Cv + \frac{1 - Cv}{1.15 * \sqrt{1 + \left(\frac{a}{h}\right)^2}} \right] \le 0.4 * Fy \quad \text{[AISC Equation G3-1]} \quad \text{(A-12)}$$

Therefore, removing the factor of safety from equation G3-1,

$$Fv = \frac{61.536}{\sqrt{3}} * \left[0.3152 + \frac{1 - 0.3152}{1.15 * \sqrt{1 + \left(\frac{19.75}{19.9375}\right)^2}} \right] = 26.2 \text{ ksi} \quad \text{(A-13)}$$

Therefore, the associated moment for this stress:

$$M_{n3} = Fv * (a * H * tw) = 26.2 * (19.75 * 19.9375 * 0.1347) = 1391 \text{ k-in} \quad \text{(A-3)}$$

4) Design of knee panel with shear stiffener added:

From frame 2: $b_{st} = 2.75$ and $t_{st} = 0.138$

From AISC table B5.1 (plates projecting from girders, built-up columns or other compression members)

$$\frac{b}{t} < \frac{95}{\sqrt{\frac{Fy}{kc}}} \Rightarrow Noncompact \text{ [AISC Table B5.1]} \quad \text{(A-14)}$$

Where $kc = \frac{4.05}{\left(\frac{h}{t}\right)^{0.46}}$ if $\frac{h}{t} > 70$; otherwise, kc = 1.0 [AISC Table B5.1] (A-15)

$\frac{b}{t} = \frac{2.75}{0.138} = 19.93$; therefore kc = 1.0 and

$\frac{95}{\sqrt{\frac{Fy}{kc}}} = \frac{95}{\sqrt{\frac{61.536}{1.0}}} = 12.11$ hence, slender and table B5.1 refers to AISC Appendix B5

From AISC Appendix B5:

When $\frac{95}{\sqrt{\frac{Fy}{kc}}} < \frac{b}{t} < \frac{195}{\sqrt{\frac{Fy}{kc}}}$ The reduction factor "Qs" is:

$$Qs = 1.293 - 0.00309 * \left(\frac{b}{t}\right) * \sqrt{\frac{Fy}{kc}} \quad \text{[AISC Equation A-B5-3]} \quad \text{(A-16)}$$

Since $12.11 < 19.93 < \frac{195}{\sqrt{61.536}}$

$$Qs = 1.293 - 0.00309 * \left(\frac{b}{t}\right) * \sqrt{\frac{Fy}{kc}} = 1.293 - 0.00309 * (19.93) * 7.844 = 0.80997$$

Moment capacity of the knee panel calculated using the equation for the thickness of shear stiffener with factor of safety (FS=23/12) removed:

$$t_{st} = \left[\frac{3 * M * \left(\frac{a}{h} + \frac{h}{a} \right) * \sqrt{a^2 + h^2}}{Q_s * \pi^2 * E * b_{st}^{\ 3}} \right] \quad \text{therefore,} \qquad \text{(A-17)}$$

$$M_{n4} = \frac{b_{st}^{\ 3} * t_{st} * Q_s * \pi^2 * E}{3 * \left(\frac{a}{h} + \frac{h}{a} \right) * \sqrt{a^2 + h^2}} = \frac{2.75^3 * 0.138 * 0.80997 * \pi^2 * 29000}{3 * \left(\frac{19.75}{19.9375} + \frac{19.9375}{19.75} \right) * \sqrt{19.75^2 + 19.9375^2}} = 3951 k - in$$

Using dimensions and properties shown in Figure A.1 and A.2, from frame 2, the predicted failure load is calculated and tabulated in Table A.1.

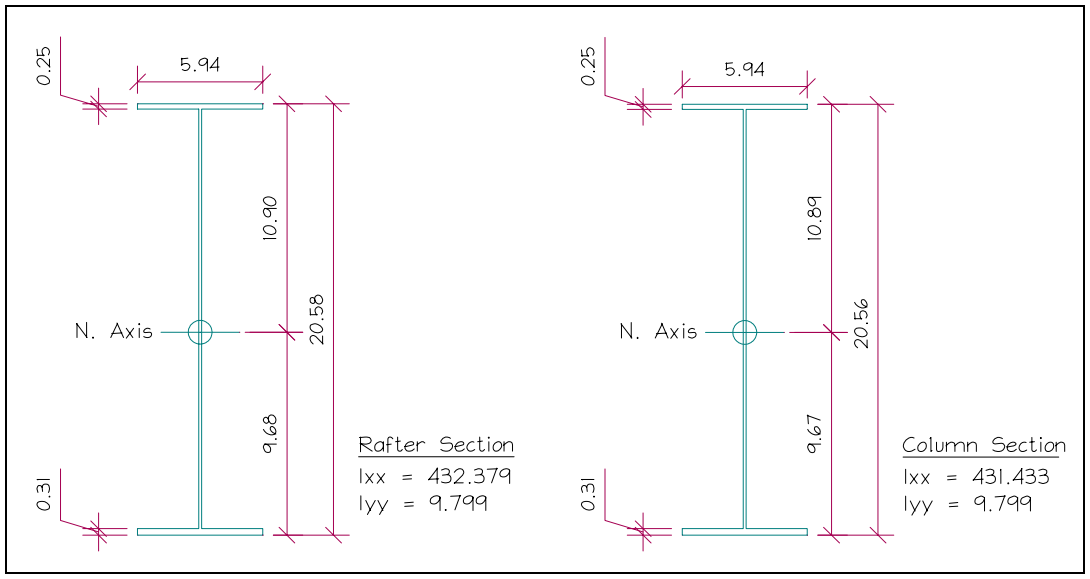

Figure A.1 Moment of Inertia and location of neutral axis

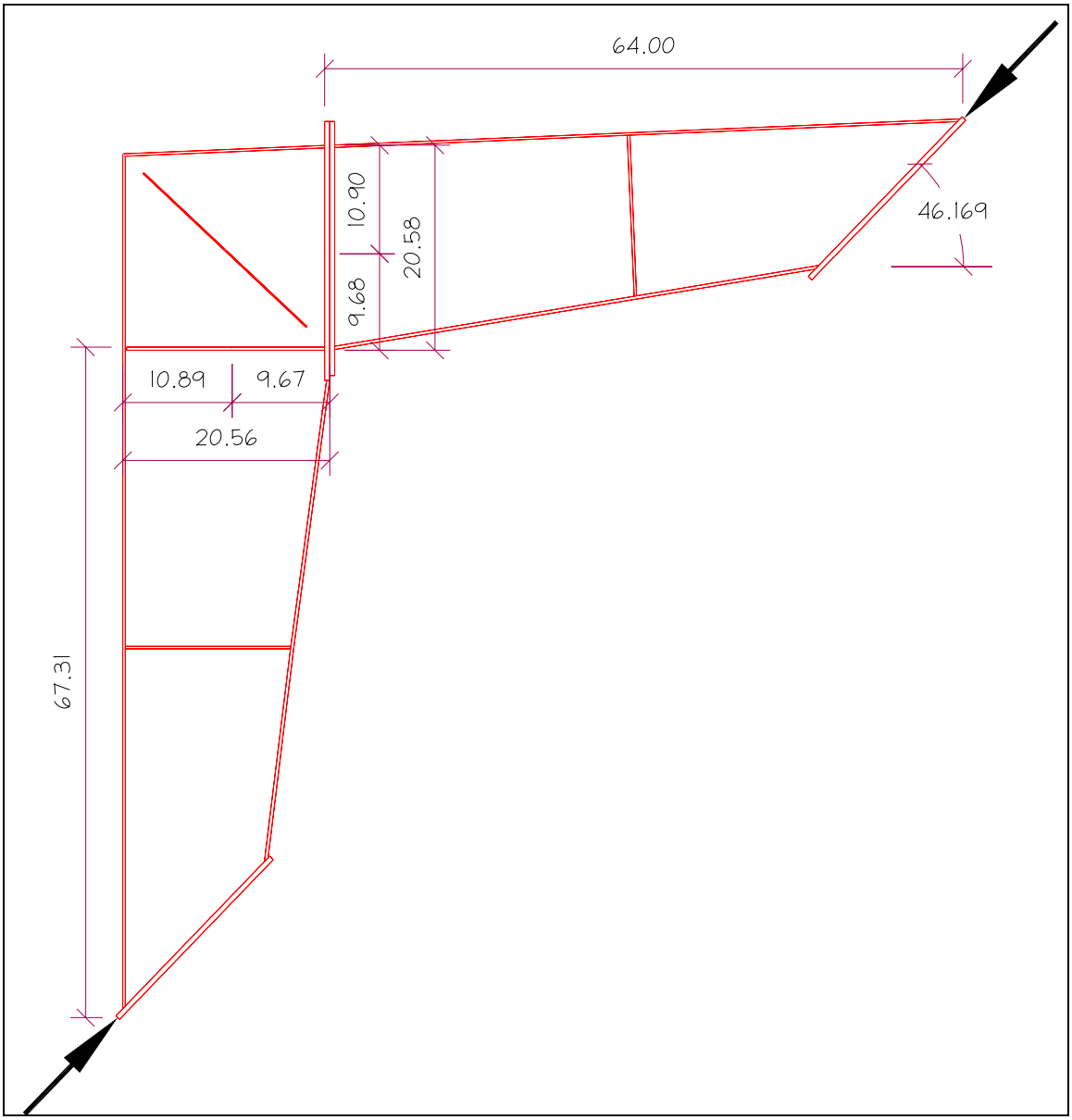

Figure A.2 Dimensions of frame 2

$$\alpha = 46.169^{\circ};\ \sin\alpha = 0.7214;\ \cos\alpha = 0.6925 \tag{A-19}$$

$$M_{column} = 0.6925 * P * 67.3125 - 0.7214 * P * 10.89 = 38.758 * P \tag{A-20}$$

$$\text{Predicted Load} = P = \frac{M_n}{38.76} \tag{A-21}$$

Table A.1 Summary of AISC predicted loads for frame 2

Failure Mode	**AISC – ASD 9th edition**	
	Predicted Moment	Predicted Load
Shear Yielding	1885 k-in	48.6 kips
Shear Buckling	594 k-in	15.56 kips
Shear Buckling w/ TFA	1391 k-in	36.39 kips
Knee Panel with shear stiffener	3951 k-in	103.5 kips (exceeds shear yielding)

APPENDIX B

LABORATORY TENSION TESTS

Material samples were taken from the webs of frame two and frame three. Tension tests were conducted on the samples to determine material properties used to calculate values in Appendix C. Table B.1 shows stress and strain data from the frame two sample, and data from the frame three sample are shown in Table B.2. Figure B.1 is a stress strain plot of the values from Tables B.1 and B.2. A simple curve fit program was used to find the curve and equation shown in Figure B.1

Table B.1 Tension test from frame 2 material sample

Frame Two Tension Test				
LOAD	Strain	STRESS	Incr. strain	Incr. E
0	0	0	0	0
400	0.000239	5861	0.000239	24,521,306
800	0.000476	11721	0.000237	24,728,236
1200	0.000722	17582	0.000246	23,823,545
1600	0.00096	23442	0.000238	24,624,336
2000	0.001191	29303	0.000231	25,370,528
2400	0.001418	35164	0.000227	25,817,586
2800	0.001652	41024	0.000234	25,045,265
3200	0.00191	46885	0.000258	22,715,473
3600	0.00226	52745	-	-
3800	0.00257	55676	-	-
4000	0.003172	58606	-	-
4100	0.004368	60071	-	-
4150	0.005797	60804	-	-
4200	0.007252	61536	-	-
4250	0.008829	62269	-	-
4300	0.010454	63001	-	-
4350	0.011956	63734	-	-
4400	0.013112	64467	-	-

Table B.2 Tension test from frame 3 material sample

Frame Three Tension Test				
LOAD	**Strain**	**STRESS**	**Inc. strain**	**Inc. E**
0	0	0	0	0
400	0.000225	5802	0.000225	25,785,019
800	0.000438	11603	0.000213	27,237,696
1200	0.000656	17405	0.000218	26,612,978
1600	0.000888	23207	0.000232	25,007,023
2000	0.001103	29008	0.000215	26,984,322
2400	0.001324	34810	0.000221	26,251,716
2800	0.001552	40611	0.000228	25,445,742
3200	0.001813	46413	-	-
3600	0.002159	52215	-	-
3800	0.002415	55115	-	-
4000	0.002846	58016	-	-
4100	0.003233	59467	-	-
4200	0.00438	60917	-	-
4250	0.006972	61642	-	-
4300	0.007827	62368	-	-
4350	0.009423	63093	-	-
4400	0.011039	63818	-	-

Dimensions (samples from frames 2 and 3):

$tw_{(2)} = 0.1347"$

$width_{(2)} = 0.5067"$

$Area_{(2)} = 0.6825"$

$tw_{(3)} = 0.1365"$

$width_{(3)} = 0.5051"$

$Area_{(3)} = 0.6895"$

$$Stress = \frac{Load}{Area} \tag{B-1}$$

$$E = \frac{Stress}{Strain} \tag{B-2}$$

Average E = 25,518,200

Fy = 61.536 ksi

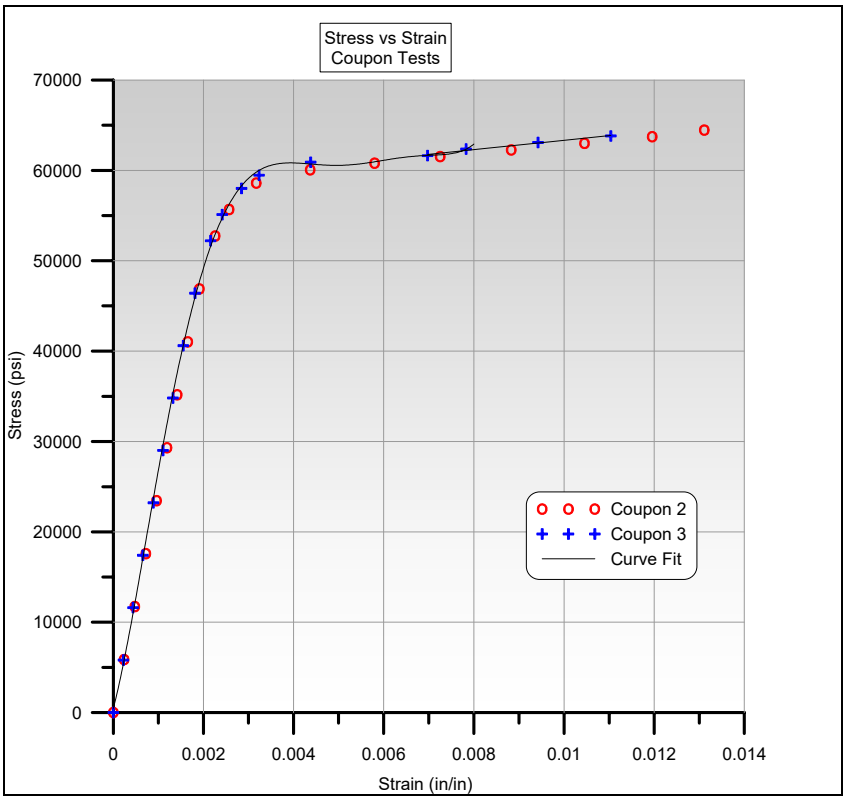

Figure B.1 Stress versus Strain for tension tests

Equation of the Curve: (B-3)

= [7360004197000000000 * ABS(X^6)] – [2000272963000000000*ABS(X^5)] + [2053247492000000*ABS(X^4)] – [9398217612000*ABS(X^3)] + [14610593290*ABS(X^2)]+ [19286417.06*ABS(X)]+ [453.4637803]

APPENDIX C

EXPERIMENTAL DATA AND SAMPLE CALCULATIONS

As stated in chapter two, strain gages were used to capture laboratory data. Table C.1 through Table C.5 presents the strain data collected during the laboratory tests. This appendix also presents the equations and sample calculations converting the laboratory strain data to stresses and shear strain. All of these values are tabulated in Table C.6 through Table C.14. Throughout the tables in this appendix, strain data is shown as 1E-6 in/in and stress is noted as kip per square inch (ksi). For gage notation and location, refer to Figure 2.9 and Figure 2.10. The following notation is used throughout:

- G1 = gage one, located on the rafter flange
- G2 = gage two, located on the column flange
- G3 = ε_y = the 0° component of a three element rectangular strain gage rosette #1
- G4 = ε_{xy} = the 45° component of a three element rectangular strain gage rosette #1
- G5 = ε_x = the 90° component of a three element rectangular strain gage rosette #1
- G6 = ε_y = the 0° component of a three element rectangular strain gage rosette #2
- G7 = ε_{xy} = the 45° component of a three element rectangular strain gage rosette #2
- G8 = ε_x = the 90° component of a three element rectangular strain gage rosette #2
- σ_1 = normal stress at location of gage one
- σ_2 = normal stress at location of gage two
- Γ_{xy} = measured shear strain, from rosette gage
- σ_3, σ_y = stress corresponding to G3
- T_{xy} = shear stress
- σ_5, σ_x = stress corresponding to G5

- σ_{max} = maximum principal stress
- σ_{min} = minimum principal stress
- T_{max} = maximum shear stress
- σ_{vm} = Von Mises stress
- E = modulus of elasticity as determined from coupon tests as 25,518,200
- ν = poissons ratio = 0.29

Table C.1 Laboratory strain data collected from frame 1

Test 1 / Frame 1					
Load (lbs)	G1	G2	G3	G4	G5
0	0	0	0	0	0
500	10	8	-2	-21	-3
1,000	29	21	-5	-65	-5
2,000	47	37	-7	-110	-11
3,000	65	54	-8	-153	-13
4,000	84	70	-10	-196	-20
5,000	101	86	-11	-239	-25
6,000	115	100	-15	-280	-31
7,000	133	115	-18	-326	-38
8,000	151	131	-23	-377	-47
9,000	166	145	-28	-423	-56
10,000	186	162	-34	-477	-67
11,000	201	177	-39	-531	-78
12,000	216	192	-47	-585	-91
13,000	232	207	-56	-643	-105
14,000	250	223	-64	-703	-119
15,000	265	240	-74	-765	-136
16,000	283	257	-84	-833	-153

Table C.1 (continued)

Test 1 / Frame 1					
Load (lbs)	G1	G2	G3	G4	G5
17,000	298	271	-94	-895	-171
18,000	315	286	-108	-969	-193
19,000	333	301	-122	-1049	-218
20,000	359	328	-139	-1137	-247
21,000	387	360	-155	-1223	-275
22,000	413	404	-173	-1317	-306
23,000	445	449	-193	-1414	-340
24,000	458	503	-217	-1520	-377
25,000	474	545	-244	-1637	-420
26,000	496	573	-273	-1762	-465
27,000	515	600	-304	-1890	-512
28,000	538	614	-341	-2036	-566
29,000	567	627	-382	-2192	-624
30,000	572	645	-426	-2351	-685
31,000	585	672	-475	-2520	-751
32,000	605	692	-533	-2722	-830
33,000	622	709	-592	-2920	-909
34,000	640	716	-667	-3170	-1010
35,000	660	718	-749	-3427	-1116
36,000	682	718	-848	-3737	-1247
37,000	700	711	-960	-4070	-1388
38,000	708	700	-1102	-4493	-1569
39,000	717	688	-1267	-4971	-1781
40,000	712	669	-1452	-5530	-2025
41,000	704	646	-1686	-6199	-2323
42,000	680	610	-1984	-7048	-2688
43,000	636	555	-2386	-8274	-3211

Table C.2 Laboratory strain data collected from frame 2

Test 2 / Frame 2								
Load (lbs)	G1	G2	G3	G4	G5	G6	G7	G8
0	0	0	0	0	0	0	0	0
500	10	8	0	-11	0	2	-8	5
1,000	29	27	2	-42	-1	6	-31	16
2,000	46	40	0	-66	-1	9	-47	25
3,000	67	62	0	-97	-6	7	-70	33
4,000	75	69	-9	-129	-8	12	-86	44
5,000	96	86	-7	-152	-4	10	-104	53
6,000	109	100	-7	-173	-5	14	-117	63
7,000	135	127	-5	-204	1	17	-137	76
8,000	149	136	-8	-233	-2	18	-156	84
9,000	196	150	-5	-259	2	22	-170	99
10,000	250	161	3	-281	8	25	-187	108
11,000	290	172	-2	-318	5	26	-209	118
12,000	312	179	-4	-343	4	26	-225	125
13,000	326	198	3	-374	9	32	-242	142
14,000	354	211	11	-403	17	40	-258	158
15,000	374	225	13	-430	19	44	-274	169
16,000	398	237	17	-458	24	49	-290	181
17,000	422	244	20	-488	28	54	-307	194
18,000	454	258	24	-512	33	59	-322	204
19,000	478	274	23	-545	32	62	-340	214
20,000	504	278	23	-577	36	68	-357	227
21,000	536	297	29	-607	44	76	-373	243
22,000	562	313	35	-635	52	84	-387	257
23,000	582	325	37	-666	58	92	-403	270
24,000	614	356	44	-703	68	102	-421	286
25,000	639	396	47	-734	73	110	-437	296

Table C.2 (continued)

Test 2 / Frame 2								
Load (lbs)	G1	G2	G3	G4	G5	G6	G7	G8
26,000	660	432	47	-773	77	117	-456	308
27,000	680	460	47	-810	82	127	-473	320
28,000	704	490	50	-850	90	136	-492	332
29,000	724	520	51	-889	98	149	-507	348
30,000	750	629	52	-934	105	162	-523	362
31,000	792	710	65	-974	128	188	-533	389
32,000	820	747	71	-1012	141	207	-541	406
33,000	851	782	78	-1056	157	231	-553	428
34,000	880	816	80	-1103	172	253	-563	449
35,000	915	859	84	-1159	191	283	-572	475
36,000	939	888	86	-1213	206	311	-579	500
37,000	962	920	86	-1270	228	347	-582	530
38,000	998	948	89	-1351	258	399	-582	572
39,000	1030	970	96	-1416	293	449	-577	615
40,000	1050	980	94	-1475	316	486	-576	649
41,000	1074	1004	89	-1562	352	546	-568	695
42,000	1101	1028	85	-1660	400	619	-551	758
43,000	1125	1049	75	-1771	460	700	-531	823
44,000	1148	1073	62	-1890	528	787	-509	897
45,000	1174	1095	39	-2039	616	888	-482	977
46,000	1183	1108	6	-2195	705	979	-459	1054
47,000	1207	1133	-25	-2373	816	1079	-430	1140
48,000	1218	1153	-69	-2619	974	1194	-392	1243
49,000	1232	1174	-106	-2919	1166	1312	-350	1352
50,000	1242	1185	-143	-3294	1384	1426	-304	1465
51,000	1255	1193	-170	-3897	1721	1586	-228	1617
52,000	1262	1192	-174	-4750	2160	1940	-137	1787
53,000	1253	1158	-102	-6440	3023	1936	9	2044

Table C.3 Laboratory strain data collected from frame 3

Test 3 / Frame 3								
Load (lbs)	G1	G2	G3L	G4	G5	G6	G7	G8
0	0	0	0	0	0	0	0	0
500	10	18	4	-9	0	0	-17	0
1000	34	27	11	-26	0	0	-51	2
2000	55	48	20	-43	-1	5	-86	3
4000	98	85	36	-81	-4	4	-159	4
6000	131	117	50	-112	-11	0	-223	5
8000	172	154	76	-139	-8	-9	-303	-2
10000	205	305	105	-150	-3	-23	-382	-16
12000	242	396	148	-147	21	-41	-482	-35
14000	278	454	204	-127	50	-70	-599	-64
16000	311	497	270	-84	95	-103	-726	-102
18000	342	561	352	-17	153	-145	-877	-149
20000	368	636	444	-7	221	-190	-1034	-200
22000	396	694	554	191	307	-249	-1234	-268
24000	424	736	674	325	412	-316	-1452	-337
25000	438	764	740	403	469	-353	-1576	-378
26000	443	775	784	456	504	-381	-1663	-407
27000	455	795	860	548	569	-428	-1809	-455
28000	468	811	946	650	642	-487	-1982	-413
29000	476	826	1024	746	711	-543	-2145	-468
30000	485	845	1110	853	799	-609	-2328	-631
31000	486	861	1169	924	855	-655	-2458	-676
32000	494	878	1275	1059	952	-746	-2706	-760
33000	496	897	1362	1165	1033	-825	-2917	-836
34000	501	914	1506	1349	1176	-959	-3267	-960
35000	500	924	1617	1490	1283	-1062	-3535	-1054
36000	502	931	1746	1657	1413	-1189	-3861	-1169
37000	504	933	1902	1861	1582	-1348	-4255	-1312

Table C.3 (continued)

Test 3 / Frame 3								
Load (lbs)	G1	G2	G3L	G4	G5	G6	G7	G8
38000	498	929	2075	2093	1763	-1524	-4689	-1468
39000	485	924	2280	2368	1977	-1733	-5197	-1752
40000	476	912	2514	2690	2238	-1983	-5806	-1866
41000	460	895	2820	3103	2573	-2280	-6540	-2120
42000	430	862	3242	3659	3033	-2668	-7519	-2448
43000	385	821	3820	4400	3659	-3145	-8802	-2844

Table C.4 Laboratory strain data collected from frame 4

Test 4 / Frame 4								
Load (lbs)	G1	G2	G3	G4	G5	G6	G7	G8
0	0	0	0	0	0	0	0	0
500	10	9	0	-10	6	3	-14	4
1000	29	28	0	-32	17	10	-41	12
2000	50	47	-2	-50	28	13	-65	16
4000	92	86	6	-82	56	22	-112	27
6000	131	122	8	-121	77	27	-163	35
8000	164	151	5	-157	97	35	-209	55
10000	208	195	7	-195	120	42	-261	60
12000	272	283	9	-235	142	55	-315	68
14000	333	403	12	-271	166	67	-365	77
16000	390	484	15	-302	189	83	-411	83
18000	501	571	13	-343	208	120	-468	83
20000	582	661	20	-376	239	168	-522	85
22000	672	722	20	-409	261	189	-573	83
24000	757	793	25	-442	292	208	-631	82
26000	847	850	31	-473	321	214	-689	78
28000	945	897	37	-503	354	211	-749	73

Table C.4 (continued)

Test 4 / Frame 4								
Load (lbs)	G1	G2	G3	G4	G5	G6	G7	G8
30000	1014	935	42	-538	384	198	-819	59
32000	1090	970	52	-569	422	182	-892	41
34000	1170	1017	69	-595	469	158	-977	13
36000	1252	1053	84	-623	516	132	-1069	-25
38000	1321	1097	106	-649	572	100	-1172	-69
40000	1386	1136	137	-671	651	74	-1301	-123
41000	1412	1156	155	-680	692	64	-1365	-148
42000	1442	1180	184	-687	750	49	-1458	-186
43000	1469	1201	213	-695	808	40	-1551	-226
44000	1490	1219	247	-695	873	37	-1650	-263
45000	1515	1233	290	-685	944	41	-1742	-295
46000	1541	1255	348	-670	1038	55	-1863	-332
47000	1570	1278	434	-635	1173	93	-2025	-372
48000	1596	1297	514	-595	1284	132	-2154	-403
49000	1670	1318	634	-520	1449	213	-2338	-428
50000	1655	1338	788	-401	1659	350	-2553	-439
51000	1682	1354	990	-218	1927	570	-2820	-423
52000	1695	1366	1316	135	2385	1111	-3296	-329
53000	1710	1373	1715	416	2933	2147	-3979	-91
53700	1654	1262	4229	4289	5005	1335	-7989	1904

Table C.5 Laboratory strain data collected from frame 5

Test 5 / Frame 5								
Load (lbs)	G1	G2	G3	G4	G5	G6	G7	G8
0	0	0	0	0	0	0	0	0
500	13	12	-4	-12	3	-3	-14	-1
1000	39	35	-12	-37	10	-10	-43	-3
2000	65	58	-19	-73	17	-12	-69	-3
4000	98	86	-36	-111	23	-22	-117	-9
6000	131	119	-44	-147	35	-26	-157	-9
10000	210	159	-68	-247	56	-39	-256	-13
14000	287	325	-86	-339	80	-46	-349	-11
18000	385	564	-101	-433	111	-53	-453	-7
22000	496	678	-119	-530	141	-64	-573	-10
26000	619	763	-140	-629	171	-79	-702	-10
30000	693	845	-161	-730	210	-96	-850	-7
34000	762	933	-190	-845	259	-121	-1019	-5
38000	855	1028	-223	-977	327	-150	-1210	-12
42000	1004	1128	-274	-1170	418	-195	-1443	-35
46000	1133	1242	-341	-1389	553	-227	-1699	-106
48000	1203	1309	-396	-1524	633	-248	-1856	-187
50000	1287	1414	-433	-1616	716	-275	-2002	-328

The following presents the methodology used to convert strain data to the values tabulated in Tables C.6-C.14. Sources for equations used, and the equation numbers, are noted in brackets.

$$G3 = \varepsilon_y \tag{C-1}$$

$$G4 = \varepsilon_{xy} = \varepsilon_x \sin^2 \alpha + \varepsilon_y \cos^2 \alpha - \Gamma_{xy} \cos\alpha \sin\alpha \quad \text{[Ref. 8 equation 2.4-1]} \tag{C-2}$$

Therefore:

$$\Gamma_{xy} = 2 * \varepsilon_{xy} - \varepsilon_x - \varepsilon_y \tag{C-3}$$

Given that we are concerned with buckling of the knee web while still in the linear elastic region, Hooke's Law (for a linear homogeneous, isotropic material) will be used to solve for stresses. Also, assuming a state of plane stress ($\sigma_z = 0$), the equations are simplified to the following:

σ_1 = stress – strain curve fit equation from tension test (see appendix B) (C-4)

σ_2 = stress – strain curve fit equation from tension test (see appendix B) (C-5)

$$\sigma_3 = \sigma_y = \frac{E}{1-\nu^2}\left(\varepsilon_y + \nu\varepsilon_x\right) \quad \text{[Ref. 8 equation 2.2-5b]} \tag{C-6}$$

$$\sigma_5 = \sigma_x = \frac{E}{1-\nu^2}\left(\varepsilon_x + \nu\varepsilon_y\right) \quad \text{[Ref. 8 equation 2.2-3a]} \tag{C-7}$$

$$T_{xy} = \frac{E}{2(1+\nu)}\Gamma_{xy} \quad \text{[Ref. 8 equation 2.2-6a and 2.2-7]} \tag{C-8}$$

$$\sigma_{\max,\min} = \frac{\sigma_x + \sigma_y}{2} \pm \sqrt{\left(\frac{\sigma_x - \sigma_y}{2}\right)^2 + T_{xy}^2} \quad \text{[Ref. 8 equation 2.3-23]} \tag{C-9}$$

$$T_{\max} = \frac{\sigma_{\max} - \sigma_{\min}}{2} \quad \text{[Ref. 8 equation 2.3-25]} \tag{C-10}$$

$$\sigma_{vm} = \sqrt{\frac{1}{2}\left[\left(\sigma_{\max} - \sigma_{\min}\right)^2 + \left(\sigma_{\max}\right)^2 + \left(\sigma_{\min}\right)^2\right]} \quad \text{[Ref. 9, eq. 4.23b]} \tag{C-11}$$

Table C.6 Calculated stresses and shear strain from frame 1

Test 1 / Frame 1										
Load (lbs)	σ_1	σ_2	Γ_{xy}	σ_3, σ_y	T_{xy}	σ_5, σ_x	σ_{max}	σ_{min}	T_{max}	σ_{vm}
0	0.5	0.5	0	0.0	0.0	0.0	0.0	0.0	0.0	0.0
500	0.6	0.6	37	-0.1	0.4	-0.1	0.3	-0.5	0.4	0.6
1,000	1.0	0.9	120	-0.2	1.2	-0.2	1.0	-1.4	1.2	2.1
2,000	1.4	1.2	202	-0.3	2.0	-0.4	1.7	-2.3	2.0	3.5
3,000	1.8	1.5	285	-0.3	2.8	-0.4	2.4	-3.2	2.8	4.9
4,000	2.2	1.9	362	-0.4	3.6	-0.6	3.0	-4.1	3.6	6.2
5,000	2.5	2.2	442	-0.5	4.4	-0.8	3.7	-5.0	4.4	7.6
6,000	2.9	2.5	514	-0.7	5.1	-1.0	4.3	-5.9	5.1	8.8
7,000	3.3	2.9	596	-0.8	5.9	-1.2	4.9	-6.9	5.9	10.3
8,000	3.7	3.2	684	-1.0	6.8	-1.5	5.5	-8.0	6.8	11.8
9,000	4.0	3.5	762	-1.2	7.5	-1.8	6.0	-9.1	7.5	13.1
10,000	4.5	3.9	853	-1.5	8.4	-2.1	6.6	-10.3	8.4	14.7
11,000	4.8	4.3	945	-1.7	9.3	-2.5	7.3	-11.5	9.4	16.3
12,000	5.2	4.6	1,032	-2.0	10.2	-2.9	7.7	-12.7	10.2	17.9
13,000	5.6	5.0	1,125	-2.4	11.1	-3.4	8.2	-14.0	11.1	19.5
14,000	6.0	5.4	1,223	-2.7	12.1	-3.8	8.8	-15.4	12.1	21.2
15,000	6.4	5.8	1,320	-3.2	13.1	-4.4	9.3	-16.8	13.1	23.0
16,000	6.9	6.2	1,429	-3.6	14.1	-4.9	9.9	-18.4	14.2	24.9
17,000	7.3	6.6	1,525	-4.0	15.1	-5.5	10.3	-19.9	15.1	26.6
18,000	7.7	7.0	1,637	-4.6	16.2	-6.2	10.8	-21.6	16.2	28.6
19,000	8.2	7.3	1,758	-5.2	17.4	-7.1	11.3	-23.5	17.4	30.8
20,000	8.9	8.0	1,888	-5.9	18.7	-8.0	11.8	-25.6	18.7	33.1
21,000	9.6	8.9	2,016	-6.5	19.9	-8.9	12.2	-27.7	20.0	35.5
22,000	10.3	10.1	2,155	-7.3	21.3	-9.9	12.7	-30.0	21.4	38.0
23,000	11.2	11.3	2,295	-8.1	22.7	-11.0	13.2	-32.3	22.7	40.5
24,000	11.5	12.8	2,446	-9.1	24.2	-12.3	13.6	-34.9	24.2	43.3
25,000	12.0	14.0	2,610	-10.2	25.8	-13.7	13.9	-37.8	25.9	46.4
26,000	12.6	14.7	2,786	-11.4	27.6	-15.2	14.4	-40.9	27.6	49.6

Table C.6 (continued)

Test 1 / Frame 1										
Load (lbs)	σ_1	σ_2	Γ_{xy}	σ_3, σ_y	T_{xy}	σ_5, σ_x	σ_{max}	σ_{min}	T_{max}	σ_{vm}
27,000	13.1	15.5	2,964	-12.6	29.3	-16.7	14.7	-44.1	29.4	53.0
28,000	13.8	15.9	3,165	-14.1	31.3	-18.5	15.1	-47.7	31.4	56.7
29,000	14.6	16.3	3,378	-15.7	33.4	-20.5	15.4	-51.6	33.5	60.8
30,000	14.7	16.8	3,591	-17.4	35.5	-22.5	15.6	-55.6	35.6	64.8
31,000	15.1	17.6	3,814	-19.3	37.7	-24.8	15.8	-59.9	37.8	69.1
32,000	15.6	18.1	4,081	-21.6	40.4	-27.4	16.0	-65.0	40.5	74.3
33,000	16.1	18.6	4,339	-23.8	42.9	-30.1	16.1	-70.0	43.0	79.3
34,000	16.6	18.8	4,663	-26.7	46.1	-33.5	16.1	-76.4	46.2	85.6
35,000	17.2	18.9	4,989	-29.9	49.3	-37.1	16.0	-83.0	49.5	92.0
36,000	17.8	18.9	5,379	-33.7	53.2	-41.6	15.7	-91.0	53.3	99.8
37,000	18.3	18.7	5,792	-38.0	57.3	-46.4	15.2	-99.6	57.4	108.1
38,000	18.6	18.3	6,315	-43.4	62.5	-52.6	14.6	-110.6	62.6	118.6
39,000	18.8	18.0	6,894	-49.7	68.2	-59.9	13.6	-123.2	68.4	130.5
40,000	18.7	17.5	7,583	-56.8	75.0	-68.2	12.7	-137.7	75.2	144.5
41,000	18.5	16.8	8,389	-65.7	83.0	-78.3	11.2	-155.3	83.2	161.1
42,000	17.8	15.8	9,424	-77.0	93.2	-90.9	9.5	-177.4	93.5	182.4
43,000	16.5	14.2	10,951	-92.4	108.3	-109	8.0	-209	108.6	213.3

Table C.7 Calculated stresses and shear strain from frame 2

Test 2 / Frame 2									
Load (lbs)	σ_1	σ_2	Γ_{xy}	σ_3, σ_y	T_{xy}	σ_5, σ_x	σ_{max}	σ_{min}	T_{max}
0	0.5	0.5	0	0.0	0.0	0.0	0.0	0.0	0.0
500	0.6	0.6	22	0.0	0.2	0.0	0.2	-0.2	0.2
1,000	1.0	1.0	85	0.0	0.8	0.0	0.9	-0.8	0.8
2,000	1.4	1.2	131	0.0	1.3	0.0	1.3	-1.3	1.3
3,000	1.8	1.7	188	0.0	1.9	-0.2	1.8	-2.0	1.9
4,000	2.0	1.9	241	-0.3	2.4	-0.3	2.1	-2.7	2.4

Table C.7 (continued)

Test 2 / Frame 2									
Load (lbs)	σ_1	σ_2	Γ_{xy}	σ_3, σ_y	T_{xy}	σ_5, σ_x	σ_{max}	σ_{min}	T_{max}
5,000	2.4	2.2	293	-0.2	2.9	-0.2	2.7	-3.1	2.9
6,000	2.7	2.5	334	-0.2	3.3	-0.2	3.1	-3.5	3.3
7,000	3.3	3.1	404	-0.1	4.0	0.0	3.9	-4.1	4.0
8,000	3.6	3.3	456	-0.2	4.5	-0.1	4.3	-4.7	4.5
9,000	4.7	3.6	515	-0.1	5.1	0.0	5.0	-5.1	5.1
10,000	6.0	3.9	573	0.1	5.7	0.2	5.9	-5.5	5.7
11,000	7.1	4.2	639	0.0	6.3	0.1	6.4	-6.3	6.3
12,000	7.6	4.3	686	-0.1	6.8	0.1	6.8	-6.8	6.8
13,000	8.0	4.8	760	0.2	7.5	0.3	7.7	-7.3	7.5
14,000	8.7	5.1	834	0.4	8.2	0.6	8.8	-7.7	8.2
15,000	9.3	5.4	892	0.5	8.8	0.6	9.4	-8.2	8.8
16,000	9.9	5.7	957	0.7	9.5	0.8	10.2	-8.7	9.5
17,000	10.6	5.9	1,024	0.8	10.1	0.9	11.0	-9.3	10.1
18,000	11.4	6.2	1,081	0.9	10.7	1.1	11.7	-9.7	10.7
19,000	12.1	6.7	1,145	0.9	11.3	1.1	12.3	-10.3	11.3
20,000	12.8	6.8	1,213	0.9	12.0	1.2	13.1	-10.9	12.0
21,000	13.7	7.2	1,287	1.2	12.7	1.5	14.0	-11.4	12.7
22,000	14.4	7.7	1,357	1.4	13.4	1.7	15.0	-11.9	13.4
23,000	15.0	8.0	1,427	1.5	14.1	1.9	15.8	-12.4	14.1
24,000	15.9	8.8	1,518	1.8	15.0	2.3	17.0	-13.0	15.0
25,000	16.6	9.8	1,588	1.9	15.7	2.4	17.9	-13.6	15.7
26,000	17.2	10.8	1,670	1.9	16.5	2.5	18.7	-14.3	16.5
27,000	17.8	11.6	1,749	2.0	17.3	2.7	19.6	-15.0	17.3
28,000	18.5	12.4	1,840	2.1	18.2	2.9	20.7	-15.7	18.2
29,000	19.0	13.3	1,927	2.2	19.1	3.1	21.7	-16.4	19.1
30,000	19.8	16.3	2,025	2.3	20.0	3.3	22.9	-17.2	20.0
31,000	21.0	18.6	2,141	2.8	21.2	4.1	24.7	-17.7	21.2
32,000	21.8	19.7	2,236	3.1	22.1	4.5	25.9	-18.3	22.1

Table C.7 (continued)

Test 2 / Frame 2									
Load (lbs)	σ_1	σ_2	Γ_{xy}	σ_3, σ_y	T_{xy}	σ_5, σ_x	σ_{max}	σ_{min}	T_{max}
33,000	22.6	20.7	2,347	3.4	23.2	5.0	27.4	-19.0	23.2
34,000	23.5	21.7	2,458	3.6	24.3	5.4	28.9	-19.8	24.3
35,000	24.4	22.9	2,593	3.9	25.6	6.0	30.6	-20.7	25.7
36,000	25.1	23.7	2,718	4.1	26.9	6.4	32.2	-21.7	26.9
37,000	25.8	24.6	2,854	4.2	28.2	7.0	33.9	-22.6	28.3
38,000	26.8	25.4	3,049	4.6	30.2	7.9	36.4	-24.0	30.2
39,000	27.6	26.0	3,221	5.0	31.9	8.9	38.9	-24.9	31.9
40,000	28.2	26.3	3,360	5.2	33.2	9.6	40.7	-25.9	33.3
41,000	28.8	26.9	3,565	5.3	35.3	10.5	43.3	-27.4	35.4
42,000	29.6	27.6	3,805	5.6	37.6	11.8	46.5	-29.0	37.8
43,000	30.2	28.2	4,077	5.8	40.3	13.4	50.1	-30.9	40.5
44,000	30.8	28.8	4,370	6.0	43.2	15.2	54.1	-32.9	43.5
45,000	31.5	29.4	4,733	6.1	46.8	17.5	58.9	-35.4	47.2
46,000	31.7	29.7	5,101	5.9	50.5	19.7	63.7	-38.1	50.9
47,000	32.4	30.4	5,537	5.9	54.8	22.5	69.6	-41.2	55.4
48,000	32.6	30.9	6,143	5.9	60.8	26.6	77.9	-45.4	61.6
49,000	33.0	31.5	6,898	6.5	68.2	31.6	88.4	-50.3	69.4
50,000	33.3	31.8	7,829	7.2	77.4	37.4	101.2	-56.6	78.9
51,000	33.6	32.0	9,345	9.2	92.4	46.6	122.2	-66.4	94.3
52,000	33.8	32.0	11,486	12.6	113.6	58.8	151.6	-80.2	115.9
53,000	33.5	31.1	15,801	21.6	156.3	83.4	211.8	-106.8	159.3

Table C.8 Additional calculated stresses and shear strain from frame 2

Test 2 / Frame 2								
Load (lbs)	Γ_{xy}	σ_6, σ_y	T_{xy}	σ_8, σ_x	σ_{max}	σ_{min}	T_{max}	σ_{vm}
0	0	0.0	0.0	0.0	0.0	0.0	0.0	0.0
500	23	0.1	0.2	0.2	0.4	-0.1	0.2	0.4
1,000	84	0.3	0.8	0.5	1.2	-0.4	0.8	1.5
2,000	128	0.5	1.3	0.8	1.9	-0.7	1.3	2.3
3,000	180	0.5	1.8	1.0	2.5	-1.1	1.8	3.2
4,000	228	0.7	2.3	1.3	3.3	-1.3	2.3	4.1
5,000	271	0.7	2.7	1.6	3.8	-1.6	2.7	4.8
6,000	311	0.9	3.1	1.9	4.5	-1.7	3.1	5.6
7,000	367	1.1	3.6	2.3	5.3	-2.0	3.7	6.6
8,000	414	1.2	4.1	2.5	6.0	-2.3	4.1	7.4
9,000	461	1.4	4.6	2.9	6.8	-2.4	4.6	8.3
10,000	507	1.6	5.0	3.2	7.5	-2.7	5.1	9.1
11,000	562	1.7	5.6	3.5	8.2	-3.0	5.6	10.1
12,000	601	1.7	5.9	3.7	8.7	-3.3	6.0	10.8
13,000	658	2.0	6.5	4.2	9.7	-3.5	6.6	11.8
14,000	714	2.4	7.1	4.7	10.7	-3.6	7.2	12.9
15,000	761	2.6	7.5	5.1	11.5	-3.8	7.6	13.8
16,000	810	2.8	8.0	5.4	12.3	-4.0	8.1	14.7
17,000	862	3.1	8.5	5.8	13.1	-4.2	8.6	15.6
18,000	907	3.3	9.0	6.2	13.8	-4.4	9.1	16.4
19,000	956	3.5	9.5	6.5	14.5	-4.6	9.6	17.3
20,000	1,009	3.7	10.0	6.9	15.4	-4.8	10.1	18.3
21,000	1,065	4.1	10.5	7.4	16.4	-4.9	10.7	19.3
22,000	1,115	4.4	11.0	7.8	17.3	-5.0	11.2	20.3
23,000	1,168	4.7	11.6	8.3	18.2	-5.2	11.7	21.3
24,000	1,230	5.2	12.2	8.8	19.3	-5.3	12.3	22.4
25,000	1,280	5.5	12.7	9.1	20.1	-5.5	12.8	23.3
26,000	1,337	5.7	13.2	9.5	21.0	-5.7	13.4	24.4

Table C.8 (continued)

Test 2 / Frame 2								
Load (lbs)	Γ_{xy}	σ_6, σ_y	T_{xy}	σ_8, σ_x	σ_{max}	σ_{min}	T_{max}	σ_{vm}
27,000	1,393	6.1	13.8	9.9	21.9	-5.9	13.9	25.4
28,000	1,452	6.5	14.4	10.3	22.9	-6.1	14.5	26.5
29,000	1,511	7.0	14.9	10.9	24.0	-6.1	15.1	27.6
30,000	1,570	7.4	15.5	11.4	25.1	-6.2	15.7	28.7
31,000	1,643	8.4	16.3	12.4	26.7	-6.0	16.4	30.2
32,000	1,695	9.0	16.8	13.0	27.9	-5.9	16.9	31.2
33,000	1,765	9.9	17.5	13.8	29.4	-5.7	17.6	32.6
34,000	1,828	10.7	18.1	14.6	30.8	-5.6	18.2	33.9
35,000	1,902	11.7	18.8	15.5	32.5	-5.3	18.9	35.5
36,000	1,969	12.7	19.5	16.4	34.1	-5.0	19.6	36.9
37,000	2,041	14.0	20.2	17.6	36.0	-4.5	20.3	38.5
38,000	2,135	15.7	21.1	19.2	38.6	-3.7	21.2	40.6
39,000	2,218	17.5	21.9	20.8	41.1	-2.9	22.0	42.6
40,000	2,287	18.8	22.6	22.0	43.1	-2.3	22.7	44.3
41,000	2,377	20.8	23.5	23.8	45.9	-1.3	23.6	46.5
42,000	2,479	23.4	24.5	26.1	49.3	0.2	24.6	49.2
43,000	2,585	26.2	25.6	28.6	53.0	1.8	25.6	52.1
44,000	2,702	29.2	26.7	31.4	57.0	3.5	26.7	55.3
45,000	2,829	32.6	28.0	34.4	61.5	5.5	28.0	58.9
46,000	2,951	35.8	29.2	37.3	65.7	7.3	29.2	62.4
47,000	3,079	39.3	30.5	40.5	70.3	9.4	30.5	66.1
48,000	3,221	43.3	31.9	44.3	75.7	11.9	31.9	70.5
49,000	3,364	47.5	33.3	48.3	81.1	14.6	33.3	74.9
50,000	3,499	51.6	34.6	52.3	86.6	17.3	34.6	79.3
51,000	3,659	57.3	36.2	57.9	93.8	21.4	36.2	85.1
52,000	4,001	68.5	39.6	65.5	106.6	27.4	39.6	95.9
53,000	3,962	70.5	39.2	72.6	110.7	32.3	39.2	98.6

Table C.9 Calculated stresses and shear strain from frame 3

Test 3 / Frame 3									
Load (lbs)	σ_1	σ_2	$\Gamma_{xy,4}$	σ_3, σ_y	$T_{xy,4}$	σ_5, σ_x	σ_{max}	σ_{min}	T_{max}
0	0	0	0	0.0	0.0	0.0	0.0	0.0	0.0
500	0.6	0.8	22	0.1	0.2	0.0	0.3	-0.1	0.2
1,000	1.1	1.0	63	0.3	0.6	0.1	0.8	-0.4	0.6
2,000	1.6	1.4	105	0.5	1.0	0.1	1.4	-0.7	1.1
4,000	2.5	2.2	194	1.0	1.9	0.2	2.5	-1.4	2.0
6,000	3.2	2.9	263	1.3	2.6	0.1	3.4	-2.0	2.7
8,000	4.2	3.7	346	2.1	3.4	0.4	4.7	-2.3	3.5
10,000	4.9	7.4	402	2.9	4.0	0.8	6.0	-2.3	4.1
12,000	5.9	9.8	463	4.3	4.6	1.8	7.8	-1.7	4.7
14,000	6.8	11.4	508	6.1	5.0	3.0	9.8	-0.7	5.3
16,000	7.6	12.6	533	8.3	5.3	4.8	12.1	1.0	5.5
18,000	8.4	14.4	539	11.0	5.3	7.1	14.8	3.4	5.7
20,000	9.1	16.5	679	14.2	6.7	9.7	19.0	4.9	7.1
22,000	9.8	18.2	479	17.9	4.7	13.0	20.8	10.1	5.3
24,000	10.6	19.4	436	22.1	4.3	16.9	24.5	14.5	5.0
25,000	11.0	20.2	403	24.4	4.0	19.0	26.5	16.9	4.8
26,000	11.1	20.5	376	25.9	3.7	20.4	27.8	18.5	4.6
27,000	11.5	21.1	333	28.6	3.3	22.8	30.1	21.3	4.4
28,000	11.8	21.5	288	31.5	2.8	25.5	32.7	24.4	4.1
29,000	12.0	21.9	243	34.3	2.4	28.1	35.1	27.3	3.9
30,000	12.3	22.5	203	37.4	2.0	31.2	38.0	30.6	3.7
31,000	12.3	22.9	176	39.5	1.7	33.3	39.9	32.8	3.6
32,000	12.5	23.4	109	43.2	1.1	36.8	43.4	36.6	3.4
33,000	12.6	23.9	65	46.3	0.6	39.8	46.4	39.7	3.3
34,000	12.7	24.4	16	51.5	0.2	44.9	51.5	44.9	3.3
35,000	12.7	24.7	80	55.4	0.8	48.8	55.5	48.7	3.4
36,000	12.8	24.9	155	60.1	1.5	53.5	60.4	53.1	3.6
37,000	12.8	25.0	238	65.8	2.4	59.4	66.6	58.7	3.9

Table C.9 (continued)

Test 3 / Frame 3									
Load (lbs)	σ_1	σ_2	$\Gamma_{xy,4}$	σ_3, σ_y	$T_{xy,4}$	σ_5, σ_x	σ_{max}	σ_{min}	T_{max}
38,000	12.6	24.8	348	72.1	3.4	65.9	73.6	64.3	4.6
39,000	12.3	24.7	479	79.5	4.7	73.5	82.1	70.9	5.6
40,000	12.0	24.4	628	88.1	6.2	82.7	92.2	78.6	6.8
41,000	11.6	23.9	813	99.4	8.0	94.5	105.3	88.5	8.4
42,000	10.8	23.0	1,043	114.8	10.3	110.7	123.3	102.2	10.5
43,000	9.6	21.8	1,321	136.0	13.1	132.8	147.6	121.2	13.2

Table C.10 Additional calculated stresses and shear strain from frame 3

Test 3 / Frame 3								
Load (lbs)	$\Gamma_{xy,7}$	σ_6, σ_y	$T_{xy,7}$	σ_8, σ_x	σ_{max}	σ_{min}	T_{max}	σ_{vm}
0	0	0.0	0.0	0.0	0.0	0.0	0.0	0.0
500	34	0.0	0.3	0.0	0.3	-0.3	0.3	0.6
1,000	104	0.0	1.0	0.1	1.1	-1.0	1.0	1.8
2,000	180	0.2	1.8	0.1	1.9	-1.6	1.8	3.1
4,000	326	0.1	3.2	0.1	3.4	-3.1	3.2	5.6
6,000	451	0.0	4.5	0.1	4.6	-4.4	4.5	7.7
8,000	595	-0.3	5.9	-0.1	5.7	-6.1	5.9	10.2
10,000	725	-0.8	7.2	-0.6	6.5	-7.9	7.2	12.4
12,000	888	-1.4	8.8	-1.3	7.4	-10.1	8.8	15.3
14,000	1,064	-2.5	10.5	-2.3	8.1	-12.9	10.5	18.4
16,000	1,247	-3.7	12.3	-3.7	8.6	-16.0	12.3	21.7
18,000	1,460	-5.2	14.4	-5.3	9.2	-19.7	14.4	25.6
20,000	1,678	-6.9	16.6	-7.1	9.6	-23.6	16.6	29.6
22,000	1,951	-9.1	19.3	-9.5	10.0	-28.6	19.3	34.7
24,000	2,251	-11.5	22.3	-11.9	10.5	-34.0	22.3	40.3
25,000	2,421	-12.9	23.9	-13.4	10.8	-37.1	23.9	43.5

Table C.10 (continued)

Test 3 / Frame 3								
Load (lbs)	$\Gamma_{xy,7}$	σ_6, σ_y	$T_{xy,7}$	σ_8, σ_x	σ_{max}	σ_{min}	T_{max}	σ_{vm}
26,000	2,538	-13.9	25.1	-14.4	10.9	-39.3	25.1	45.7
27,000	2,735	-15.6	27.1	-16.1	11.2	-42.9	27.1	49.5
28,000	3,064	-16.9	30.3	-15.4	14.1	-46.5	30.3	54.9
29,000	3,279	-18.9	32.4	-17.4	14.3	-50.6	32.4	59.1
30,000	3,416	-22.1	33.8	-22.5	11.5	-56.1	33.8	62.6
31,000	3,585	-23.7	35.5	-24.1	11.5	-59.4	35.5	65.9
32,000	3,906	-26.9	38.6	-27.2	11.6	-65.7	38.6	72.2
33,000	4,173	-29.7	41.3	-30.0	11.4	-71.1	41.3	77.5
34,000	4,615	-34.5	45.6	-34.5	11.2	-80.1	45.6	86.3
35,000	4,954	-38.1	49.0	-37.9	11.0	-87.0	49.0	93.0
36,000	5,364	-42.6	53.1	-42.2	10.7	-95.4	53.1	101.2
37,000	5,850	-48.2	57.9	-47.4	10.1	-105.7	57.9	111.0
38,000	6,386	-54.3	63.2	-53.2	9.4	-116.9	63.2	121.9
39,000	6,909	-62.4	68.3	-62.8	5.7	-131.0	68.3	133.9
40,000	7,763	-70.3	76.8	-68.0	7.6	-146.0	76.8	149.9
41,000	8,680	-80.7	85.9	-77.5	6.8	-164.9	85.9	168.4
42,000	9,922	-94.1	98.1	-89.8	6.2	-190.1	98.2	193.3
43,000	11,615	-110.6	114.9	-104.6	7.3	-222.5	114.9	226.3

Table C.11 Calculated stresses and shear strain from frame 4

Test 4 / Frame 4									
Load (lbs)	σ_1	σ_2	$\Gamma_{xy,4}$	σ_3, σ_y	$T_{xy,4}$	σ_5, σ_x	σ_{max}	σ_{min}	T_{max}
0	0	0	0	0.0	0.0	0.0	0.0	0.0	0.0
500	0.6	0.6	26	0.0	0.3	0.2	0.4	-0.2	0.3
1,000	1.0	1.0	81	0.1	0.8	0.5	1.1	-0.5	0.8
2,000	1.5	1.4	126	0.2	1.2	0.8	1.7	-0.8	1.3
4,000	2.3	2.2	226	0.6	2.2	1.6	3.4	-1.2	2.3
6,000	3.2	3.0	327	0.8	3.2	2.2	4.8	-1.8	3.3
8,000	4.0	3.7	416	0.9	4.1	2.7	6.0	-2.4	4.2
10,000	5.0	4.7	517	1.2	5.1	3.4	7.5	-3.0	5.2
12,000	6.6	6.9	621	1.4	6.1	4.0	9.0	-3.6	6.3
14,000	8.2	10.0	720	1.7	7.1	4.7	10.5	-4.1	7.3
16,000	9.7	12.3	808	1.9	8.0	5.4	11.8	-4.5	8.2
18,000	12.7	14.7	907	2.0	9.0	5.9	13.1	-5.2	9.2
20,000	15.0	17.2	1011	2.5	10.0	6.8	14.9	-5.6	10.2
22,000	17.6	19.0	1099	2.7	10.9	7.4	16.2	-6.1	11.1
24,000	20.0	21.0	1201	3.1	11.9	8.3	17.9	-6.5	12.2
26,000	22.5	22.6	1298	3.5	12.8	9.2	19.5	-6.8	13.2
28,000	25.3	23.9	1397	3.9	13.8	10.2	21.2	-7.1	14.2
30,000	27.2	25.0	1502	4.3	14.9	11.0	22.9	-7.6	15.2
32,000	29.3	26.0	1612	4.9	15.9	12.2	24.9	-7.8	16.4
34,000	31.4	27.3	1728	5.7	17.1	13.6	27.2	-7.9	17.5
36,000	33.5	28.3	1846	6.5	18.3	15.1	29.5	-8.0	18.8
38,000	35.2	29.5	1976	7.6	19.5	16.8	32.3	-7.9	20.1
40,000	36.8	30.5	2130	9.1	21.1	19.2	35.8	-7.5	21.7
41,000	37.5	31.0	2207	9.9	21.8	20.5	37.7	-7.2	22.5
42,000	38.2	31.7	2308	11.2	22.8	22.4	40.3	-6.7	23.5
43,000	38.8	32.2	2411	12.5	23.8	24.2	42.9	-6.2	24.6
44,000	39.3	32.7	2510	13.9	24.8	26.3	45.7	-5.5	25.6
45,000	39.8	33.0	2604	15.7	25.8	28.6	48.7	-4.4	26.6

Table C.11 (continued)

Test 4 / Frame 4									
Load (lbs)	σ_1	σ_2	$\Gamma_{xy,4}$	σ_3, σ_y	$T_{xy,4}$	σ_5, σ_x	σ_{max}	σ_{min}	T_{max}
46,000	40.4	33.6	2726	18.1	27.0	31.7	52.7	-2.9	27.8
47,000	41.1	34.2	2877	21.6	28.5	36.2	58.3	-0.5	29.4
48,000	41.6	34.7	2988	24.7	29.6	39.9	62.8	1.8	30.5
49,000	43.2	35.2	3123	29.4	30.9	45.5	69.4	5.5	31.9
50,000	42.9	35.7	3249	35.4	32.1	52.6	77.2	10.7	33.3
51,000	43.4	36.1	3353	43.2	33.2	61.7	86.9	18.0	34.4
52,000	43.7	36.4	3431	55.9	33.9	77.1	102.1	31.0	35.5
53,000	44.0	36.5	3816	71.5	37.7	95.6	123.1	43.9	39.6
53,700	42.8	33.8	656	158.3	6.5	173.6	176.0	155.9	10.1

Table C.12 Additional calculated stresses and shear strain from frame 4

Test 4 / Frame 4								
Load (lbs)	$\Gamma_{xy,7}$	σ_6, σ_y	$T_{xy,7}$	σ_8, σ_x	σ_{max}	σ_{min}	T_{max}	σ_{vm}
0	0	0.0	0.0	0.0	0.0	0.0	0.0	0.0
500	35	0.1	0.3	0.1	0.5	-0.2	0.3	0.6
1,000	104	0.4	1.0	0.4	1.4	-0.6	1.0	1.8
2,000	159	0.5	1.6	0.6	2.1	-1.1	1.6	2.8
4,000	273	0.8	2.7	0.9	3.6	-1.8	2.7	4.8
6,000	388	1.0	3.8	1.2	5.0	-2.7	3.8	6.7
8,000	508	1.4	5.0	1.8	6.6	-3.4	5.0	8.9
10,000	624	1.7	6.2	2.0	8.0	-4.3	6.2	10.9
12,000	753	2.1	7.4	2.3	9.7	-5.2	7.4	13.1
14,000	874	2.5	8.6	2.7	11.2	-6.1	8.6	15.2
16,000	988	3.0	9.8	3.0	12.8	-6.8	9.8	17.2
18,000	1,139	4.0	11.3	3.3	14.9	-7.6	11.3	19.9
20,000	1,297	5.4	12.8	3.7	17.4	-8.3	12.9	22.7

Table C.12 (continued)

Test 4 / Frame 4								
Load (lbs)	$\Gamma_{xy,7}$	σ_6, σ_y	$T_{xy,7}$	σ_8, σ_x	σ_{max}	σ_{min}	T_{max}	σ_{vm}
22,000	1,418	5.9	14.0	3.8	19.0	-9.2	14.1	24.8
24,000	1,552	6.5	15.4	4.0	20.6	-10.2	15.4	27.2
26,000	1,670	6.6	16.5	3.9	21.8	-11.3	16.6	29.2
28,000	1,782	6.5	17.6	3.7	22.8	-12.6	17.7	31.0
30,000	1,895	6.0	18.7	3.2	23.4	-14.2	18.8	32.9
32,000	2,007	5.4	19.9	2.6	23.9	-15.9	19.9	34.7
34,000	2,125	4.5	21.0	1.6	24.1	-18.0	21.1	36.6
36,000	2,245	3.5	22.2	0.4	24.2	-20.3	22.3	38.6
38,000	2,375	2.2	23.5	-1.1	24.1	-23.0	23.5	40.8
40,000	2,553	1.1	25.3	-2.8	24.4	-26.2	25.3	43.9
41,000	2,646	0.6	26.2	-3.6	24.7	-27.8	26.3	45.5
42,000	2,779	-0.1	27.5	-4.8	25.1	-30.0	27.6	47.8
43,000	2,916	-0.7	28.8	-6.0	25.6	-32.3	29.0	50.3
44,000	3,074	-1.1	30.4	-7.0	26.5	-34.6	30.5	53.1
45,000	3,230	-1.2	31.9	-7.9	27.6	-36.7	32.1	55.8
46,000	3,449	-1.2	34.1	-8.8	29.3	-39.3	34.3	59.7
47,000	3,771	-0.4	37.3	-9.6	32.6	-42.6	37.6	65.3
48,000	4,037	0.4	39.9	-10.2	35.4	-45.1	40.3	69.9
49,000	4,461	2.5	44.1	-10.2	40.7	-48.4	44.6	77.3
50,000	5,017	6.2	49.6	-9.4	48.6	-51.8	50.2	87.0
51,000	5,787	12.5	57.2	-7.2	60.7	-55.4	58.1	100.6
52,000	7,374	28.3	72.9	-0.2	88.4	-60.3	74.3	129.5
53,000	10,014	59.1	99.0	14.8	138.4	-64.5	101.5	179.6
53,700	19,217	52.6	190.1	63.8	248.4	-131.9	190.2	334.5

Table C.13 Calculated stresses and shear strain from frame 5

Test 5 / Frame 5									
Load (lbs)	σ_1	σ_2	$\Gamma_{xy,4}$	σ_3, σ_y	$T_{xy,4}$	σ_5, σ_x	σ_{max}	σ_{min}	T_{max}
0	0.5	0.5	0	0.0	0.0	0.0	0.0	0.0	0.0
500	0.7	0.7	23	-0.1	0.2	0.1	0.2	-0.3	0.2
1,000	1.2	1.1	72	-0.3	0.7	0.2	0.7	-0.8	0.7
2,000	1.8	1.6	144	-0.4	1.4	0.3	1.4	-1.5	1.5
4,000	2.5	2.2	209	-0.8	2.1	0.3	1.9	-2.4	2.1
6,000	3.2	2.9	285	-0.9	2.8	0.6	2.8	-3.1	2.9
10,000	5.1	3.9	482	-1.4	4.8	1.0	4.7	-5.1	4.9
14,000	7.0	8.0	672	-1.7	6.6	1.5	6.7	-7.0	6.8
18,000	9.6	14.5	876	-1.9	8.7	2.3	9.1	-8.7	8.9
22,000	12.6	17.7	1,082	-2.2	10.7	3.0	11.4	-10.6	11.0
26,000	16.0	20.1	1,289	-2.5	12.7	3.6	13.7	-12.6	13.1
30,000	18.2	22.5	1,509	-2.8	14.9	4.6	16.3	-14.5	15.4
34,000	20.1	25.0	1,759	-3.2	17.4	5.7	19.2	-16.7	18.0
38,000	22.8	27.6	2,058	-3.6	20.4	7.3	22.9	-19.2	21.1
42,000	26.9	30.3	2,484	-4.3	24.6	9.4	28.1	-22.9	25.5
46,000	30.4	33.3	2,990	-5.0	29.6	12.7	34.7	-27.1	30.9
48,000	32.3	35.0	3,285	-5.9	32.5	14.4	38.3	-29.8	34.0
50,000	34.4	37.5	3,515	-6.3	34.8	16.5	41.7	-31.5	36.6

Table C.14 Additional calculated stresses and shear strain from frame 5

Test 5 / Frame 5								
Load (lbs)	$\Gamma_{xy,7}$	σ_6, σ_y	$T_{xy,7}$	σ_8, σ_x	σ_{max}	σ_{min}	T_{max}	σ_{vm}
0	0	0.0	0.0	0.0	0.0	0.0	0.0	0.0
500	24	-0.1	0.2	-0.1	0.2	-0.3	0.2	0.4
1,000	73	-0.3	0.7	-0.2	0.5	-1.0	0.7	1.3
2,000	123	-0.4	1.2	-0.2	1.0	-1.5	1.2	2.1
4,000	203	-0.7	2.0	-0.4	1.5	-2.6	2.0	3.5
6,000	279	-0.8	2.8	-0.5	2.1	-3.4	2.8	4.8
10,000	460	-1.2	4.5	-0.7	3.6	-5.5	4.6	7.9
14,000	641	-1.4	6.3	-0.7	5.3	-7.4	6.3	11.0
18,000	846	-1.5	8.4	-0.6	7.3	-9.5	8.4	14.6
22,000	1,072	-1.9	10.6	-0.8	9.3	-11.9	10.6	18.4
26,000	1,315	-2.3	13.0	-0.9	11.4	-14.6	13.0	22.6
30,000	1,597	-2.7	15.8	-1.0	14.0	-17.7	15.8	27.5
34,000	1,912	-3.4	18.9	-1.1	16.7	-21.2	18.9	32.9
38,000	2,258	-4.3	22.3	-1.5	19.5	-25.3	22.4	38.9
42,000	2,656	-5.7	26.3	-2.6	22.2	-30.5	26.3	45.8
46,000	3,065	-7.2	30.3	-4.8	24.4	-36.3	30.3	52.9
48,000	3,277	-8.4	32.4	-7.2	24.6	-40.2	32.4	56.7
50,000	3,401	-10.3	33.6	-11.4	22.8	-44.5	33.6	59.3

APPENDIX D

FINITE ELEMENT RESULTS

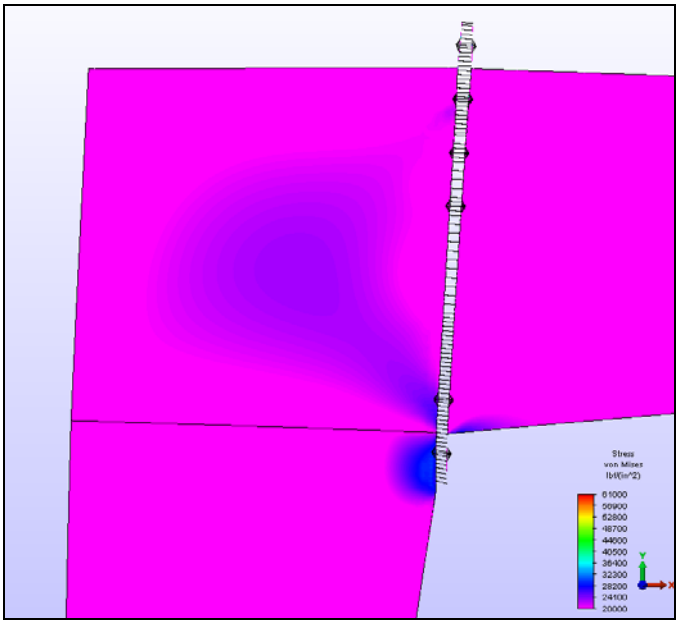

Figure D.1 Frame 1 von Mises Stress in knee web with a 20 kip load applied

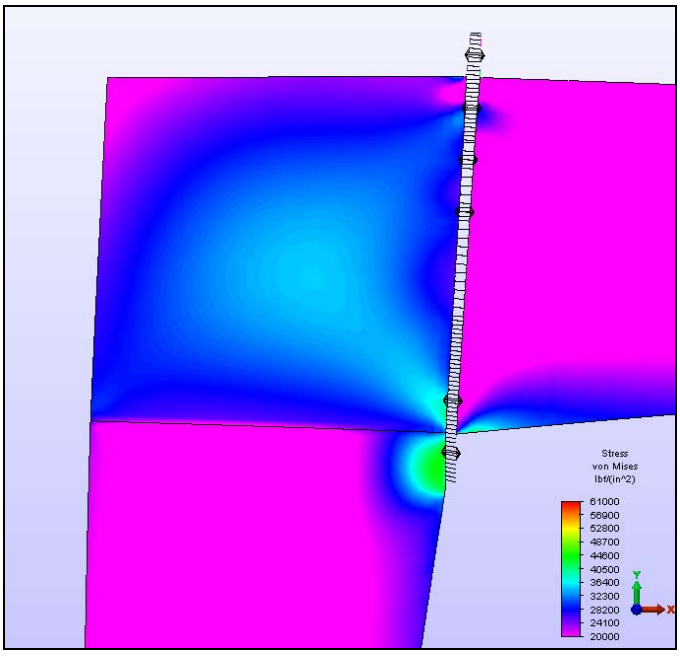

Figure D.2 Frame 1 von Mises Stress in knee web with a 30 kip load applied

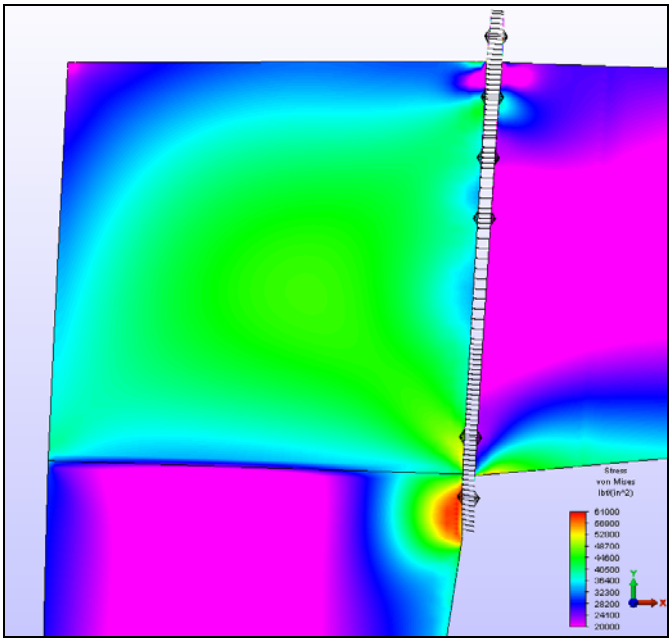

Figure D.3 Frame 1 von Mises Stress in knee web with a 40 kip load applied

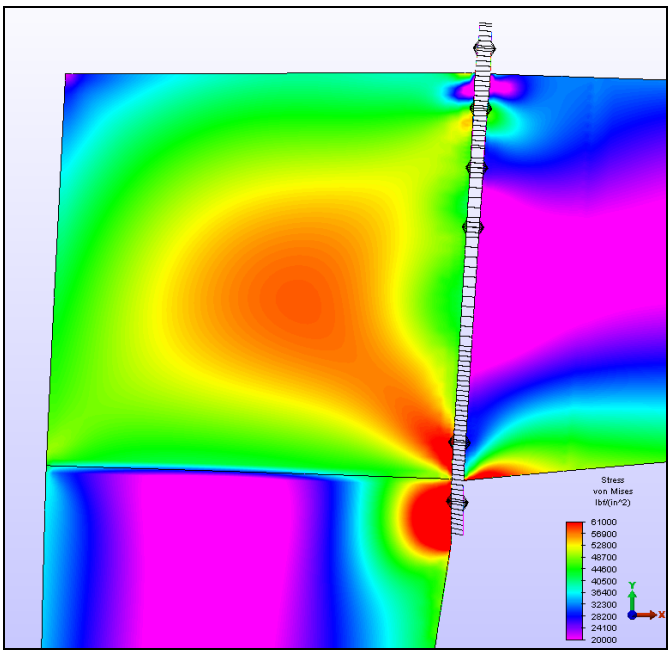

Figure D.4 Frame 1 von Mises Stress in knee web with a 50 kip load applied

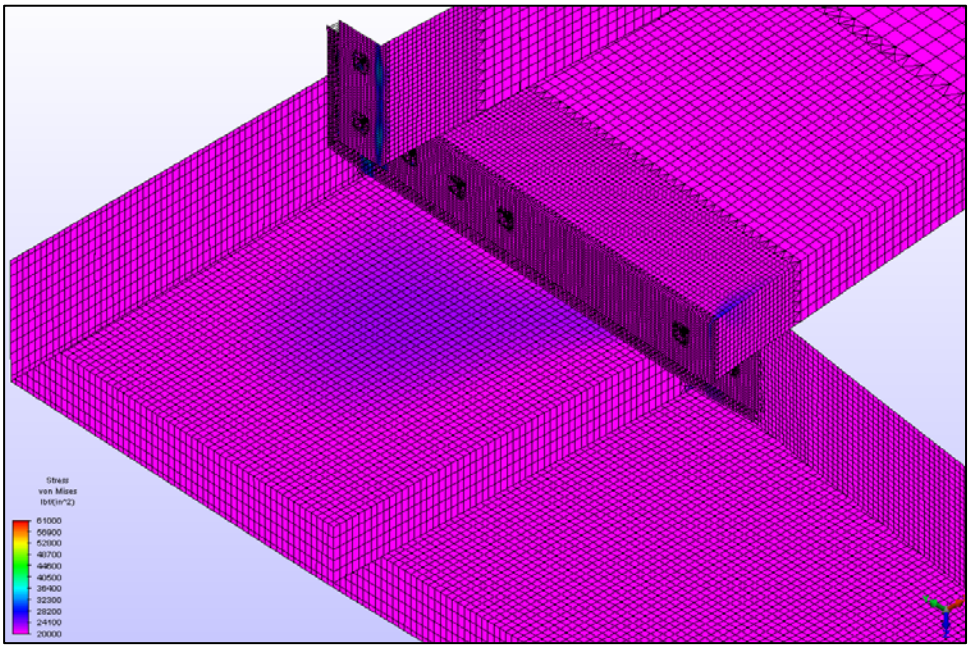

Figure D.5 Frame 1 von Mises Stress in knee with a 20 kip load applied

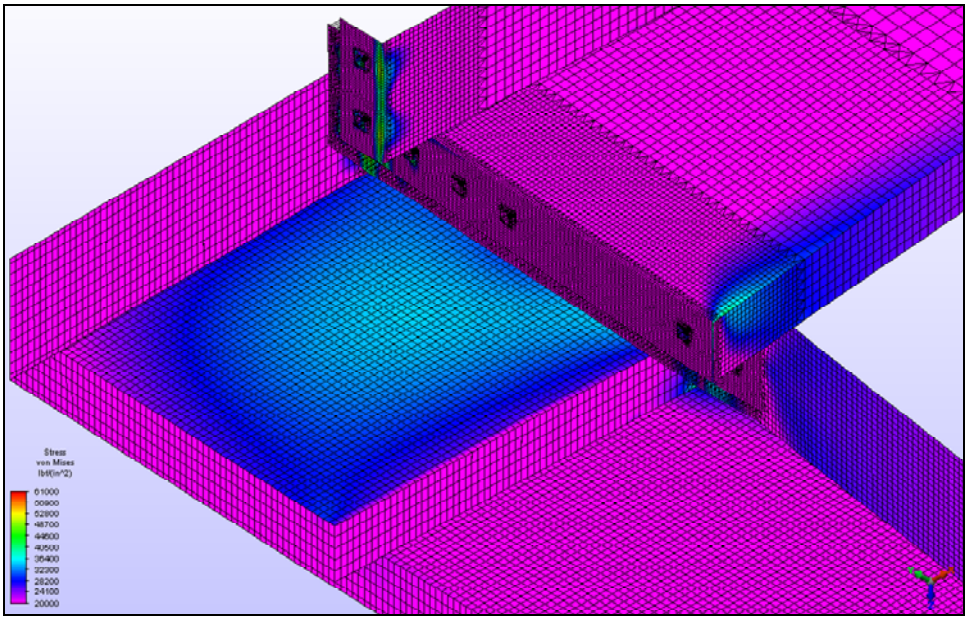

Figure D.6 Frame 1 von Mises Stress in the knee with a 30 kip load applied

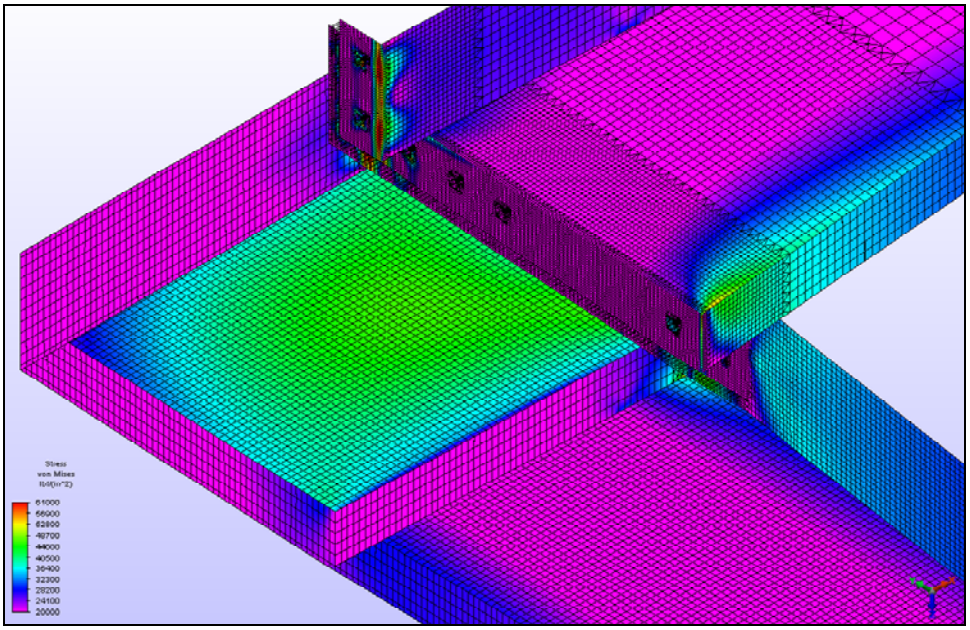

Figure D.7 Frame 1 von Mises Stress in the knee with a 40 kip load applied

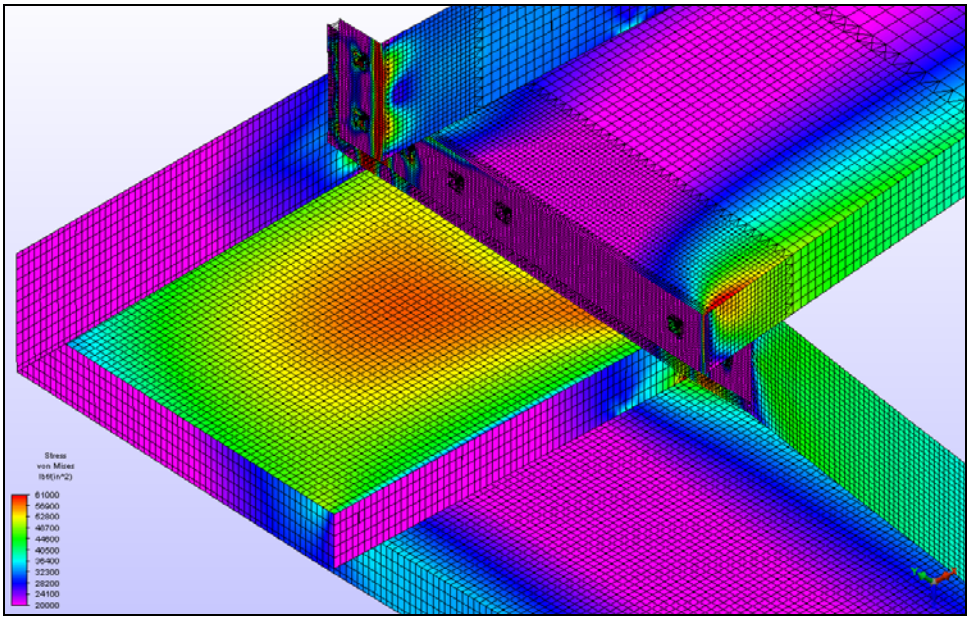

Figure D.8 Frame 1 von Mises Stress in the knee with a 50 kip load applied

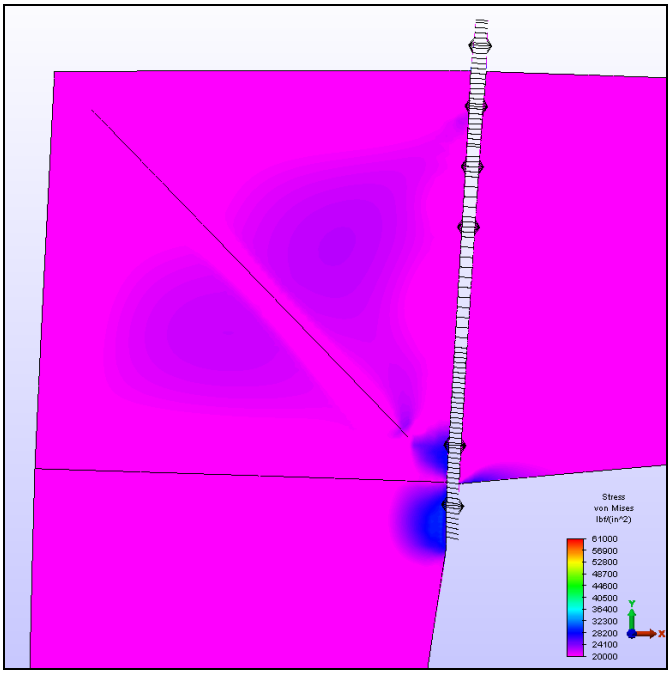

Figure D.9 Frame 2 von Mises Stress in knee web with a 20 kip load applied

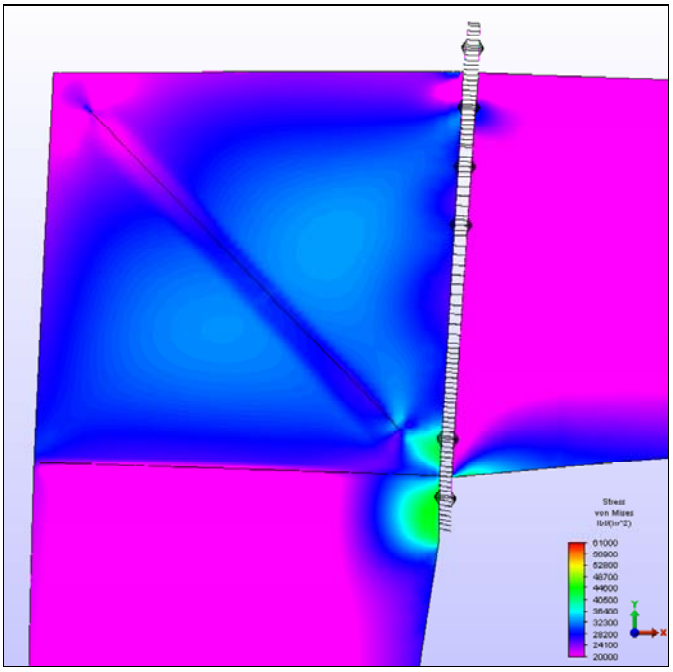

Figure D.10 Frame 2 von Mises Stress in knee web with a 30 kip load applied

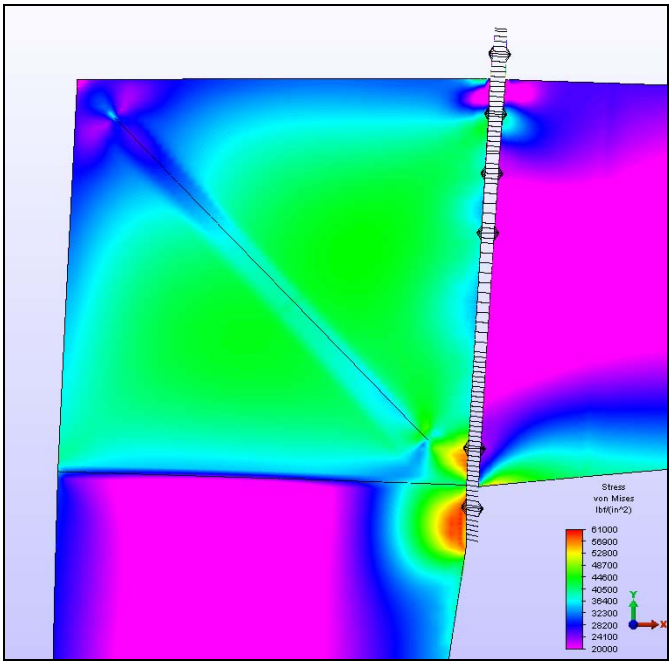

Figure D.11 Frame 2 von Mises Stress in knee web with a 40 kip load applied

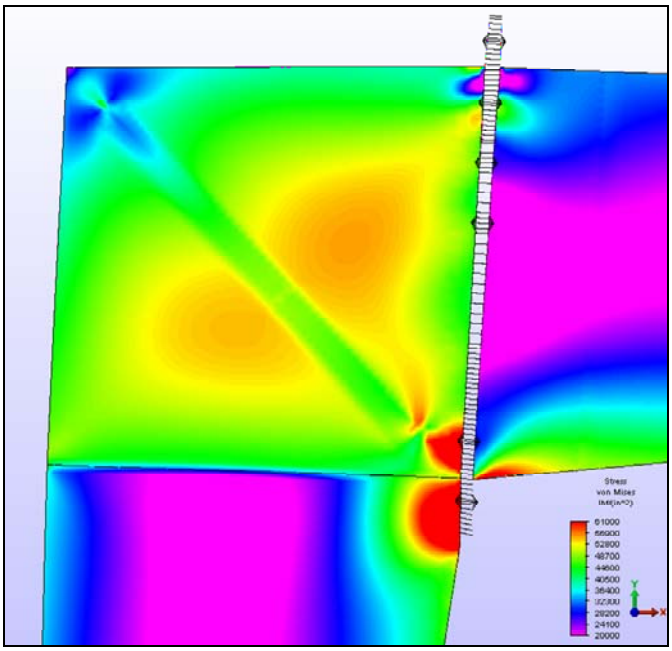

Figure D.12 Frame 2 von Mises Stress in knee web with a 50 kip load applied

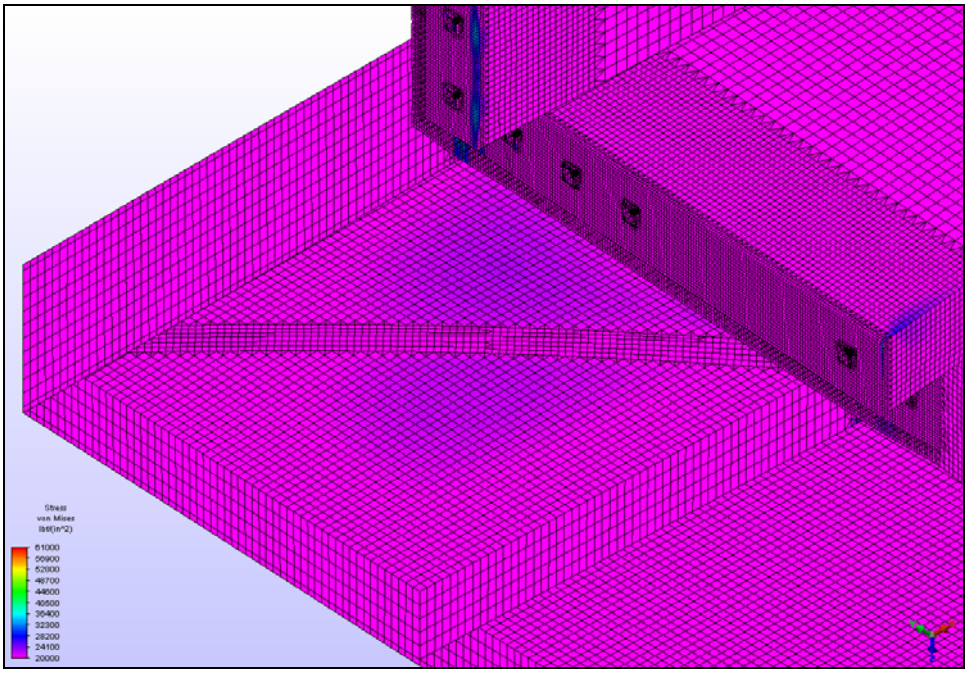

Figure D.13 Frame 2 von Mises Stress in knee with a 20 kip load applied

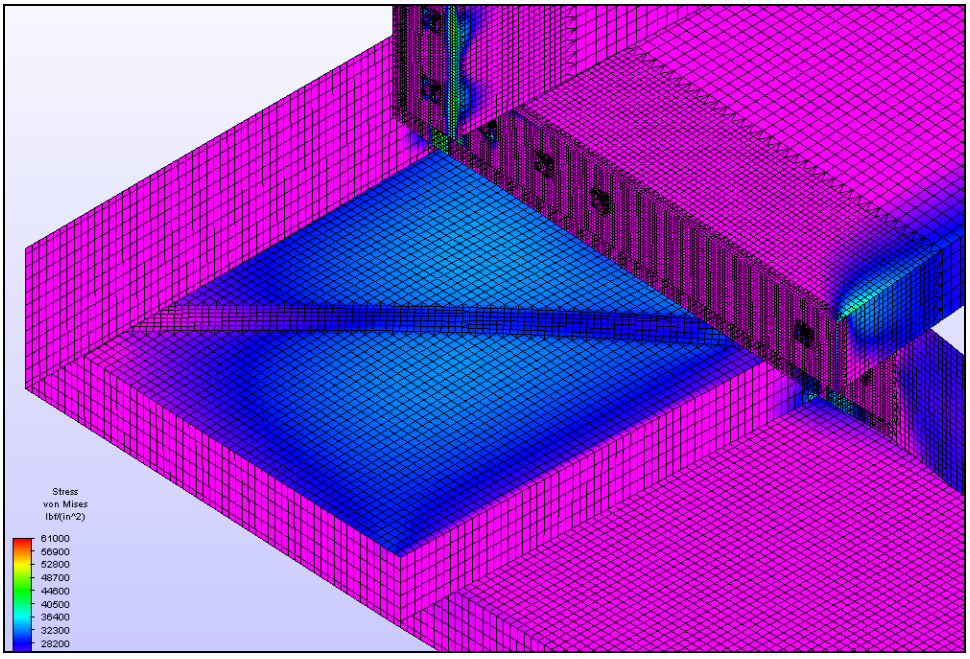

Figure D.14 Frame 2 von Mises Stress in knee with a 30 kip load applied

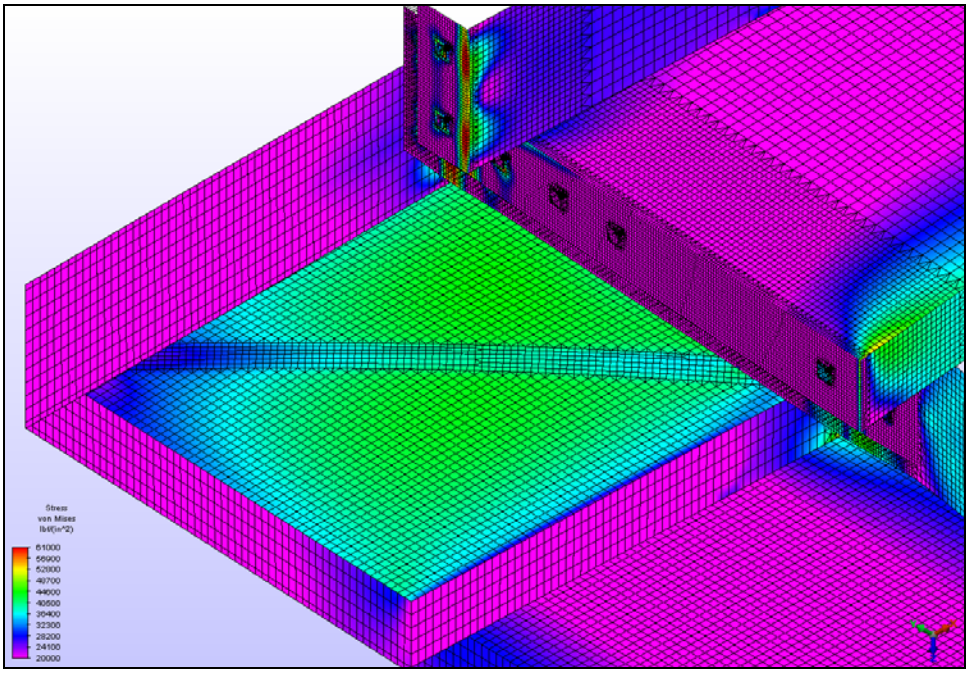

Figure D.15 Frame 2 von Mises Stress in knee with a 40 kip load applied

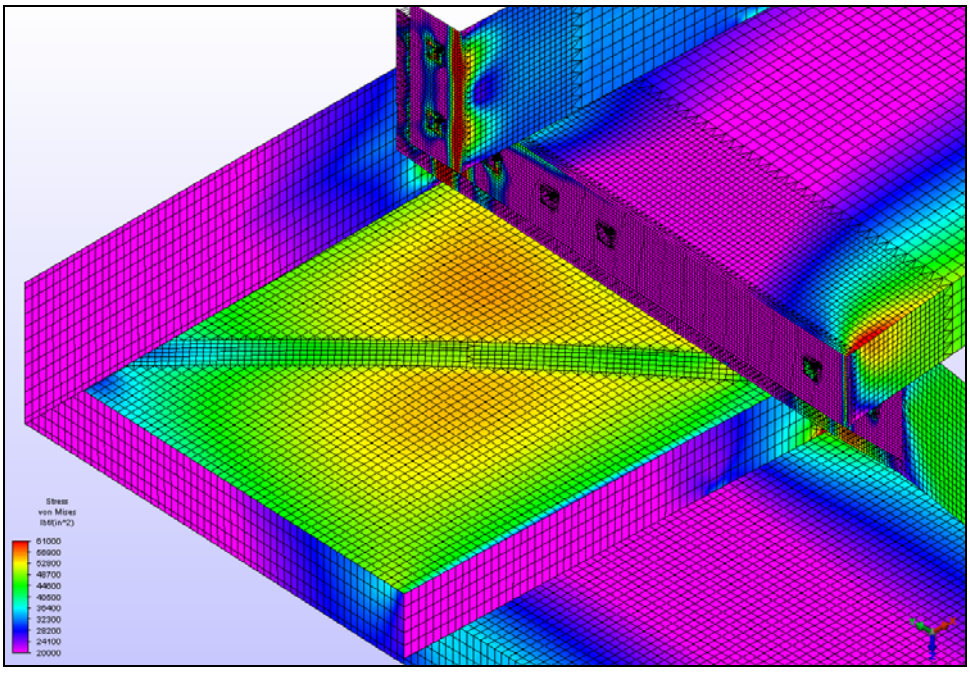

Figure D.16 Frame 2 von Mises Stress in knee with a 50 kip load applied

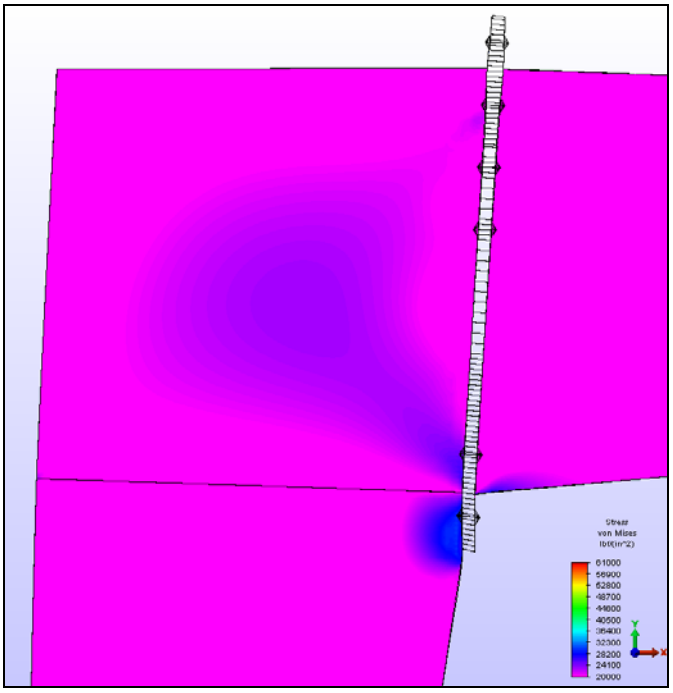

Figure D.17 Frame 3 von Mises Stress in knee web with a 20 kip load applied

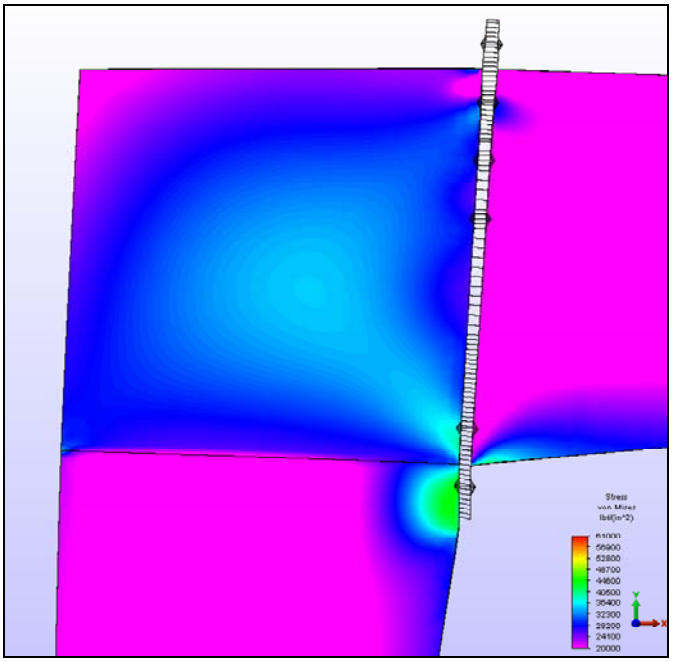

Figure D.18 Frame 3 von Mises Stress in knee web with a 30 kip load applied

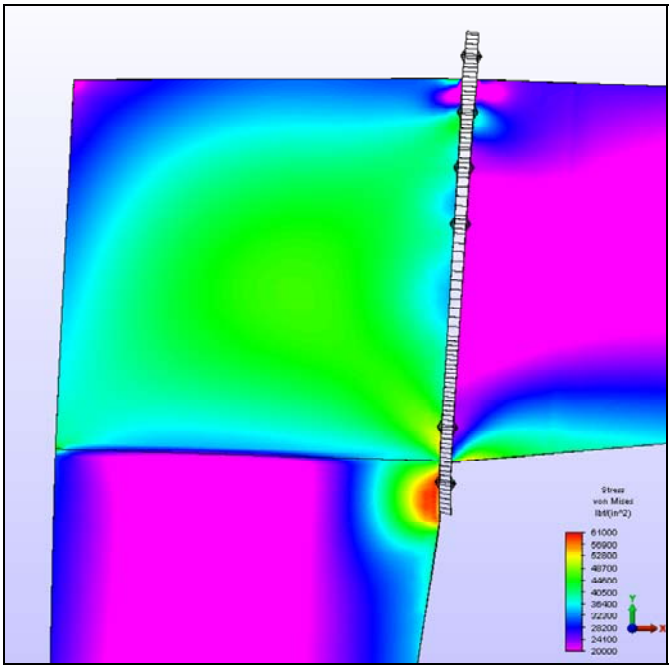

Figure D.19 Frame 3 von Mises Stress in knee web with a 40 kip load applied

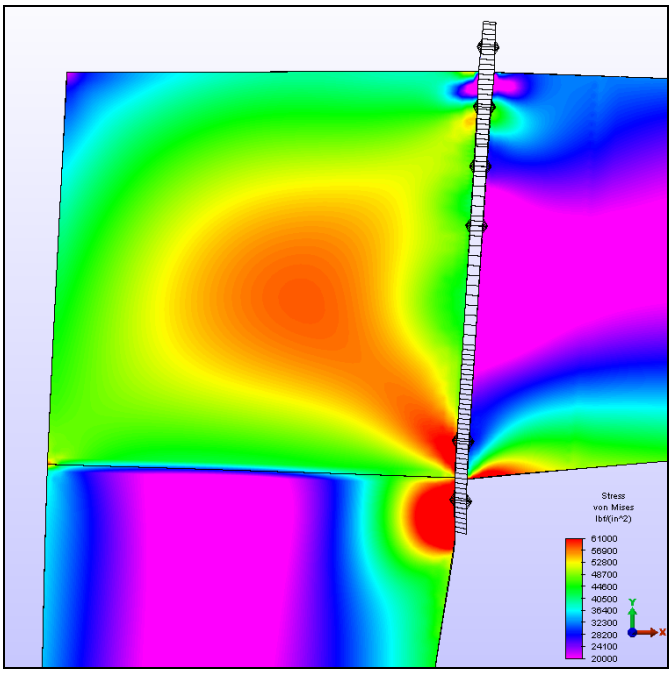

Figure D.20 Frame 3 von Mises Stress in knee web with a 50 kip load applied

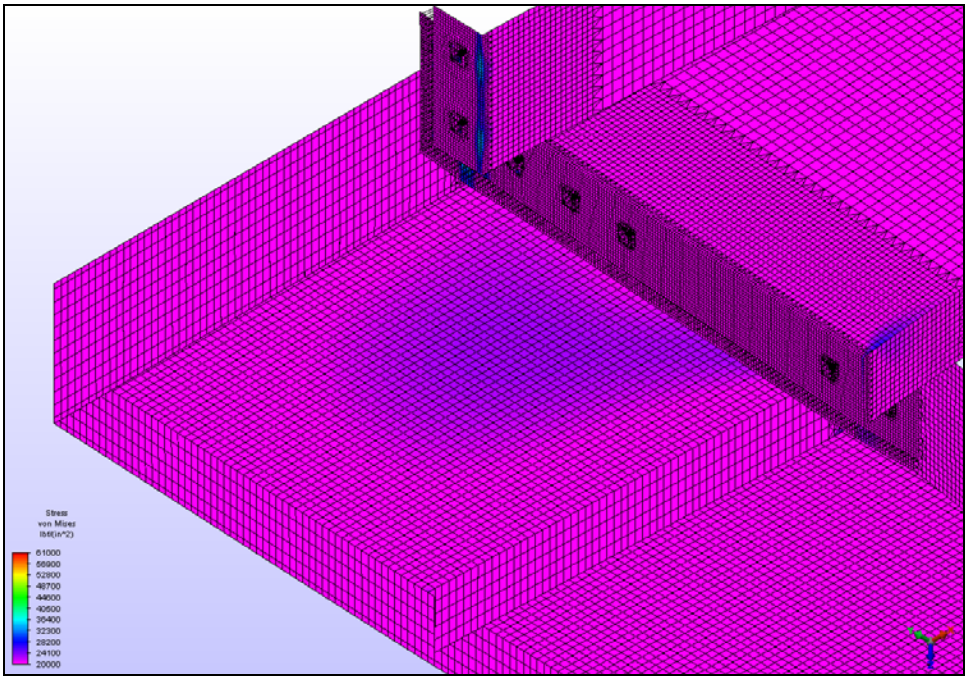

Figure D.21 Frame 3 von Mises Stress in knee with a 20 kip load applied

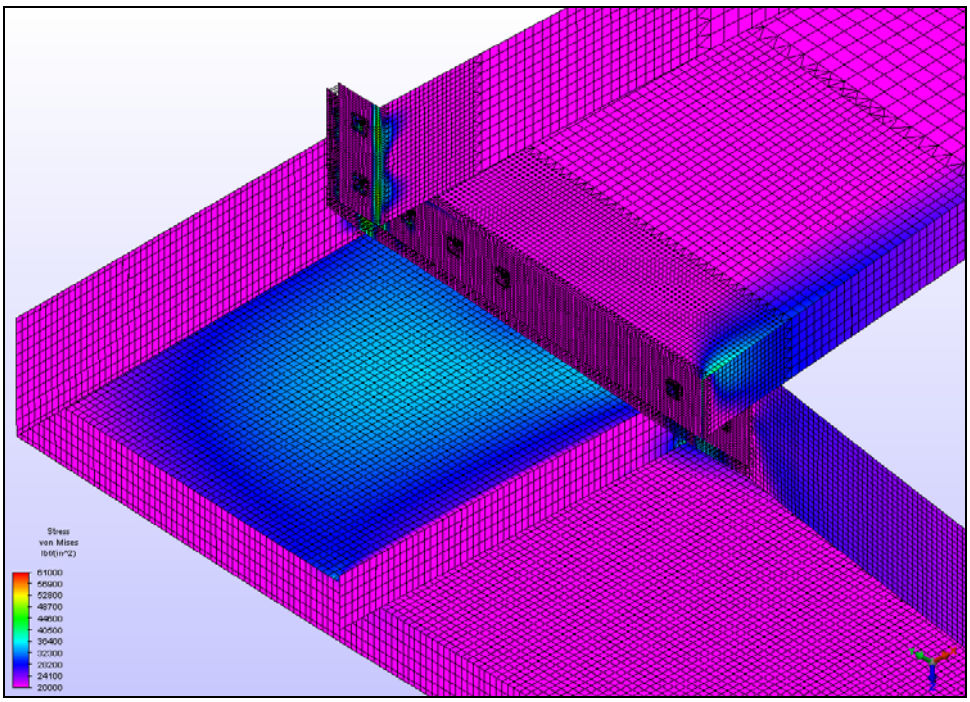

Figure D.22 Frame 3 von Mises Stress in knee with a 30 kip load applied

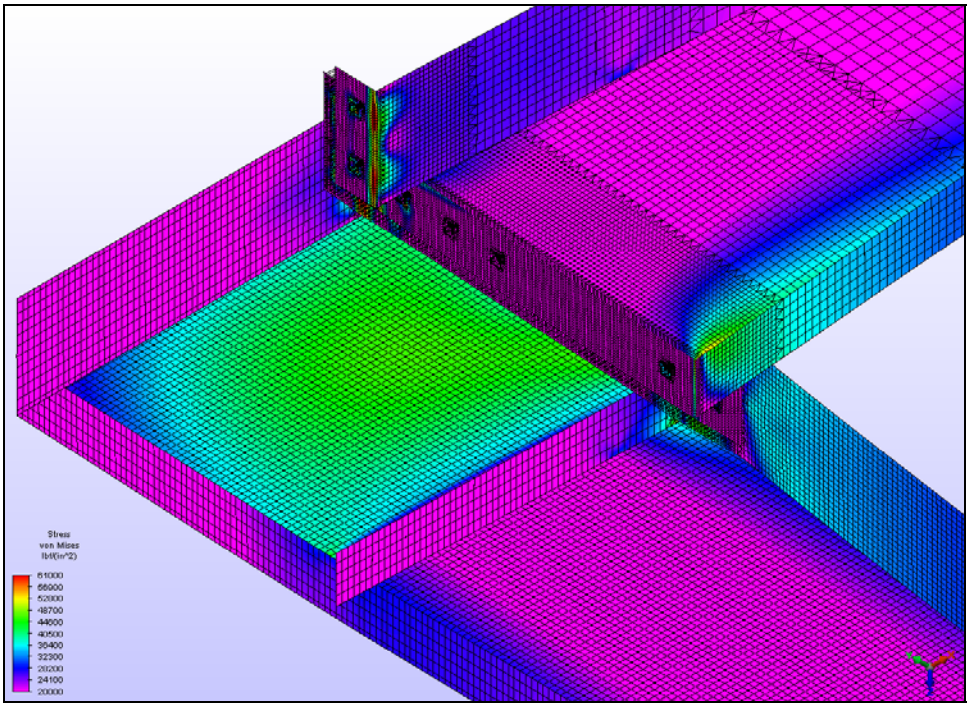

Figure D.23 Frame 3 von Mises Stress in knee with a 40 kip load applied

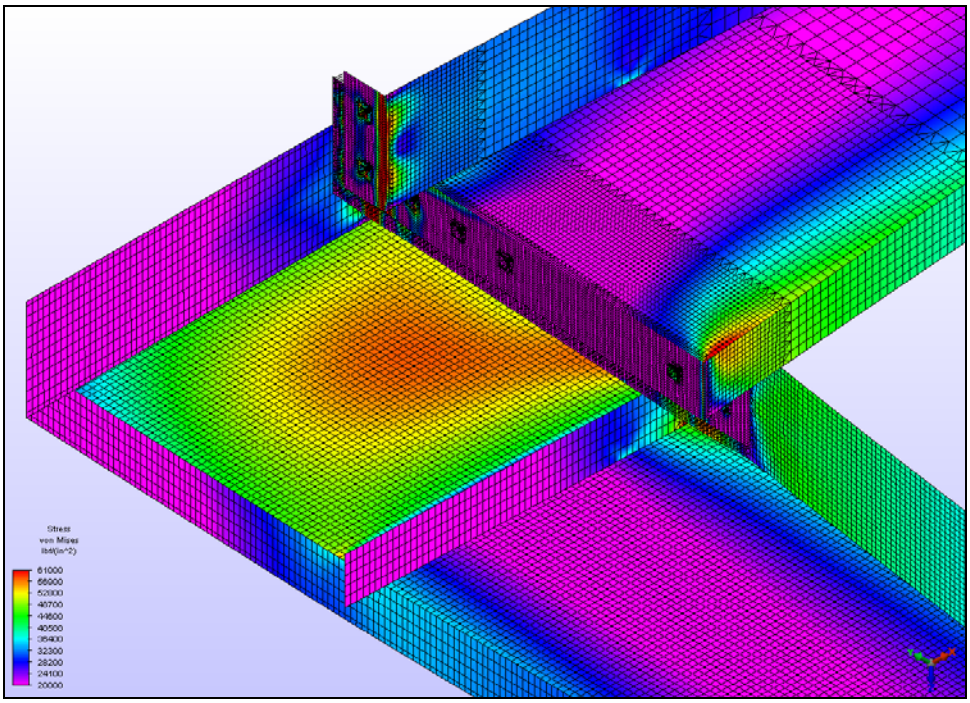

Figure D.24 Frame 3 von Mises Stress in knee with a 50 kip load applied

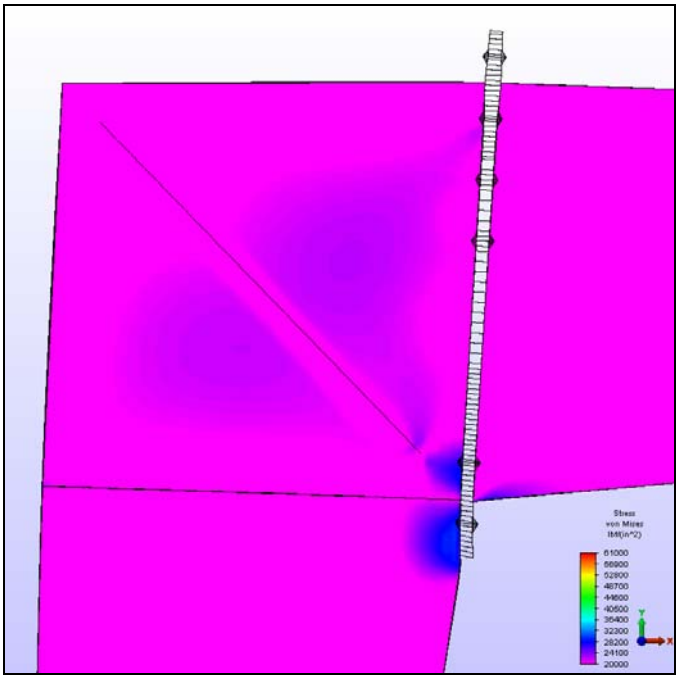

Figure D.25 Frame 4 von Mises Stress in knee web with a 20 kip load applied

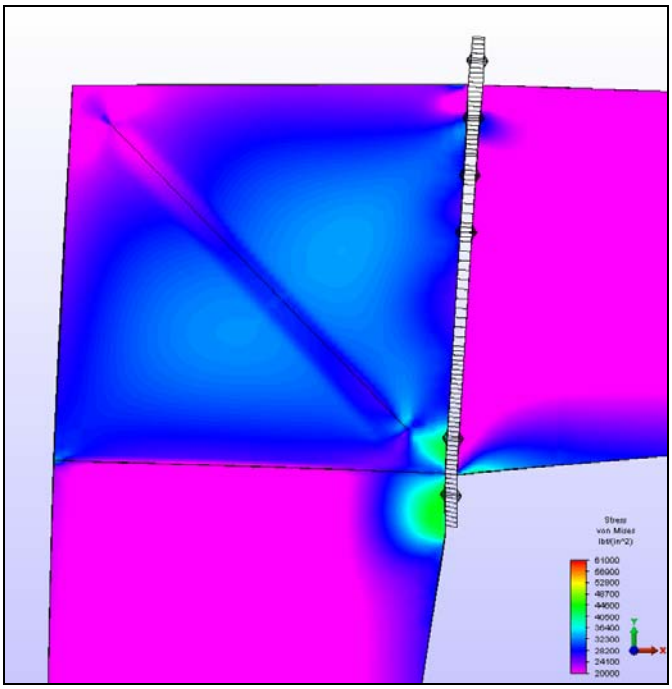

Figure D.26 Frame 4 von Mises Stress in knee web with a 30 kip load applied

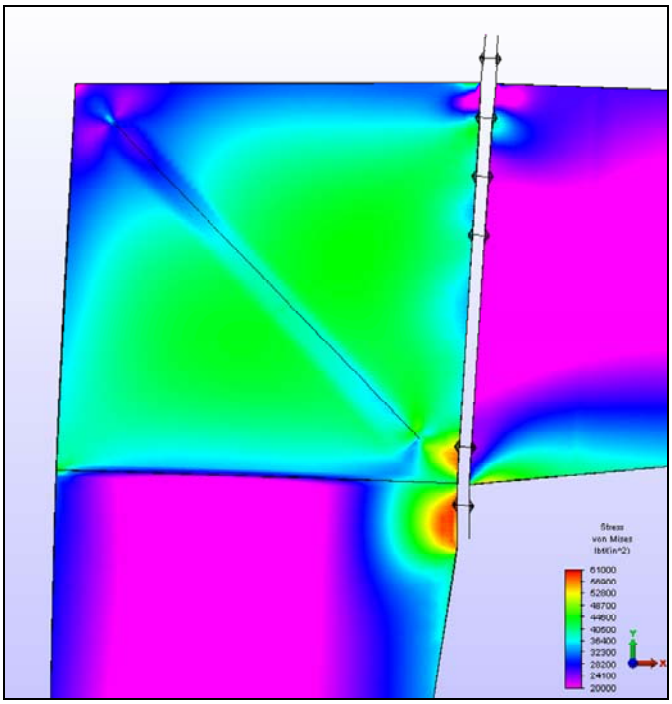

Figure D.27 Frame 4 von Mises Stress in knee web with a 40 kip load applied

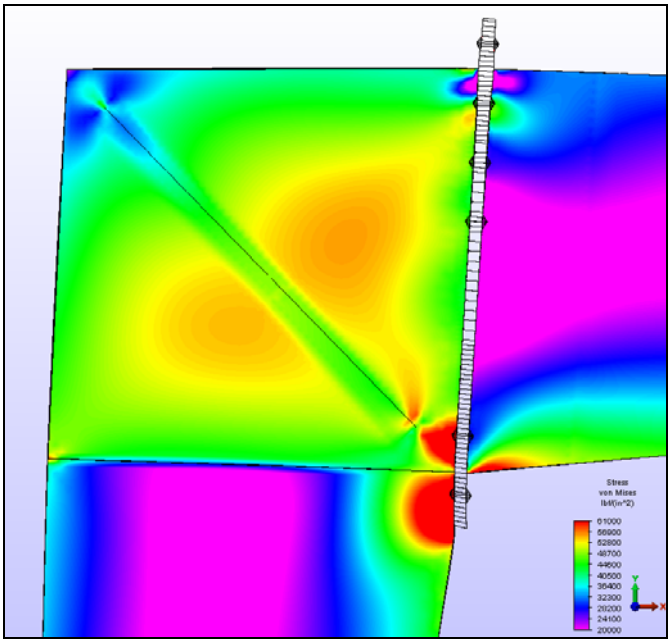

Figure D.28 Frame 4 von Mises Stress in knee web with a 50 kip load applied

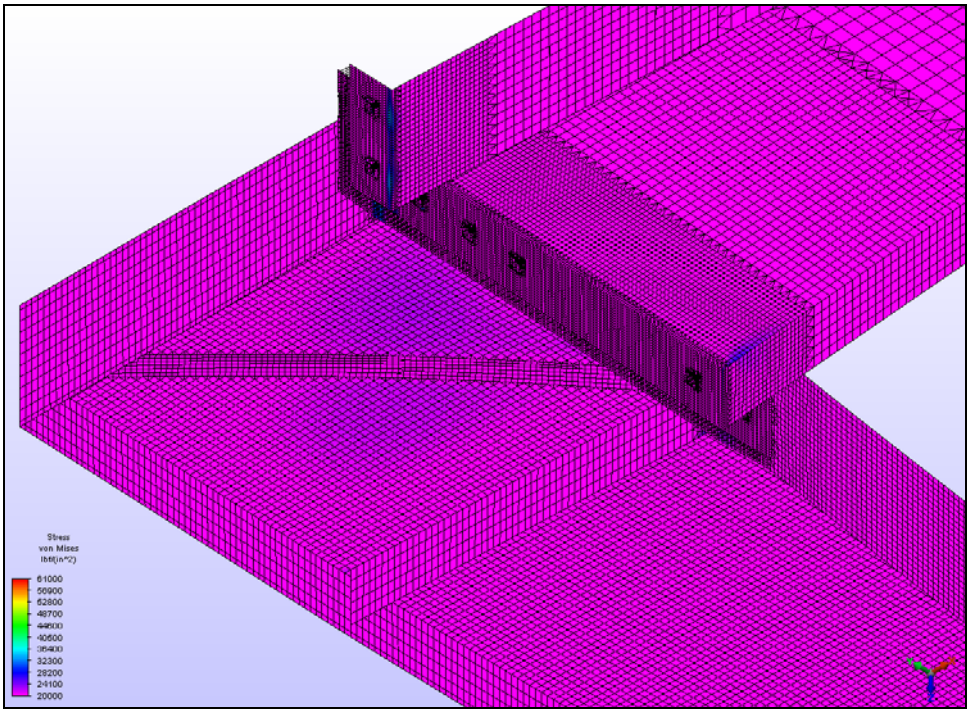

Figure D.29 Frame 4 von Mises Stress in knee with a 20 kip load applied

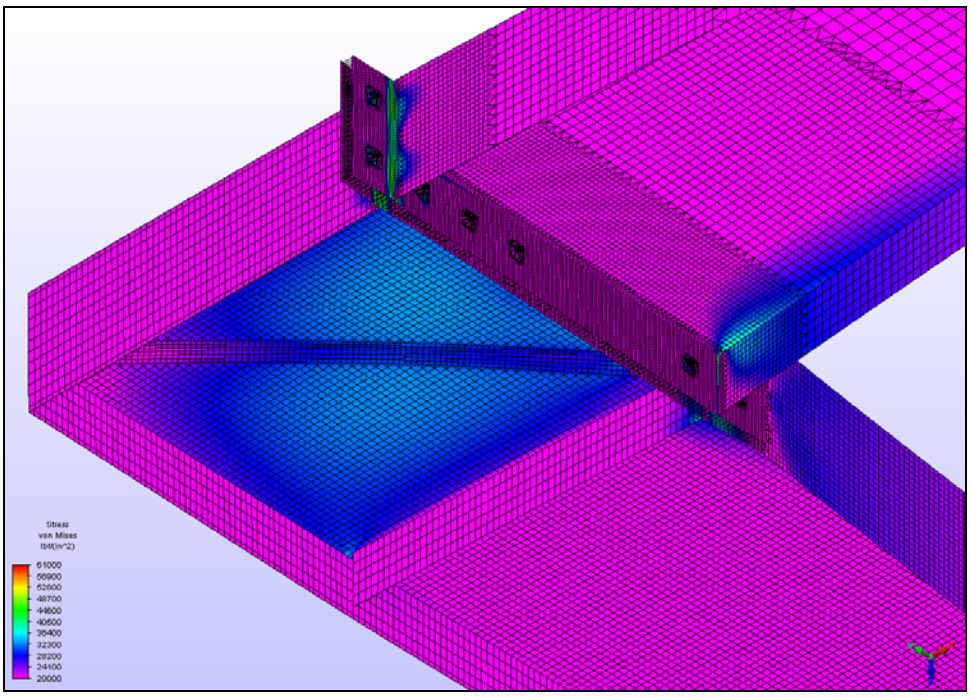

Figure D.30 Frame 4 von Mises Stress in knee with a 30 kip load applied

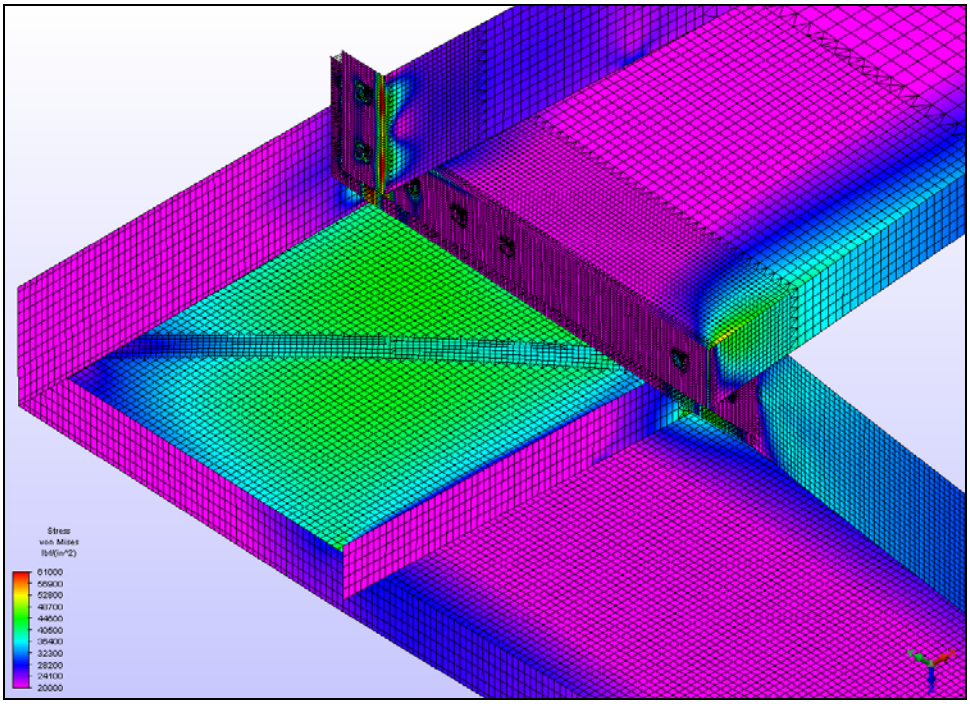

Figure D.31 Frame 4 von Mises Stress in knee with a 40 kip load applied

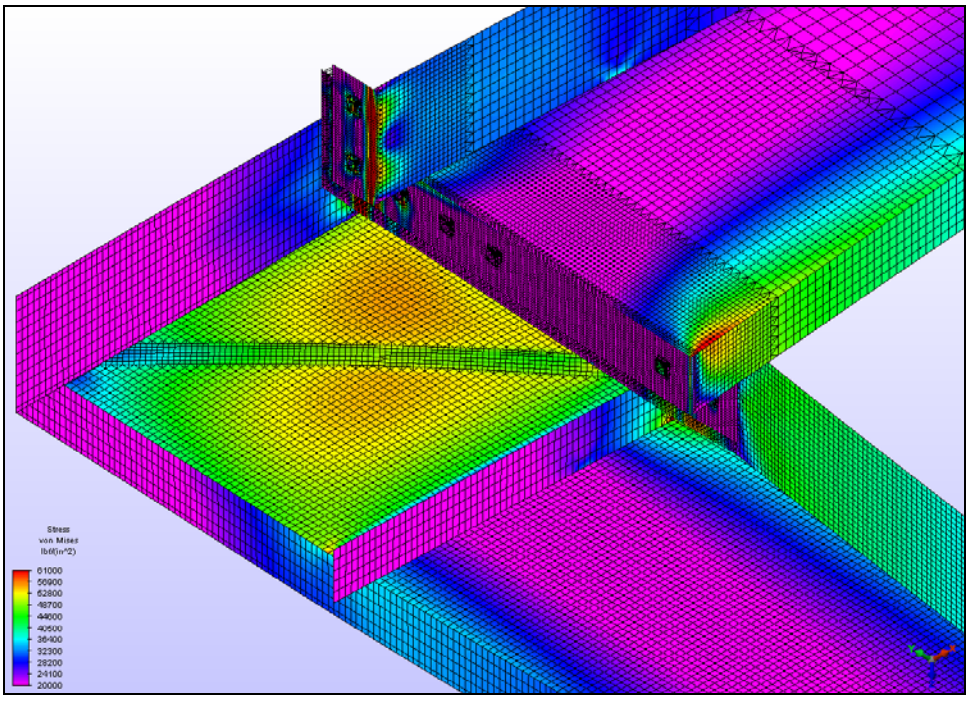

Figure D.32 Frame 4 von Mises Stress in knee with a 50 kip load applied

APPENDIX E

BUCKLING ANALYSIS WITH VARYING LENGTHS OF DIAGONAL STIFFENERS

The purpose of this additional finite element buckling analysis was to determine the minimal length of the diagonal stiffener that will adequately restrain the knee web from buckling. As tested and modeled, the original length of the diagonal stiffener was 22 ½ inches. As shown in this research, this length adequately stiffened the knee web and prevented shear web buckling until failure occurred in the column web and flange, below the square knee. Given this, an additional finite element buckling analysis was conducted to determine the shortest length of diagonal stiffener that would still prevent buckling of the knee web. This analysis would provide valuable information for determining a balanced design of the square knee and the column web and flange, clearly the region of the frame that was prone to instability if the knee web was stiffened. As shown in Chapter 4, the un-stiffened knee web buckled (frames 1 and 3). With a 22 ½ inch diagonal stiffener (frames 2 and 4), the frame failed in the column web and flange with an additional load carrying capacity of approximately 20% above that of frames 1 and 3. By changing the length of the diagonal stiffener in the FEA model for frames 2 and 4, the required length of stiffener can be determined that will achieve this same increase in load capacity. Figures E.1 through E.4 present the FEA buckling results of varying the diagonal stiffener lengths. Figure E.5 is a graph of load versus diagonal stiffener length. As shown in Figure E.5, a 10 inch diagonal stiffener would restrain buckling in the knee web just to the point of buckling of the column web and flange.

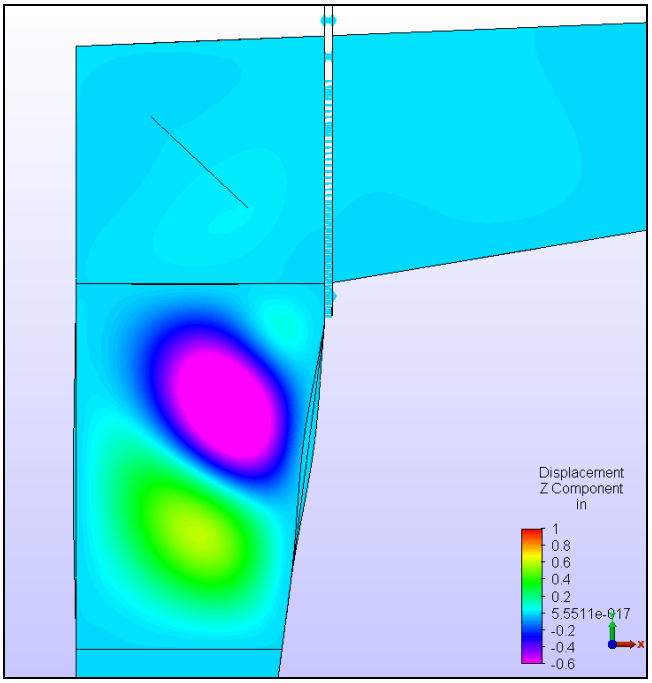

Figure E.1 Frame 2 with an 11 inch diagonal stiffener, buckling occurred in the column web and flange at a 35.7 kip load

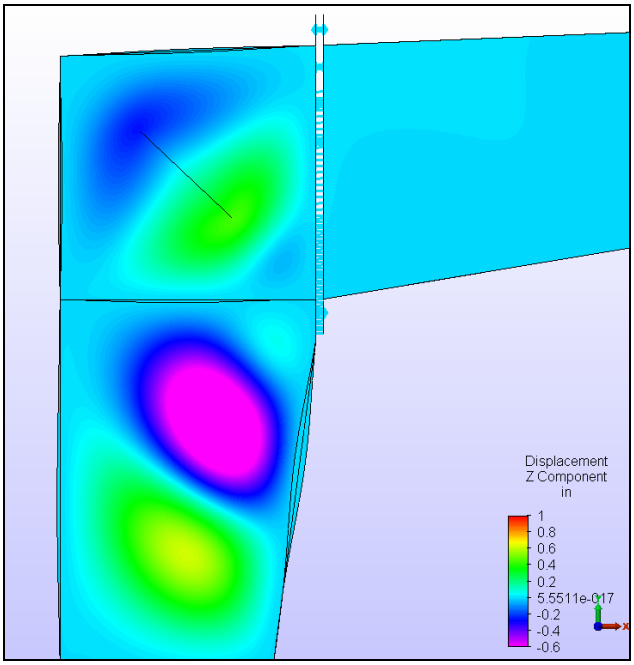

Figure E.2 Frame 2 with a 10 inch diagonal stiffener, buckling occurred in the column web and flange, and the knee web at a 35.7 kip load

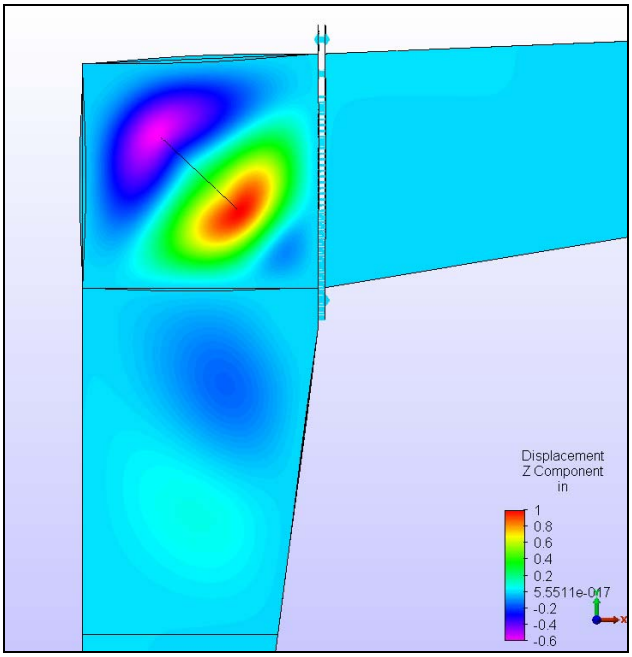

Figure E.3 Frame 2 with a 9 inch diagonal stiffener, buckling occurred in the knee web at a 33.1 kip load

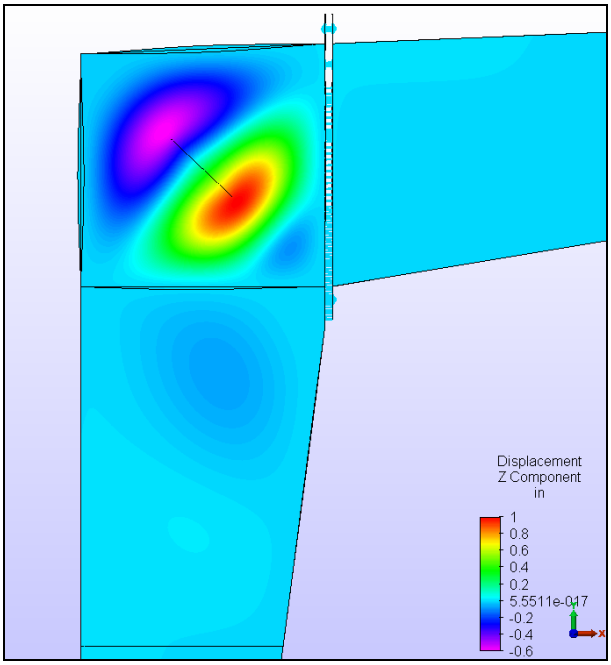

Figure E.4 Frame 2 with a 7 inch diagonal stiffener, buckling occurred in the knee web at a 29.6 kip load

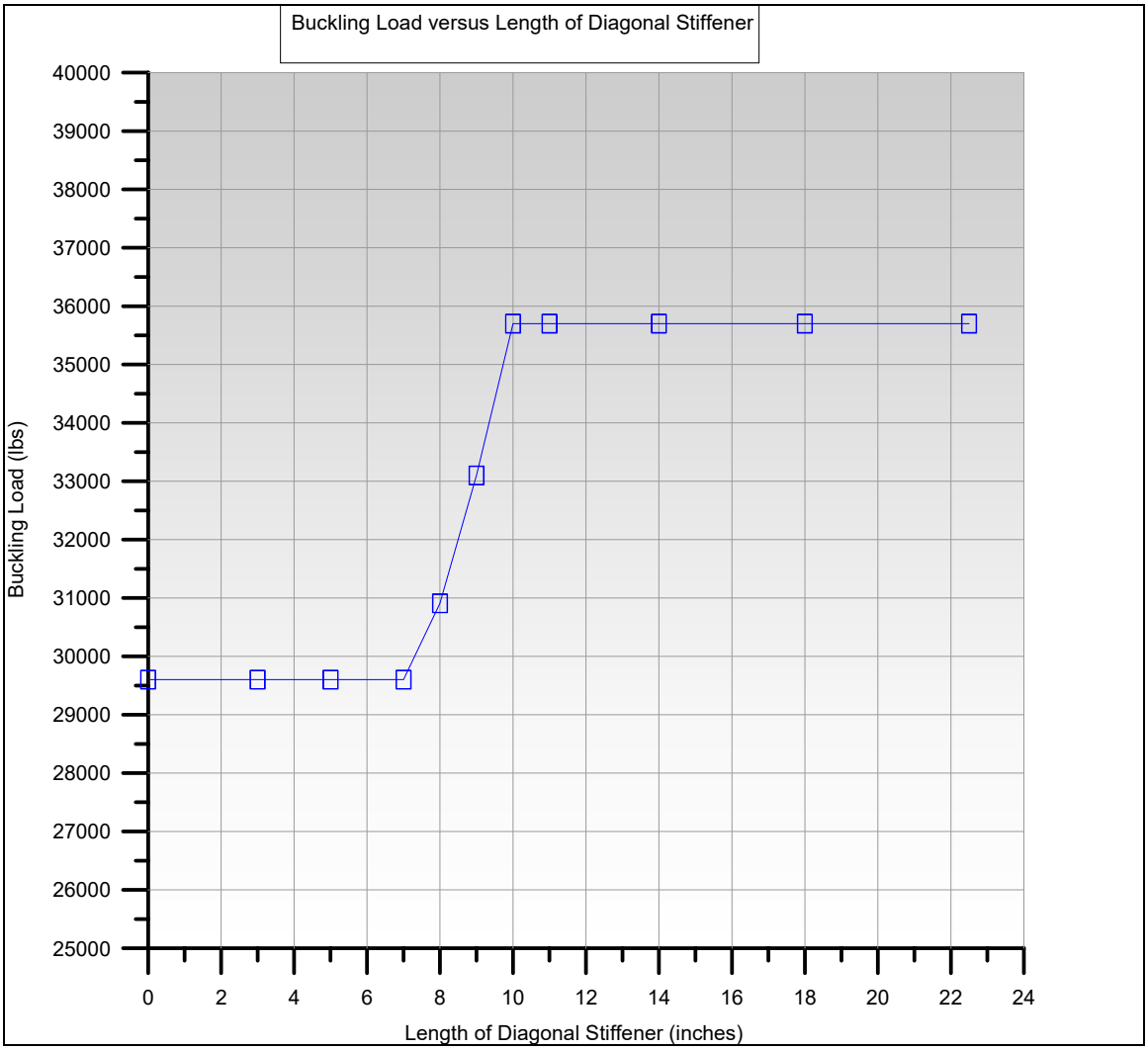

Figure E.5 Buckling load versus length of diagonal stiffener